CONTENTS

	Page	
SUMMARY	1	1/A7
INTRODUCTION	2	1/A8
SYMBOLS	4	1/A10
VEHICLE DESCRIPTION	6	1/A12
Baseline	7	1/A13
Mod 1	7	1/A13
Conventional	7	1/A13
FLIGHT DYNAMIC SIMULATION DESCRIPTION	13	1/B10
STUDY APPROACH	15	1/B12
RESULTS AND DISCUSSION (Tasks I, II, III)	17	1/B14
Literature Survey (Task I)	17	1/B14
Aerodynamics and Performance	24	1/C7
Flight Control	29	1/C12
Configuration Design	47	1/E3
Subsystem Design	54	1/E10
Mass Properties Analysis	67	1/F9
CCV/Conventional Vehicle Performance Summary	74	1/G2
ADVANCED TECHNOLOGY FOR CCV DESIGNS (Task IV)	76	1/G4
CCV Vehicle Performance	76	1/G4
CCV Design Process	78	1/G6
Structures/Subsystem	79	1/G7
CONCLUSIONS	81	1/G9
RECOMMENDATIONS	82	1/G10
REFERENCES	83	1/G11
APPENDICES	84	1/G12

NAS 1.26:2723

SEP 5 1978

NASA Contractor Report 2723

COMPLETED

ORIGINAL

Applicability of the Control Configured Design Approach to Advanced Earth Orbital Transportation Systems

Andrew K. Hepler, Howard Zeck,
William H. Walker, and Daniel E. Shafer

CONTRACT NAS1-14833
AUGUST 1978

NASA

106

NASA Contractor Report 2723

Applicability of the Control Configured Design Approach to Advanced Earth Orbital Transportation Systems

Andrew K. Hepler, Howard Zeck,
William H. Walker, and Daniel E. Shafer
Boeing Aerospace Company
Kent, Washington

Prepared for
Langley Research Center
under Contract NAS1-14833

National Aeronautics
and Space Administration

Scientific and Technical
Information Office

1978

Blank Page

FOREWORD

This study was performed by Boeing Aerospace Company; Kent, Washington under NASA Contract 1-14833 from March 1977 through December 1977.

Study Manager was Mr. Howard Zeck under the administration of Mr. A. K. Hepler. Contributors to the study are as follows:

B. Pulk	Flight Control
R. T. Savage	Aerothermodynamics
D. E. Shafer	Flight Control
A. R. Swegle	Stress
W. H. Walker	Subsystems
H. Zeck	Aerodynamics and Performance

Blank Page

SUMMARY

The next generation of Advanced Earth Orbital Transportation Systems are currently being studied by NASA to assess their potential cost/performance payoff. The present study addresses the applicability of the control configured design approach to Advanced Earth Orbital Transportation Systems. The baseline system chosen to investigate is a fully reusable vertical take-off/horizontal landing Single Stage to Orbit vehicle and had mission requirements similar to the Space Shuttle Orbiter.

The applicability and benefits were identified by technical analyses of aerodynamic, flight control, and subsystem design characteristics. Evaluations were made in terms of time responses to step disturbances, static margins and trim control, and subsystem design actuator and fluid control power. Figures of merit were assessed on vehicle dry weight and orbital payload. The study results, indicated that the major design parameters for CCV designs are the hypersonic trim, aft c.g. and control surface heating.

The study demonstrated the ability to control a longitudinally unstable vehicle (up to four percent of body length unstable) operating through a Mach number range from subsonic to hypersonic. However, external surface temperatures resulting from displacement of aerodynamic control surfaces into the hypersonic air stream must be restricted to a temperature level for which acceptable materials exist. This significantly limits hypersonic trim capability at aft center of gravity positions. A critical task for CCV designs is the development of a wing/body hypersonic configuration. It is shown that optimized CCV designs can be controllable and provide substantial payload gains over conventional non-CCV design VTO vehicles.

INTRODUCTION

The fundamental objective of this study is to achieve a better understanding of the basic vehicle design approaches for development of a Control Configured Vehicle (CCV). Thus, the overall aim of this study was to assess the applicability and potential performance gains of Control Configured Vehicle Design Concepts as applied to the development of a Single Stage to Orbit (SSTO) Vertical Take-Off/Horizontal Landing Vehicle.

Specific objectives include:

- Applicability of CCV to NASA Langley SSTO Technology study. (Task I - Literature Survey)
- Optimization of range of static stability and control power over entire entry mission profiles. (Task II).
- Establish levels of required damping and vehicle rigid mode augmented frequency and determine if current handling qualities criteria are applicable to CCV,or else establish alternate criteria (Task III).
- Identify technology advances most promising to CCV designs (Task IV).

Since the preliminary NASA in-house studies have provided the first bench mark of CCV designs to follow-on Space Shuttle missions, this study provides the next logical bench mark in understanding the more general vehicle design approach for development of a CCV. Successful CCV designs are measured not only in terms of handling qualities, but also in terms of dry weight/payload in orbit.

The scope of this study included the necessary engineering studies, analyses, trade-offs, and planning to accomplish the objective of this study consistent with the guidelines and constraints delineated. As a starting point, a baseline configuration of a CCV design was supplied by NASA. An Entry Mission Profile (Mach, Altitude, Angles of Attack and Bank) was also initially supplied by NASA. This baseline configuration was modified for the selection of the final design and designated, Mod 1. For comparisons with conventional designs, a configuration without a (subsonic) canard surface and the reference wing area increased 50 percent was also included in the study (designated conventional).

Certain commercial materials are identified in this paper in order to specify adequately which materials were investigated in the research effort. In no case does such identification imply recommendation or endorsement of the product by NASA, nor does it imply that the materials are necessarily the only ones or the best ones available for the purpose. In many cases equivalent materials are available and would probably produce equivalent results.

SYMBOLS

CCV	Control Configured Vehicle
CONV	Conventional Configured Vehicle
SSTO	Single-Stage-to-Orbit
VTO	Vertical Take-Off
HL	Horizontal Landing
A. C.	Aerodynamic Center, Measured from Nose Reference
C. G.	Center of Gravity, Measured from Nose Reference
L_B	Reference Body Length
Static Margin	$(A.C. - C.G.)/L_B$
GLOW	Gross Lift-Off Weight
EASY	Flight Control Dynamic Analysis Program
$C_{L\alpha}$	Slope of Lift Coefficient
C_L	Lift Coefficient L/qS_{REF}
α	Angle of Attack
β	Angle of Sideslip
S_{REF}	Reference Wing Area
I	Moment of Inertia
q	Dynamic Pressure $\frac{\rho V^2}{2}$
V	Velocity
M	Mach Number $V/_a$
a	Speed of Sound
ρ	Atmospheric Density
$\Delta\alpha$	Delta Pitch Angle
$\Delta\phi$	Delta Roll Angle
δ	Control Surface Deflection
a_z	Normal Acceleration
P	Roll Rate
T	Thrust

SYMBOLS

$\bar{V}$	Tail Volume Coefficient
Ka	Flight Control Gain
S	Complex Frequency
σ	Real and Part of Complex Frequency(s).
$j\omega$	Imaginary Part of Complex Frequency(s)

Subscripts:

A	Aileron
R	Rudder
e	Elevon
BF	Body Flap

VEHICLE DESCRIPTION

Three vehicles were studied: the baseline vehicle, the Mod I and the conventional. General characteristics of the three vehicles are shown on table 1. These characteristics are parametrically trended from previous space transportation studies (reference (1)). These vehicles employed delta wings and six LOX-hydrogen engines located at the aft end. These engines consist of three (3) fixed expansion engines and (3) two position nozzle engines. A 4.57m (15 ft) diam X 18.29m (60 ft) long payload bay is located on the top of the body forward of the vertical fin and approximately 2/3 of the length forward of the estimated c.g. The payload bay is partially submerged. The crew cab is situated immediately forward of this. A tri-cycle landing gear was utilized in all cases. The external dimensions were provided by NASA Langley Research Center and were adjusted as necessary by variations in body height and width for the required tankage. All three vehicles are configured with the hydrogen tank located forward in the body and the LOX tank aft immediately forward of the engine thrust structure. An interbay compartment between tanks provided space for the secondary power and related subsystems.

Table 1 Design Characteristics

	CONVENTIONAL	BASELINE MOD 1	
GLOW kg (LB)	1632929 (3599992)	1469332 (3239323)	1469332 (3239323)
ASCENT PROPELLANT kg (LB)	1412198 (3113363)	1269418 (2798588)	1269418 (2798538)
EMPTY WEIGHT kg (LB)	166552 (367185)	149770 (330187)	153587 (338602)
WING AREA m^2 (FT^2)	836 (9000)	557 (6000)	557 (6000)
EXPOSED m^2 (FT^2)	387 (4164.6)	242.6 (2611.3)	285.3 (3071.3)
FIN AREA m^2 (FT^2)	65.7 (707)	65.7 (707)	65.7 (707)
T/W AT LIFTOFF	1.3	1.3	
C.G. % B.L. LIFTOFF (EMPTY)	79.3 (78.4)	79.2 (77.1)	79.3 (77.6)
PROPULSION			
(3) 40:1 $THRUST_{VAC}$ MN (LB)	3.8889 (874260	3.4993 (786671)	
(3) 50/150:1 $THRUST_{VAC}$ MN (LB)	4.1052 (922885)	3.6939 (830425)	

Baseline Vehicle.-The vehicle identified as the baseline is shown on figure 1. This vehicle is configured as previously described with a 557.4m^2 (6000 ft^2) wing and a 27.9m^2 (300 ft^2) forward located canard (figure 2). A small strake provides volume at the intertank and wing juncture for the retracted main landing gear. The nose gear retracts into a well in the hydrogen tank. A retractable canard used for subsonic trim is mounted on the upper, forward surface of the body.

Mod I Vehicle.-The Mod I vehicle is configured identical to the Baseline with the exception that an extension of 0.91m (3 ft) was added to the elevon trailing edge and a 1.52m (5 ft) extension added to the body flap. These extensions are necessary to achieve hypersonic trim when preliminary estimates of the actual c.g. of the baseline indicated a much further aft c.g. than previously assumed. This vehicle is shown on Figure 3.

Conventional Vehicle.-As the study evolved, it became evident that for a meaningful assessment of the benefits of CCV design, a comparable non-CCV configuration should be shown in sufficient depth to define weights and c.g. To achieve comparable landing characteristics, the reference wing area was increased by 50%. This necessitated an increase in GLOW, thrust, and internal tankage volume. In addition, one alternate configuration was developed in an effort to achieve the most forward c.g. possible by locating the LOX tank forward. This alternate "conventional" configuration is shown on figure 4 and 5. Figure 5 which shows cross section details is typical of all vehicles.

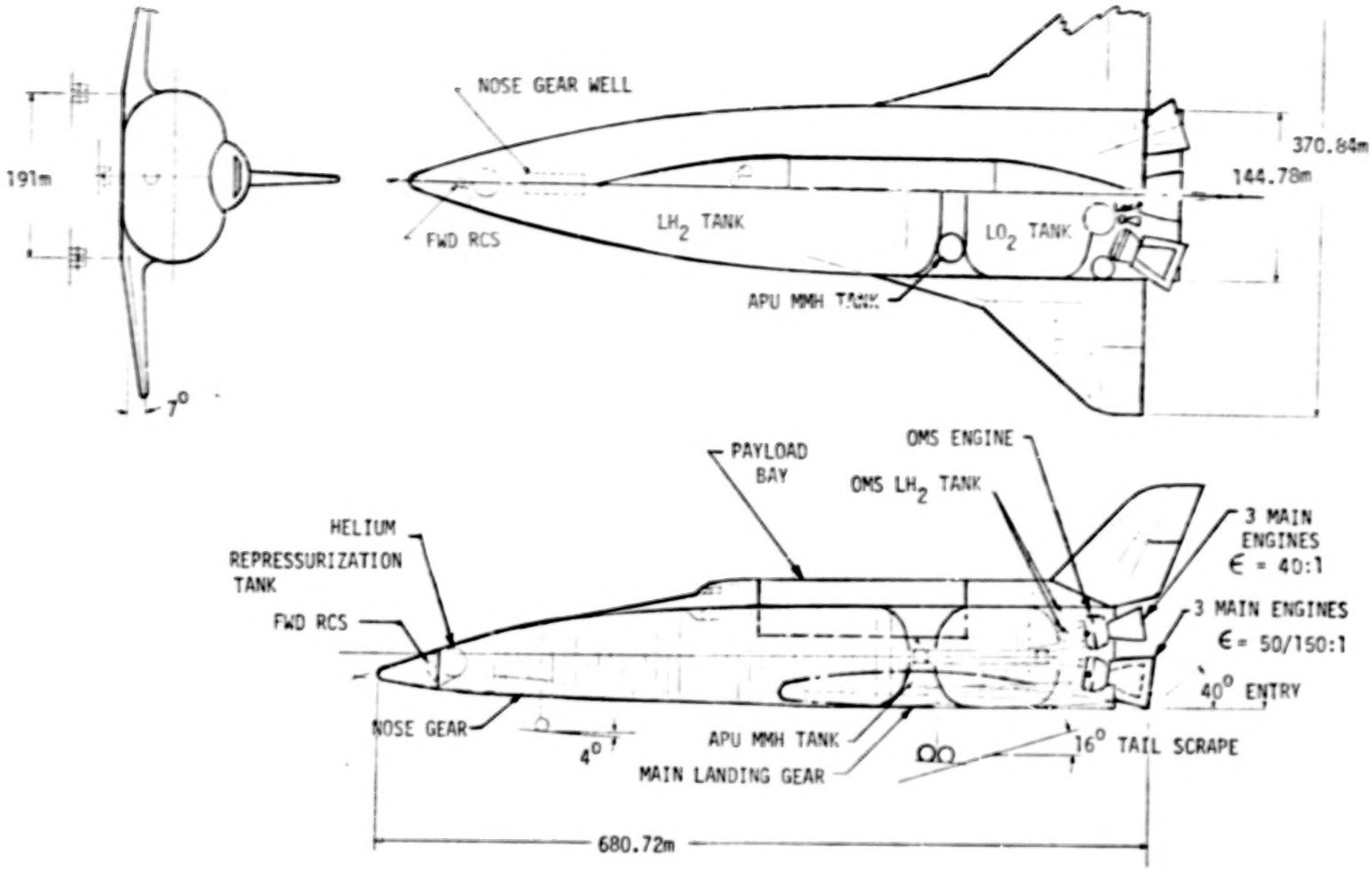

Figure 1 Vehicle Baseline Design

REFERENCE DIMENSIONS

AREA	= 27.87	m^2
SPAN	= 11.79	m
CHORD	= 2.35	m
SWEEP	= 10°	
DIHEDRAL	= 10°	

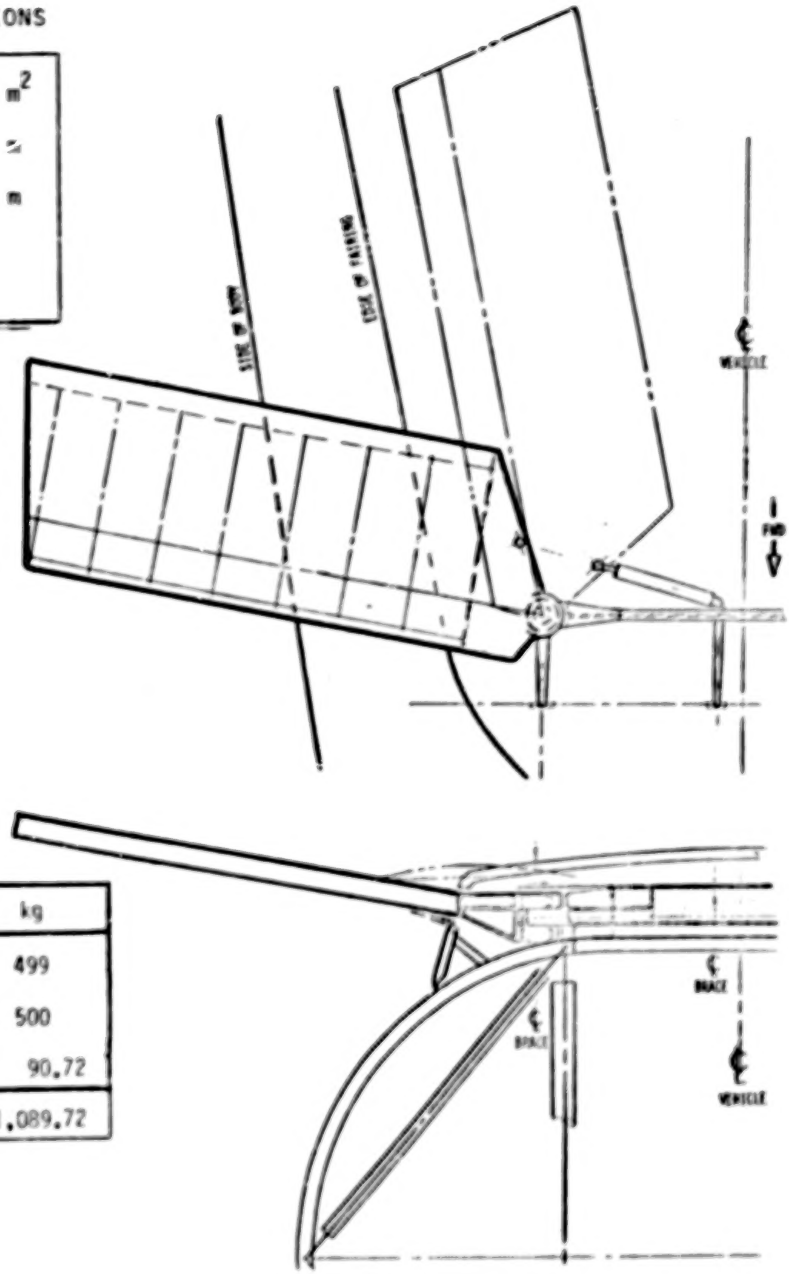

COMPONENT WEIGHTS

	kg
BODY FITTINGS	499
CANARD	500
ACTUATION SYSTEM	90.72
	1,089.72

Figure 2 Canard Installation - Subsonic

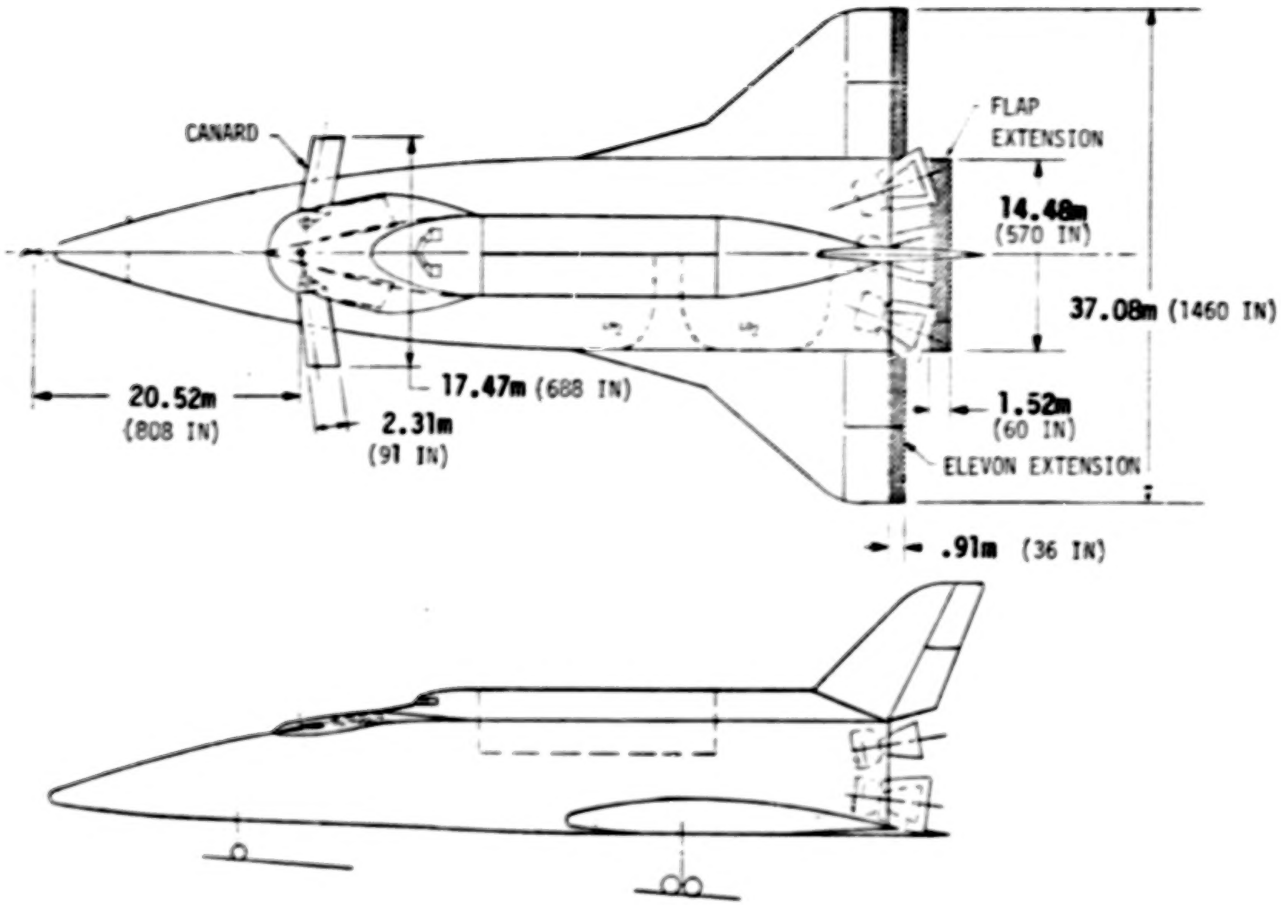

Figure 3 Modification 1 (MOD 1)

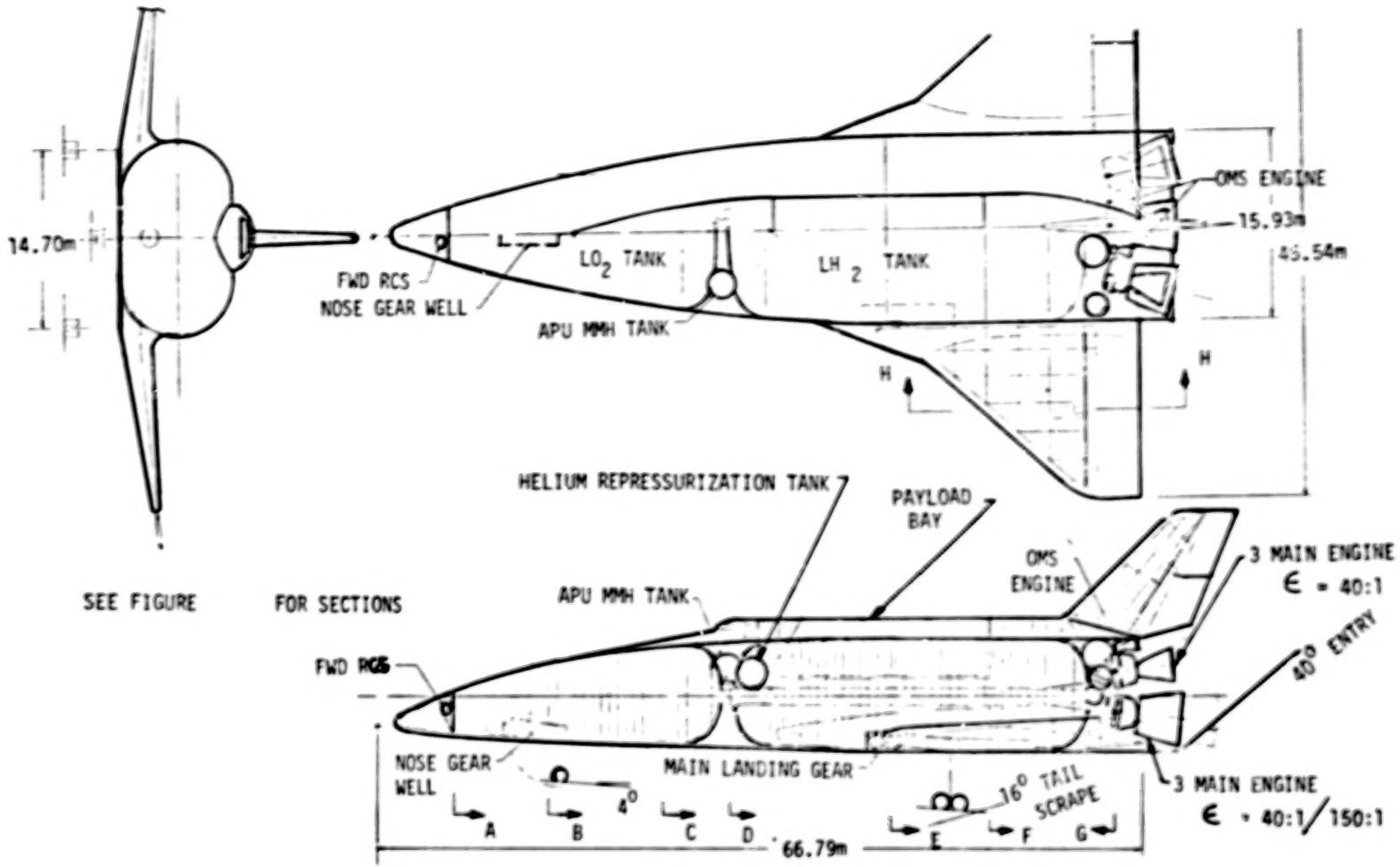

Figure 4 Conventional Design (CONV)

SEE FIGURE
FOR LOCATION OF
SECTION CUTS.

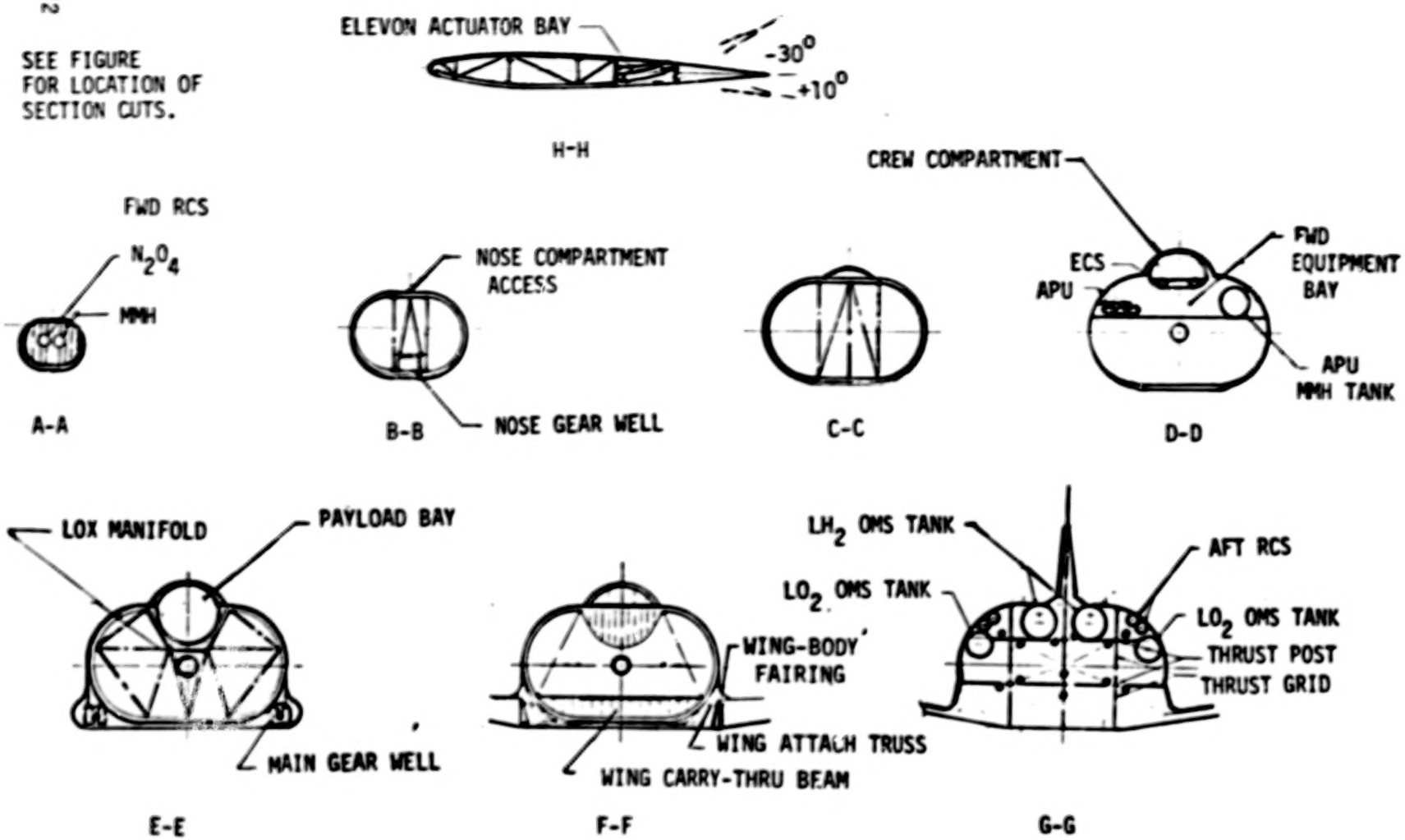

Figure 5 Vehicle Cross Section Details

FLIGHT DYNAMICS SIMULATION DESCRIPTION

EASY Dynamic Analysis Program - The EASY program was developed for the Air Force by Boeing Computer Services in 1976 under contract F33615-76-C-3165. (reference 5) EASY was selected as the dynamic analysis tool for this study for several reasons. The program is highly user oriented. The system model is created from a large library of standard components. These components represent such things as longitudinal aerodynamics, lateral aerodynamics, six degree of freedom kinematics and aerodynamic variables for representing the airframe. Numerous transfer function forms are available to represent autopilot compensation networks. Integrators with saturation and limiters can be used to model rate and position limited control surface actuators. The program can easily handle any aerodynamic non-linearities that can be described by tables or equations.

The standard components are simply called by the user and the connections indicated, much like wiring an analog computer. The program draws a block diagram of the system model and indicates any unsatisfied input requirements of each standard component. The computer drawn diagram used for the subsonic dynamic analyses of this study is shown in appendix B. The program also accepts fortran statements to model anything not covered by standard components.

The kinematics represent a flat earth model. The version used for this study was improved to include a centrifugal acceleration term that correctly represents the effect of near orbital velocities on vertical accelerations with respect to the flat earth. The atmospheric data tables were extended to 121.92 km (400,000 ft) to accommodate this study. Comparison of portions of reentry trajectory obtained from this version with a NASA trajectory using Post showed consistent agreement in the hypersonic speed region, see figure 6. (Note: Initial speed and altitude conditions for EASY trajectory are slightly higher.)

One of the biggest advantages of EASY is that the same program will do both the analysis and the simulation. This results in a significant time saving, since only one model need be developed and the aero data (which can be quite voluminous) need only be input once. Furthermore, since only one program is used for both analysis and simulation, configuration control

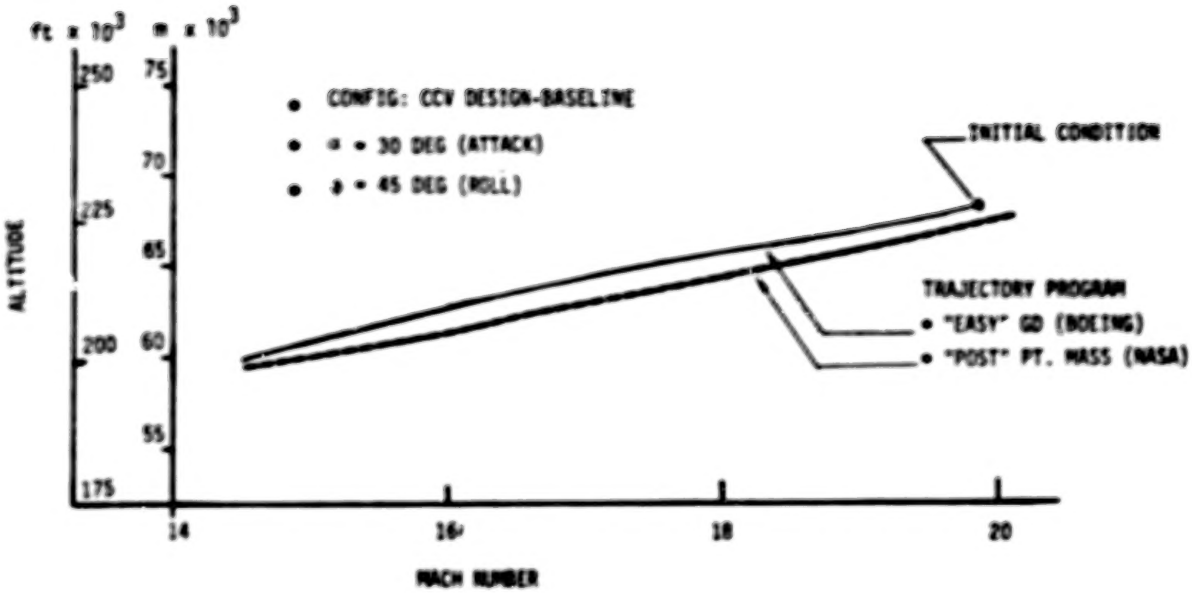

Figure 6 "Easy"/"Post" Entry Trajectory Comparison

is simplified and discrepancies in the results are eliminated since there is no question of the analysis and simulation models being different due to different computer formulations.

Simple command cards cause the program to generate root locus and Nichols or Bode plots. To perform these analyses, the program linearizes the model about the set point over an interval for each state, which is user controlled. The program will also determine the steady state as a function of any parameter and will design optimum controllers of the linear optional regulator type.

The problem can be simplified for any of the options by shutting off any of the states, which is equivalent to keeping an analog integrator in the initial condition mode. Three integration methods are available: 1) variable step, variable order gear, 2) variable step 4th order Runge-Kutta, 3) fixed step Euler. The integration step size for the latter is under user control, as are the plots, scales and print-out.

STUDY APPROACH

As a starting point, a baseline CCV configuration was supplied by NASA. The configuration has been wind tunnel tested over a wide range of speeds and this aerodynamic test data was used extensively during the study. For other configurations, such as Mod 1 and conventional, their aerodynamic characteristics were estimated. During the early phase of the study, it was determined that four fixed design points would be flight control analyzed rather than the complete trajectory. These four design points covered the entire entry trajectory range from subsonic to hypersonic speeds. This type of analysis permitted detailed insights of flight control characteristics at various points along the entry trajectory which are essential before a complete entry 6D simulation is undertaken. This agreed upon approach kept the analysis within the scope and cost of the present study contract.

The following study guidelines were adhered to:

<u>Vehicle Definition</u>

- SSTO VTO/HL
- Initial c.g./L_B 0.69
- Payload 29.483 kg(65,000 lb)sized 4.572 X 18.288m (15 X 60 ft)
- Landing Speed not to exceed 84.94 m/sec (165 knots) at an angle of attack no greater than 15 degrees.
- Hypersonically trimmable over angle of attack from 25 to 50 degrees.
- Baseline configuration characteristics initially supplied by NASA/Langley (i.e. Layout, Aero and Entry Profile)

Microfilmed From
Best Available Copy

Fixed Design Points (for Flight Control Analyses)

	M	ALT. km (ft X 10^3)	ATTACK DEG	ROLL DEG
. SUBSONIC	0.3	S.L.	7-12 ▷	0
. TRANSONIC	1.2	16.764 (55)	10	0
. SUPERSONIC	2.86	27.432 (90)	13	25
. HYPERSONIC	20.0	68.885 (226)	30	45

▷ Trim depends on configuration and c.g. location

The chart (figure 7 presents the overall flow of the study as broken down by task and technical disciplines. The main disciplines included flight control, aerodynamics, performance, vehicle design, and subsystems. Preliminary analysis of the baseline configuration indicated

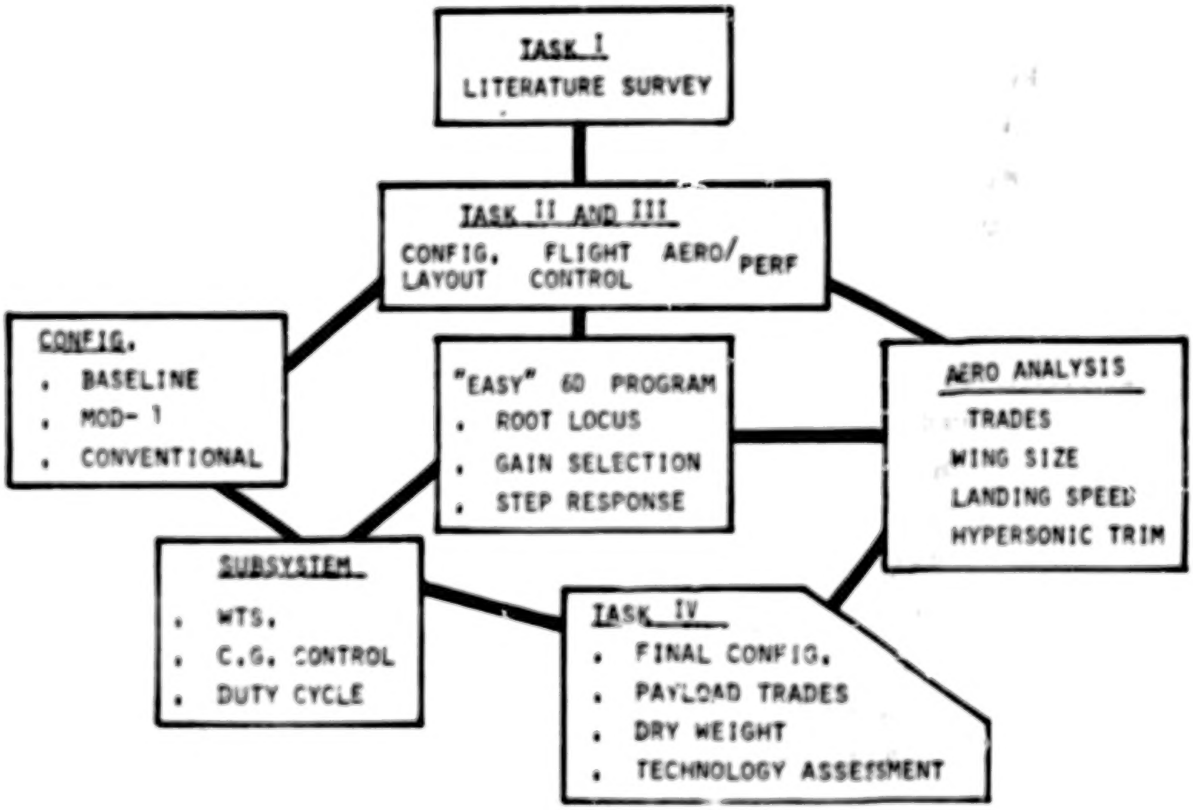

Figure 7 Study Activities

Microfilmed From
Best Available Copy

problem areas particularly in hypersonic trim at aft Center of Gravity (C.G.) positions. This result, gave rise to the Mod-1 configuration in which the sizes of the elevons and body flap were increased. Mid-way through the study, it was decided that a conventional configuration with an increased wing size and no canard, should be included in the study in order to provide the standard for assessing the payload benefits of a CCV design vehicle. This conventional configuration was evaluated to determine its aerodynamic performance and weights and balance characteristics. However, it was not analyzed for its handling qualities since it was assumed that it would be similar to that of the shuttle orbiter. Task IV, Technology Assessment, was limited to those areas and technical disciplines where the present study results indicated potential payoffs of CCV designs in improving payload performance.

RESULTS AND DISCUSSION

Study results for Tasks I to III are given in this section for the various technical disciplines. The literature search of Task I is presented first followed by Aerodynamics/Performance, Flight Control, Configuration Design and Subsystems, respectively. This section concludes with finalized vehicle performance comparisons and the potential benefits of CCV designs. The results of this section provide a lead in to Task IV, Technology Assessment.

Literature Survey

An automated literature search was conducted by the Boeing Technical Library using the key words "CCV" and "Space Shuttle" separately. A list of well over 200 titles has been obtained from NASA, DDC and Boeing sources. A representative set is presented in table 2 at the end of this section.

Very brief descriptions of the contents of most of the papers in the bibliography are given when the title is not adequately descriptive. Since many of the papers scanned are repetitive, only a fraction of the titles available have been included. It is believed that they are representative.

Microfilmed From
Best Available Copy

The resulting titles were scanned for articles dealing with response requirements or CCV design techniques. Numerous articles dealt with handling qualities item 16, table 2. Many articles such as item 6 cited shortcomings in MIL-8785B, however, there were also numerous cautions regarding application of the c* transient response criteria to highly augmented designs. The most appropriate data on the required responses for a vehicle under automatic guidance were found in item 25 of table 2. In this document, allowable time response envelopes for the pertiment vehicle states are given for inputs such as $\Delta\alpha$ and $\Delta\phi$ commands, which originate in the guidance system. These response criteria will be used in the current study, since it is assumed that the SSTO response requirements will closely resemble those of the Space Shuttle for the reentry and subsequent portions of the mission. It may be reasonable, however, to time scale the envelopes in order to accommodate the greater size of the SSTO vehicle.

Many of the papers were broad surveys of the field (items 2 and 9 for example). The requirements for system reliability and various techniques of redundancy management are also widely discussed (for example: item 8). Papers describing the performance advantages of reduced pitch static stability were numerous, but none formulated generalized limitations on this approach.

Lateral directional problems of shuttle type vehicles are discussed in items 18 and 30 of table 2 . Control surface requirement trends are given in item 18 that are different from those found in the present study. This indicates a strong dependence of the trends on the baseline vehicle configuration. A lateral-directional "phugoid" motion was found in item 30. This characterisitc, which causes unusual dynamic responses, also showed up in the present study.

The following applications of CCV concepts have been addressed in the literature surveyed:

1. Reduction of required airplane static margins, which can be used to reduce stabilizer and fin size, reduce trim drag, reduce wing size because of more favorable balancing tail loads, etc.
2. Gust load alleviation to reduce wing structural weight.
3. Maneuver load alleviation, which uses auxiliary controls to distribute the maneuver air loads more inboard, thus reducing wing root bending moments.
4. Fatigue reduction, designed to reduce critical response to turbulence.
5. Ride control, similar to four but with different responses.
6. Maneuver limiting uses feedback loops to prevent the vehicle from excluding a predetermined load factor.
7. Auto-land and direct lift control to reduce design vertical velocity at impact and, therefore, the landing gear weight.
8. Direct side force controls to improve tracking, landing in side winds, etc.
9. Direct control of structural modes through additional control surfaces.

Of the foregoing applications, numbers 1, 7, 8 and 9 appear to have potential advantages to the SSTO vehicle. Only the first is within the scope of the current study.

The low lift curve slope of the SSTO delta wing keeps gusts from being a structural design condition, so application 2 is not relevant to the present study. Similarly, the thicker low aspect ratio wing is primarily designed by pressure rather than root bending moment,so application 3 is not relevant. The vehicle spends but little time in turbulence so fatigue alleviation and ride control improvement are not attractive areas for additional study. The mission profile is such that inadvertently exceeding the g limit is not a likely problem.

It is of some interest to note that there were no unconventional configurations nor innovative suggestions for control effectors suitable for SSTO type vehicles to be found in the literature. The following table summarizes the literature survey:

Table 2 Itemized Flight Control CCV Literature Survey

ITEM

1 "Report on the Joint Meeting of the DGLR Specialist Committees for Flight Characteristics and Flight Control or Control Configured Vehicles" Hamburg 10/73

ESRO TT-164 (ASTIC 144846 C1) 5/75

English translation of German papers. Performance gains for unstable vehicles, manuevers and gust load control are discussed. Several papers describing control system functional design for CCV.

2 "Fly-by-Wire and Control Configured Vehicles - Rewards and Risks" B.R.A. Burns Aeronautical Journal 2/75 Survey

3 "Establishing Confidence in CCV/Alt Technology" - R. B. Holloway and H. A. Shomber (Boeing) NASA Flight Research Center - Advanced Control Technology and its Potential for Future Transport Aircraft. July 1974 - Recommends flight demonstration programs. NASA TMX 70240. (Limited to U. S. Government and contractors only. No results may be lifted from it without prior written approval of the originating installation).

4 "Application of Advanced Model Following Techniques to the Design of FCS for Control Configured Vehicles.

G. Hirzinger in AGARD Conference Proceedings #157 (10/74)

A good how-to article. Differentiates between "tracking" and disturbance performance. Extends regulator problem to following non-zero input (tracking).

5 "Development of an Active Fly-by-Wire Control System"

C. A. Anderson NASA TMX-3409 8/76
(Symposium on Advanced Control Technology Los Angeles July 1974)

Description of F-16; performance improvements and reliability requirements.

6 "Handling Qualities Requirements for Control Configured Vehicles". R. J. Woodcock and F. L. George. NASA TM-X-3409 8/76

Considers MIL-F-8785B, C* criteria And others.

Various considerations are expounded but no firm conclusions developed.

7 "Flight Control Principles for CCV's

E. G. Rynaski and N. C. Weingarten (Cornell Acro Lab)

AFFDL-TR-71-154 Jan. 1972

Describes technique of flight control system design for varying configuration parameters while maintaining good handling qualities.

Table 2 (Cont'd)

8 "Integrated Flight Control System Design for CCV "

J. A. Bondreau (Gramman) AIAA 76-941 Aircraft Systems and Technology meeting, Dallas, Texas - September, 1976.

Reliability goals are established and system design/redundancy concepts to meet them are formulated. Considerable discussion of actuation and auxiliary power systems.

9 Active Control as an Integral Tool in Advanced Aircraft Design"

W. J. G. Pinsker, 1974

AGARD Symposium, Paris October, 1974 (629-135-SYM68IM ASTIC 143664)

10 Overall survey of benefits of CCV and prerequisities for realizing them. Unique thoughts on CCV-autoband design for reduced landing gear weight. Emphasizes requirements to design surfaces for high total control force or movement.

11 "Recent Advances in Aerodynamics for Transport Aircraft"

L. T. Goodmanson and L. B. Gratzer

Astronautics and Aeronautics, Jan 74

Statically unstable in pitch plus load alleviation for reduction of gross weight

12 "New Short Period Handling Quality Criteria for Fighter Aircraft" Boeing Document D6-17841 T/N

L. G. Malcom and H. N. Tobie 9/65

Early Development of C* criteria

13 "CCV's: Active Control Technology Creating New Military Aircraft Design Potential" M. A. Ostgaard and F. R. Snortzel

Astronautics and Aeronautics Feb. 77

Another Survey

14 "Ride Quality Sensitivity to SAS Control Law and to Handling Quality Variations" R. A. Roberts, D. K. Schmidt and R. L. Swain

NASA-CR-148207 (N76-26189)

Found that ride quality for flexible airplanes in turbulance is independent of control law (rigid vehicle) designed for some handling qualities. If vehicle is allowed to become unstable (aft. c.g.) and handling qualities are maintained by SAS, the ride quality (gust response) gets worse.

15 "Design Freedom Offered by Fly-by-Wire" C. F. Newberry (Boeing)

SAE 750144 National Aerospace and Mfg. Mtg., Los Angeles 11/76

Survey Advocates FWB & CCV

Table 2 (Cont'd)

16 "Effects of Artificial Stability on Aircraft Performance"

D. Reich NASA TTF 15953 (N74 32442) 9/74

Presents performance gains of a fighter aircraft as a function of allowable longitudinal instability

17 "Survivable Flight Control Systems, Interim Report 1 Studies, Analyses and Approach, Supplement for Control Criteria Studies" R. L. Kisslinger and M. J. Wendl

AFFDL TR-71-20, Supplement 1 5/71

Studies C* type criteria on piloted, 60 simulator. Concludes criteria can be based on short period handling qualities rather than on mission modes or tasks, except for landing and inflight refueling. Establishes recommended criteria boundaries. Contains an excellent bibliography.

18 "An In-Flight Investigation to Develop Control System Design Criteria for Fighter Airplanes" T. P. Neal and R. E. Smith

AFFDL-TR-70-74 12/70

Concludes that dynamic modes of the flight control system can cause serious flying qualities problems even while satisfying MIL-F-8785B and C* criteria. Another criteria is suggested. (Limited to U. S. Government and contractors only. No results may be lifted from it without prior written approval of the orginating installation).

19 "Application of the Control Configured Vehicle Concept to a Space Shuttle Configuration" M. E. Wawrzniak (McDonnell Douglas) AIAA Paper #73-158 11th Aerospace Sciences Meeting, Washington, D. C. Jan/73

Interesting concept for lateral-directional control system analysis. Baseline vehicle of this study is quite different from ours. Different trends on control surface rate requirements results.

20 "AGARD Conference Proceedings 157 on Impact of Active Control Technology on Airplane Design" Paris Oct. 74 629.135 SY68 IM-1974

Wide range of analytical papers and descriptions of flight test results. Subjects covered are:

Advanced aircraft design

Analysis and simulation programs

Flight test programs

Advanced FCS

Systems in operation today

21 "Application of Advanced Flight Control Techniques to the Design of CCV's, Status Report" (Boeing D180-18007 May 1975)

ASTIC 142388

Table 2 (Cont'd)

22 MIL-F-8785B (ASG) Military Specification, Flying Qualities of Piloted Airplanes August 1969 (Restricted "For Official Use Only")

23 MIL-F-83300 Military Specification, Flying Qualities of Piloted V/STOL Aircraft

24 "Background Information and Users Guide for MIL-F-8785 (ASG), "Military Specification - Flying Qualities of Piloted Airplanes"

C. R. Chalk, T. P. Neal, T. M. Harris, F. E. Pritchard

(Cornell Aero Lab) and R. J. Woodcock (AFFDL) Aug. 69

25 "Recommended Revisions to Selected Portions of MIL-F-8785B (ASG) and Background Data"

AFFDL-TR-73-76 I. L. Ashkenas, R. H. Hob, S. J. Craig Aug 1973

26 Space Shuttle Flight Control System Data Book, Vol. II, Orbiter

SD73-SH-0097-20, May 1975

27 "Preliminary Analysis of the MSC Orbiter Space Shuttle Vehicle Handling Qualities" Aug. 1970

(Prepared by Boeing at the request fo MSC Guidance and Control Div.)

28 Internal Note 72-FM-197 Aug 1972

"A Representative Re-entry and Landing Trajectory for the Space Shuttle

Orbiter: J. W. Tolin and J. H. Alphin

29 JSC Internal Note 73-FM-84 May 1973 "Control System Requirements for Trajectory Control During Entry" J. C. Harpold

30 "Effects of Modifications to the Space Shuttle Entry Guidance and Control Systems" R. W. Powell and H. W. Stone NASA TN-D-8273 Oct 76

Contains useable Space Shuttle FCS block diagrams for various modes

31 "Flight Test Results Pertaining to the Space Shuttlecraft"

A symposium held at Flt Res Center - Edwards, California

June 1970 NASATM X-2101 10/70

Describes wind tunnel and flight test results for M2-F2, 3, HL-10 and X-24A. Discusses "lateral phugoid and other effects of lateral-directional control interaction.

Aerodynamics and Performance

Much of the Aerodynamic characteristics of the Baseline CCV Configuration are based upon preliminary wind tunnel test data of a similar configuration (from unpublished NASA test data). Where sufficient test data did not exist on elevon, body flap and rudder, effectiveness estimates are made based upon scaling factors from the Space Shuttle orbiter design. For configuration changes from the baseline (i.e. Mod-1) in-house estimating techniques, consistent with DATCOM methods, are used to establish the Aerodynamic characteristics.

The scope of these analyses included: the effects of wing size on subsonic aerodynamics and landing speed, static margin and trim over the entire ascent and entry trajectory regime, and hypersonic stability and trim characteristics for various configurations. In addition to these characteristics, Aerodynamic stability derivatives and control effectiveness determined for these configurations to provide inputs to the Flight Control Analyses.

Subsonic Aerodynamics of Various Wing Sizes.-Since the "conventional" and "baseline CCV" configurations, have large differences in their respective wing sizes, it is instructive to examine the effect of wing area on subsonic lift slope ($C_{L\alpha}$) and Aerodynamic Center (A.C.) characteristics. Along with the estimated data are shown in figure 8 wind tunnel test points for the baseline CCV configurations (body alone and wing/body). Agreement of the estimates with test data is very good. So long as the wing size does not decrease below about 464.5 square meters (5000 square feet) there are small changes in $C_{L\alpha}$ or A.C. The destabilizing effect of "Canard On" is readily apparent. For these configurations, the estimated center of gravity (c.g.) locations without ballast weight are appreciably aft of these A.C. locations, thus, resulting in statically unstable subsonic configurations. Flight control analyses considers the impact of these aft c.g. locations in the sections which follow.

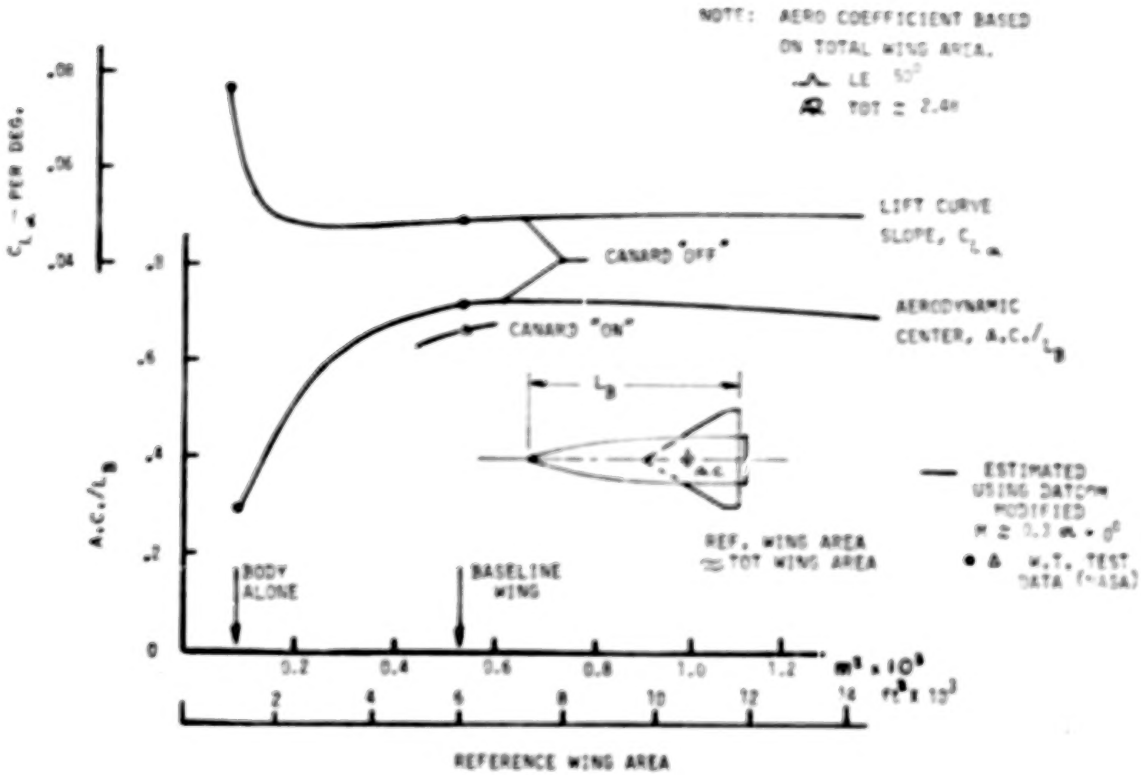

Figure 8 Subsonic Aerodynamics With Various Wing Size

Landing Speed/Wing Size Trade.-Along with the effects of wing size on L_L and A.C., the effects on landing speed have also been determined. Design guidelines for landing speed is 84.94 m/sec (165 knots) for trimmed angle of attack to not exceed 15 degrees. The additional benefits of deploying a canard surface subsonically are also shown in figure 9 . Both the "conventional" and "CCV" designs do not exceed these guidelines at an aft c.g. location of 0.730 L_B. Aft c.g. locations reduce landing speeds through their effect on trimming with relatively increased down elevons (down elevons increase wing lift). The effect of c.g. location on landing speed is presented in later charts for the Task IV studies.

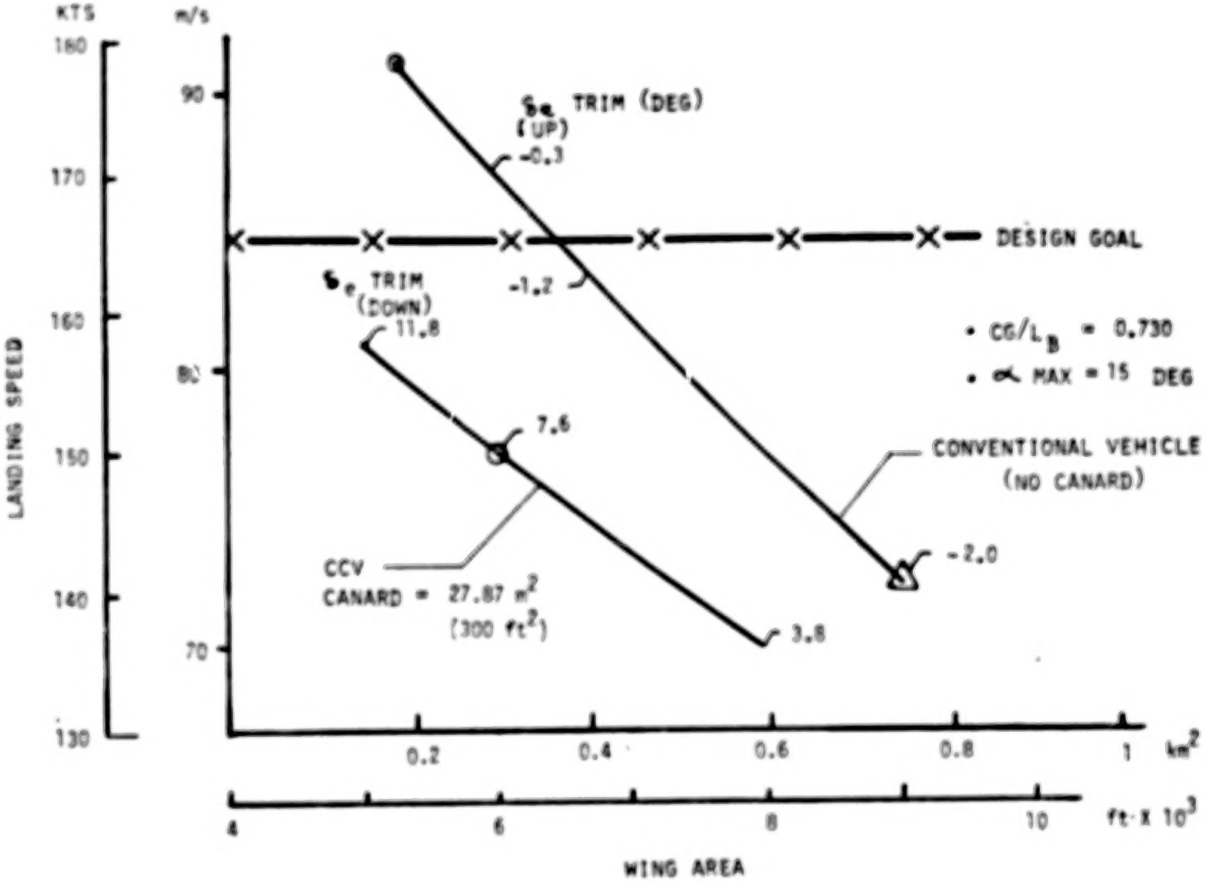

Figure 9 Landing Speed - Wing Size Trades

Shuttle/CCV Static Margin.-The static margin is conveniently defined as the difference between the A.C. and c.g. (in ratios of body length or MAC) with positive values being statically aerodynamically stable and are called stable margins. For a reference of comparison, the shuttle orbiter is also shown on figure 10 over a representative entry speed range. The four design points for the CCV designs are highlighted. Relative to the shuttle, the CCV design has much greater static margin excursions through the transonic and low supersonic speed range. These excursions have a significant effect on required elevon trim deflections as shown on the following chart. Other effects are noticed on increased flight control gain changes and activity in this speed range.

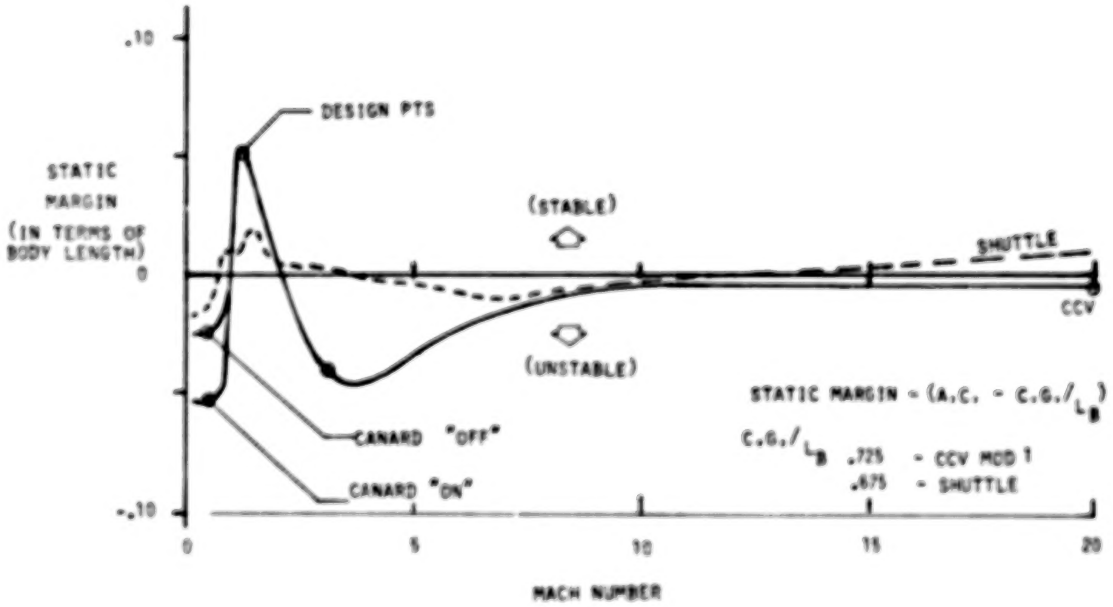

Figure 10 Shuttle - CCV Static Margin

Shuttle/CCV Static Trim.-For angle of attack requirements along a representative (supplied by NASA) entry trajectory the elevon deflections required for static trim are estimated and compared to the Shuttle Orbiter figure 11 . Like the static margin comparison, the CCV design has relatively much greater excursions in the transonic and supersonic speed ranges. These elevon trim characteristics have a very significant overall effect on the overall payload performance of the CCV designs. The greatest impact is at the hypersonic speeds where large down elevons are required to trim aft c.g. locations (i.e. c.g./L_B> 0.72). This comes about from the resulting high thermal environment with large down elevon deflections as shown on following charts. The TPS material limits are soon exceeded when down elevon deflections are greater than about five degrees. In the technology assessment of Task IV, approaches to reducing down elevon trim requirements at hypersonic speeds are suggested and a Mod-2 configuration is briefly studied.

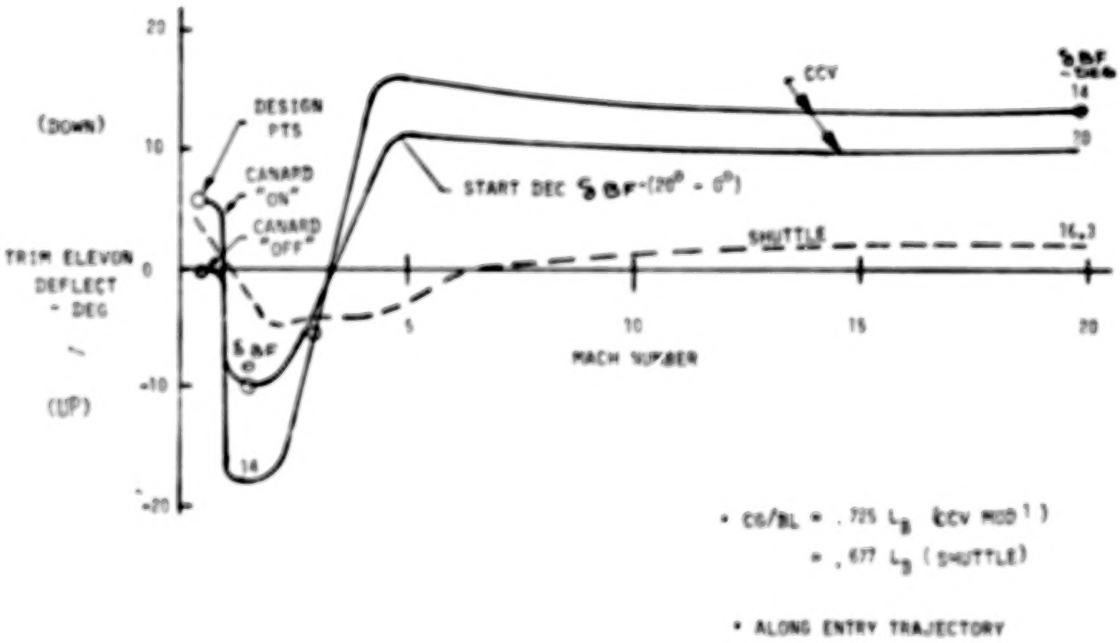

Figure 11 Shuttle - CCV Static Trim Elevon Requirements

Hypersonic Trim and Stability Comparisons.-Hypersonic trim is a major design consideration as already indicated from previous figures. For the "baseline" CCV configuration down elevons exceed ten degrees for c.g. locations aft of 0.70 of body length (see figure 12 .) For "Mod 1 configuration with increased body flap and elevon size, the c.g. location for ten degree down elevon moves aft to 0.715 L_B, thus reducing ballast penalties (i.e. c.g./L_B = .01 requires ballast $\approx$ 6000 lb). The "conventional" design with large wing size 836.1m^2 (9000 ft^2) is trimmable to about 0.72 L_B with ten degree of down elevon. Further aft movement in c.g. location is possible by aerodynamic shape changes in the configuration. Such changes are illustrated in the technology assessment of Task IV.

Hypersonic Temperature/Elevon Deflection Trade.-This trade is a major driver in evaluating the impact of CCV design on performance/payload gains. As the elevon is deflected to down positions for trim, the lower elevon surface is subjected to increasingly more severe heating environments. Entry temperatures quickly climb to temperatures above 1367K (2000°F) and come close to exceeding TPS material limits for down deflection greater than about five degrees (See figure 13 . By superimposing c.g. locations for trimmed down elevon deflections on these plots, limits on aft c.g. locations due the high temperatures are established. A slight relief with increased wing size of the conventional design is apparent (due mainly to a higher equilibrium glide entry trajectory). Some of these limitations can be eased by changes in the hypersonic aerodynamic configuration as illustrated in Task IV with Mod 2 configuration.

Flight Control

A major task of this study was to determine and assess the penalties associated with incorporation of CCV concepts. The flight control part of the study concentrated on a single, conventionally shaped vehicle configuration with variations in center of gravity location (static stability) and elevon size. In this context, redundancy considerations frequently associated with CCV design was not an issue. All of the control

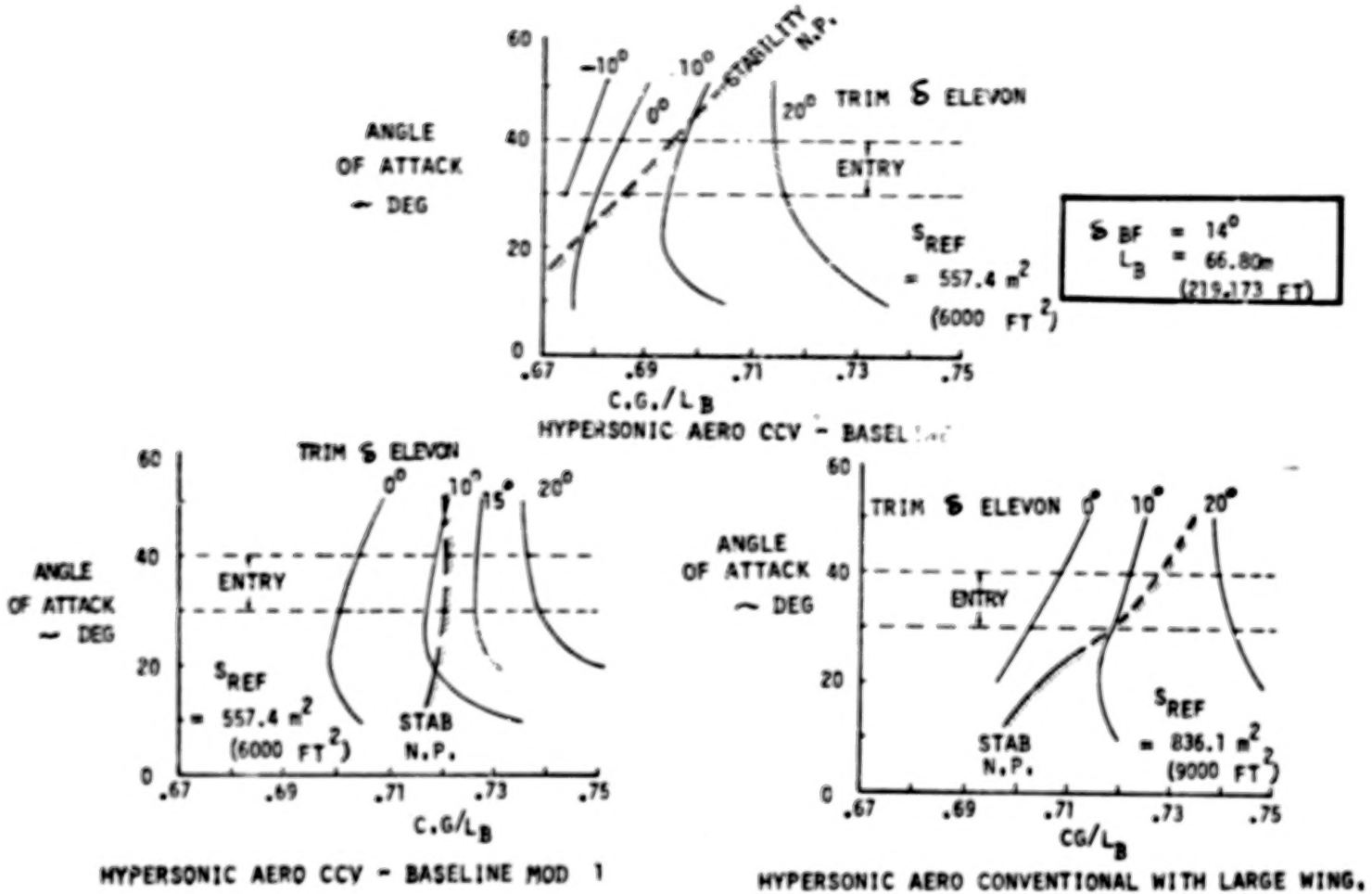

Figure 12 Hypersonic Trim and Stability for Various Configurations

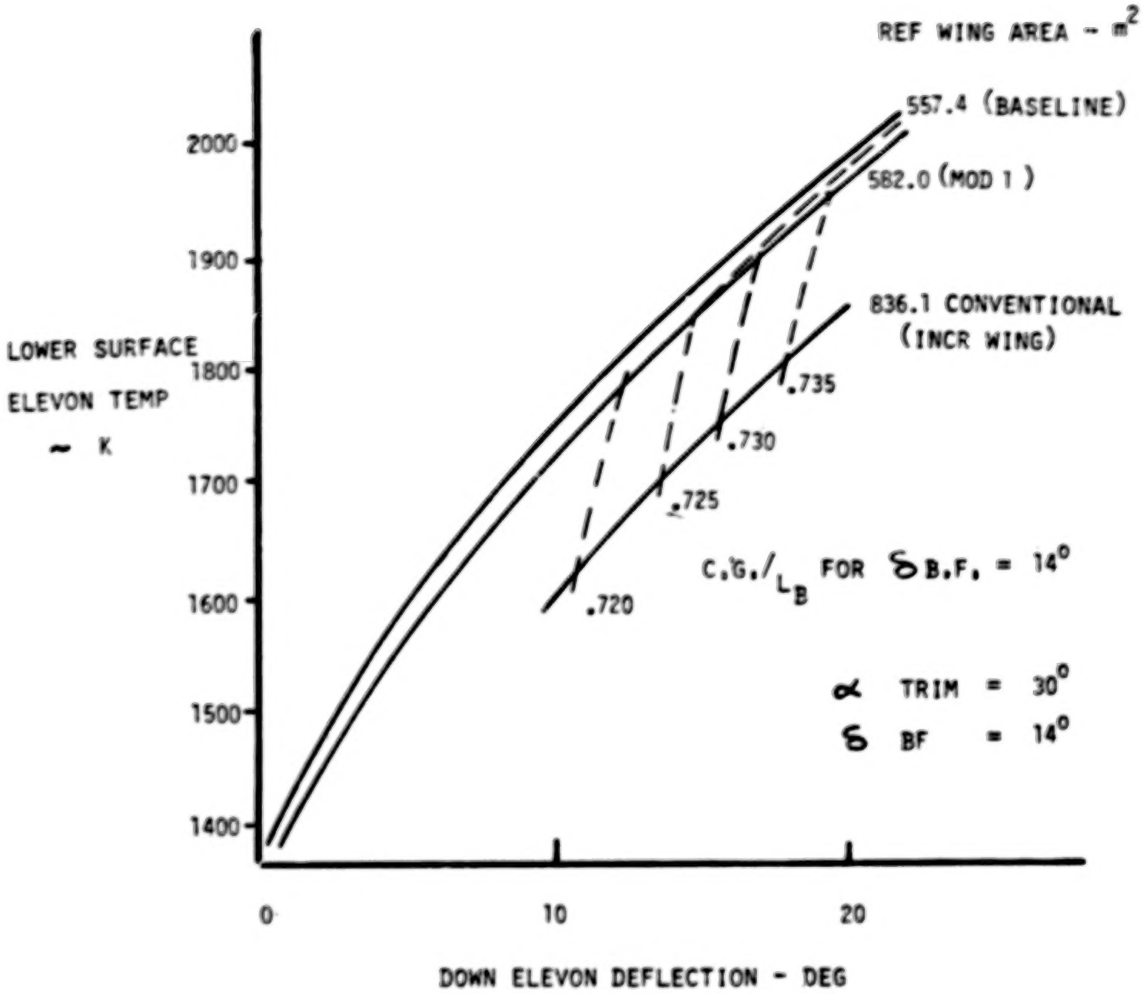

Figure 13 Hypersonic Temperature - Elevon Deflection Trade

surfaces depend on power operation, so even the conventionally designed vehicle requires redundancy sufficient to assure completely reliable operation. The only difference here between CCV and conventional design is the allowable degradation resulting from partial failures. It was felt that this would not result in significant weight difference, and in any case, this level of detail was beyond the scope of the present study. Redundant sensors and computers required for CCV reliability represent an insignificant weight increment on a vehicle of the size considered in this study.

The penalties for a CCV design that are associated with the flight control dynamics are related to the hinge moment and rate requirements generated by the unstable vehicle. These requirements determine the actuator size, hydraulic tubing size and the horsepower required of the hydraulic supply system.

Control surface actuation requirements depend on the autopilot design and the maneuvers and disturbances, as well as on the basic airframe stability. In selecting the autopilot gains for the several configuration variations, a number of handling quality criteria were considered and were rejected in favor of the Shuttle response time history envelopes (item 26 of table 2). It was felt that this approach would emphasize the dependence of the actuation requirements on the configuration.

The autopilot gains for each configuration variation were tuned to produce transient responses to the maneuver commands that were as nearly identical (for normal acceleration and roll angle) as possible. This was needed to make the variation in actuation requirements meaningful. In order to find the effect of configuration modifications on the control actuation requirements, a discreet maneuver at one flight condition was simulated for each variation. A simultaneous 0.5g pullup and 30 degree roll and stop was selected for the maneuver. The control surface deflections, rates and hinge moments were compared with each other and with the results of the same simulated maneuver performed by the Shuttle. The comparison with the Shuttle provided the basis for estimating the actuation system and hydraulic power supply weights for the configurations studied herein.

Ideally, each configuration modification would have been flown over a complete trajectory and the actuation requirements derived from the results. However, this could not be adequately done within the scope of this study. Instead, four fixed point flight conditions were selected for study. They were:

1. Entry: $M = 20$, $h = 67$ km (220,000 ft.), $\alpha = 30^0$
2. Supersonic: $M = 2.86$, $h = 27.4$ km (90,000 ft), $\alpha = 13^0$
3. Transonic: $M = 1.2$, $h = 16.8$ km (55,000 ft), $\alpha = 10^0$
4. Subsonic: $M = 0.3$, h = sea level, $\alpha = 7^0$ to 12^0 function of c.g. and configuration

The entry condition dynamics are dominated by the reaction control forces and moments. The Space Shuttle entry control system was used directly. It was taken from item 26 of table 2 and it is shown in appendix B. The reaction jet forces were scaled using the appropriate lever arm and moment of inertia ratios to give the same angular accelerations on the CCV as on the Shuttle. As shown in figure 19 , this results in nearly identical transients, independent of the static stability. As a result, this flight condition is of little interest to the CCV comparison problem.

Good transient responses may be somewhat difficult to attain in pitch in the transonic region and in yaw-roll in the supersonic. However, it is expected that the requirements in these regions can be, to some extent, tailored to the capabilities of the vehicle. In the subsonic landing condition, on the other hand, the response requirements are expected to be rather rigidly fixed by the landing maneuver. Therefore, most of the control system analysis was done at the landing condition. Rather simple autopilots proved to be adequate for this flight condition. The Space Shuttle autopilot configurations were used for the transonic and supersonic cases. Only the MOD 1 vehicle with the c.g. at 73.5 percent was simulated at these two flight conditions. The objective being simply to show that adequate responses were attainable. The Shuttle autopilot gains had to be changed to produce good responses with the MOD 1 vehicle. The autopilots used are shown in appendix B, which were taken from item 30 of table 2 and modified.

Dynamic Analysis - Subsonic.-The NASA baseline configuration has rather conventional dynamics. It is stable and well damped in both pitch and yaw-roll. As successive changes are made, i.e. added canard, successive rearward c.g. shifts and added elevon area, the vehicle becomes progressively less stable. This is illustrated in figure 14 which shows the static stability variation in both pitch and yaw as a function of c.g. for both the baseline and the Mod 1 configurations.

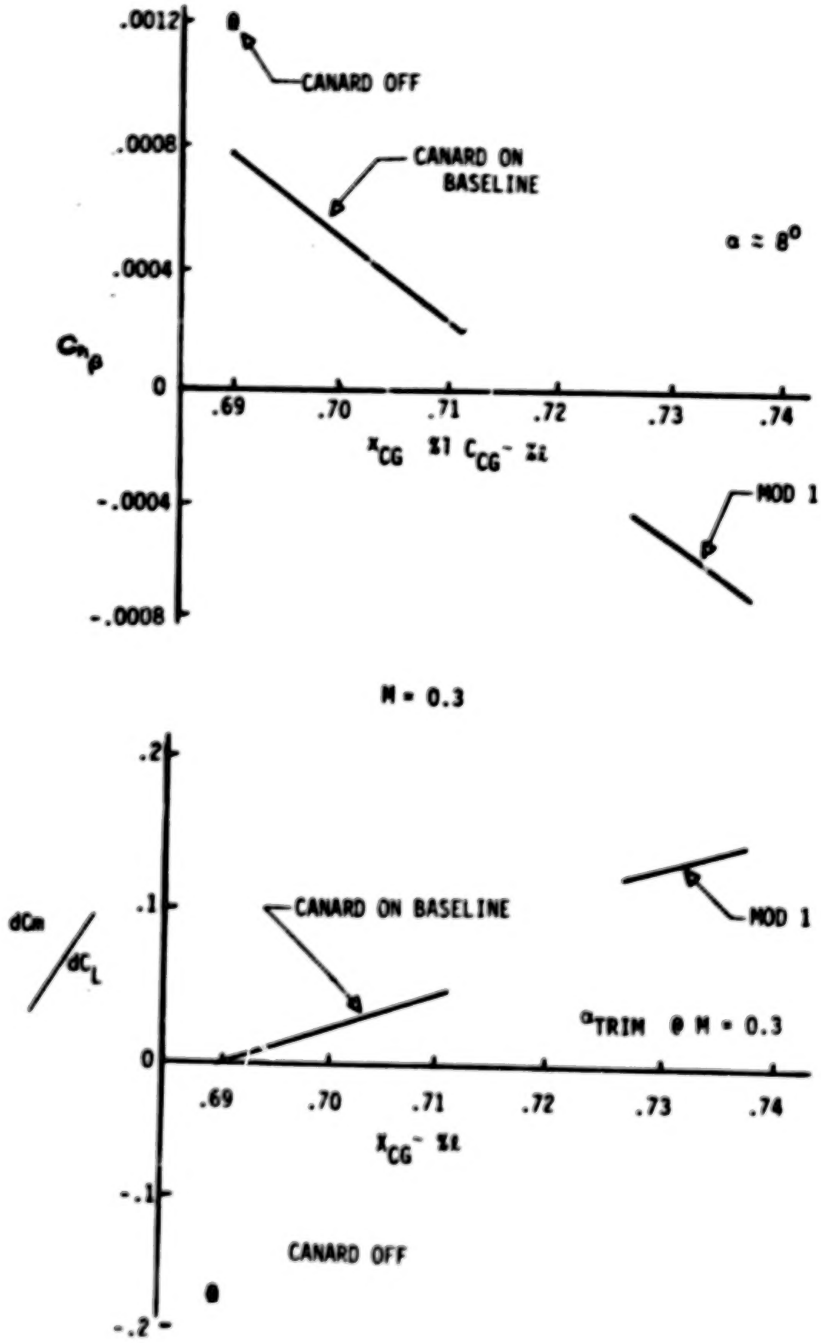

Figure 14 Static Stability in Pitch and Yaw

The static margin does not follow the expected linear variation with center of gravity because of significant nonlinearity in the basic aero data $C_{m_{.69}}$ vs. α (See figure 15). The data shows an increase in static stability between 6 and 12 degrees angle of attack. The Mod 1 vehicle trim at about 7° while the baseline vehicles trim near 8.5^{o}. Therefore, the change in static margin, in going from baseline to Mod 1 configuration is the sum of the effects of configuration change (stabilizing) center of gravity change (destabilizing) and trim angle of attack (destabilizing).

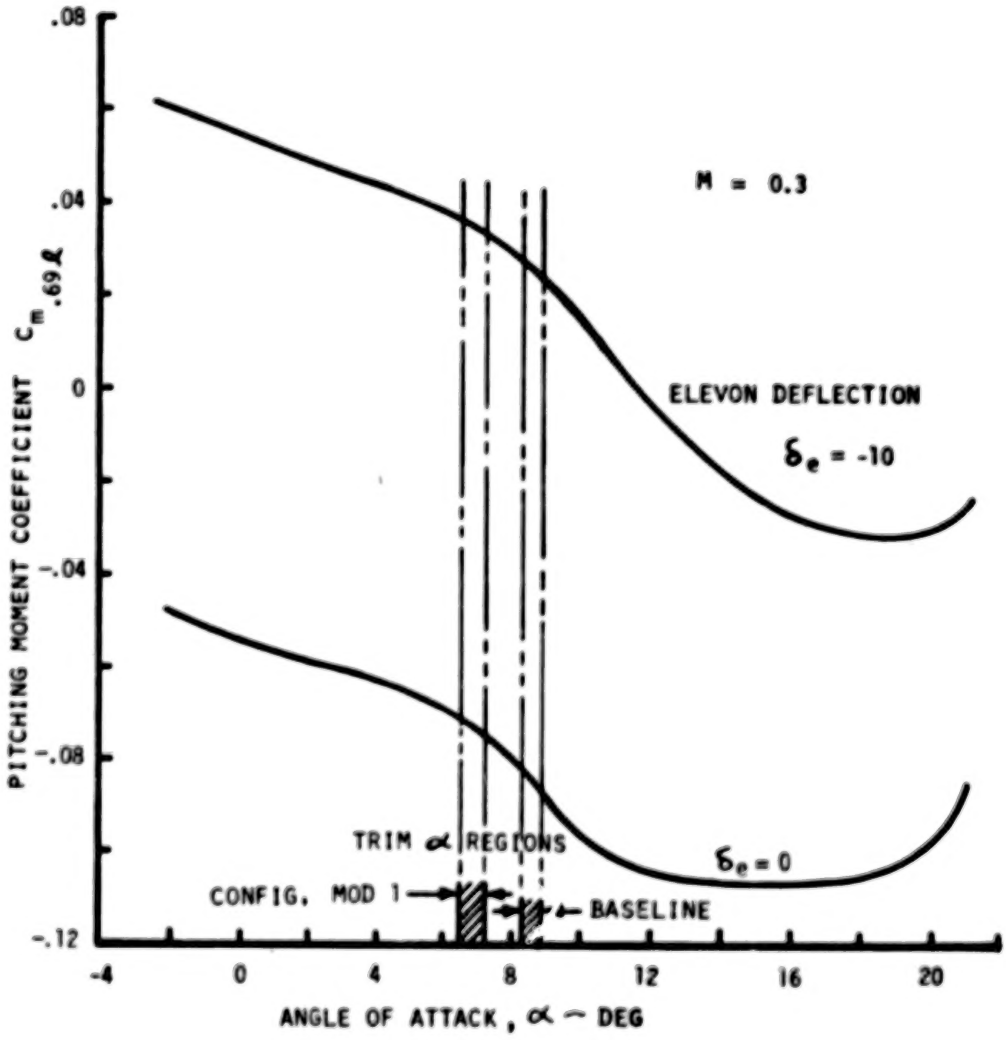

Figure 15 Subsonic Pitching Moments

The following mass properties, representative of the entry condition, have been used for all of the dynamic analyses.

$$I_{xx} = 16.27 \times 10^6 \quad kg\text{-}m^2$$
$$I_{yy} = 65.08 \times 10^6 \quad kg\text{-}m^2$$
$$I_{zz} = 73.21 \times 10^6 \quad kg\text{-}m^2$$
$$Mass = .1901 \times 10^6 \quad kg$$

These static stabilities result in vehicle dynamics that can be shown by the pole locations of the characteristic equations. These pole locations are shown in figure 16 for pitch and figure 17 for yaw-roll.

The pitch short period for the NASA baseline without canard is seen to be dynamically stable, with conventional short period and plugoid. Addition of the canard results in aperiodic real roots, with one being unstable. Aft movement of the center of gravity causes the appearance of a pole configuration that gives rise to the "third mode" oscillation in which all three (pitch) degrees of freedom are significantly and all three diverge due to the unstable root.

Meeting the response criteria requires that the frequency be increased from the low values in figure 16 to about 4 radians per second. The poles for the yaw-roll motion show an interesting change as the instability increases from the baseline to the Mod 1 configuration. Instead of the conventional complex pair representing the dutch roll and the two real roots that characterize the roll and spiral motions, there are now two complex pairs. This is the so called lateral phugoid (see item 30, table 2). These pole locations result in slow, large amplitude oscillations.

The pitch and yaw-roll autopilots are shown in appendix B. The set of gains finally selected for the simulations are given in table 3. Root locus techniques were used iteratively with simulations in order to arrive at this set of gains. The goal was not only to find a set of gains for each configuration that gave responses within the shuttle envelope, but to match the responses of all five of the configuration variations.

An example of the root locus plotting, gain selection and simulation is shown in appendix B. This represents one of the earlier iterations. The procedure was followed for each configuration variation and was gone through several times to arrive at the gains in table 3. The resulting transient responses are shown and discussed in the following sections.

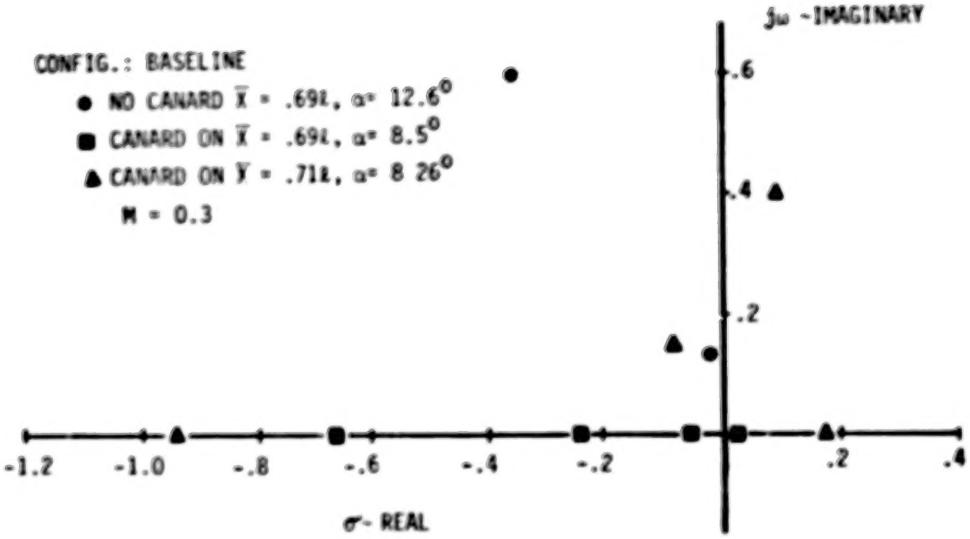

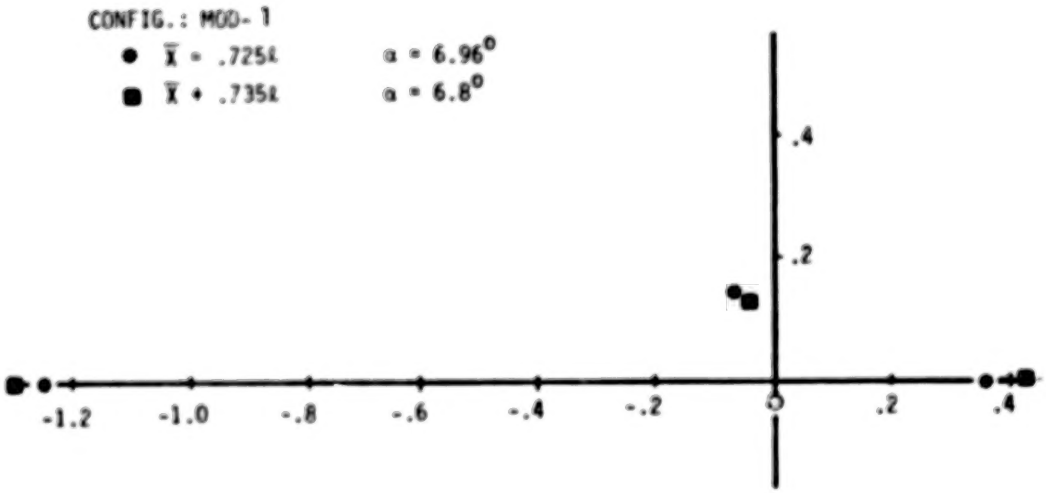

Figure 16 Pitch Axis Roots - Free Airplane M = 0.3

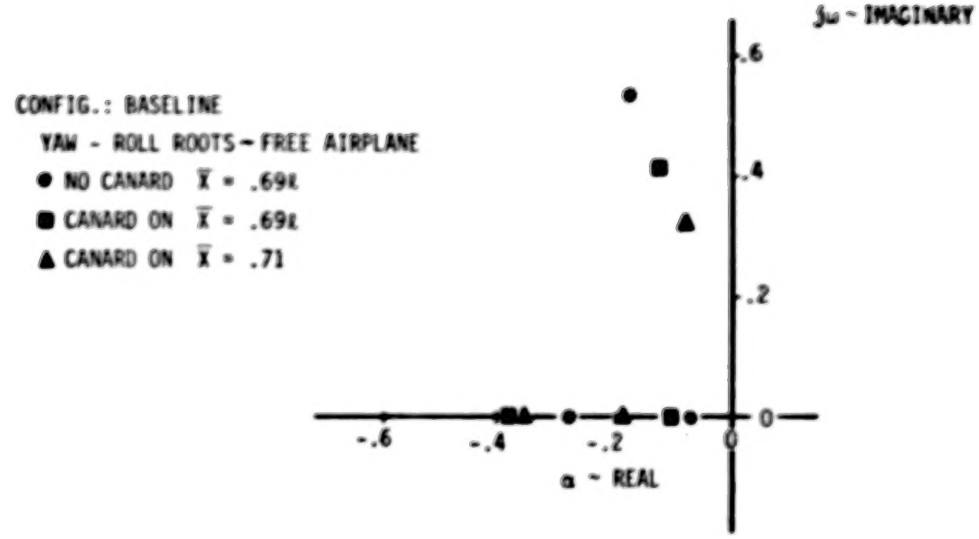

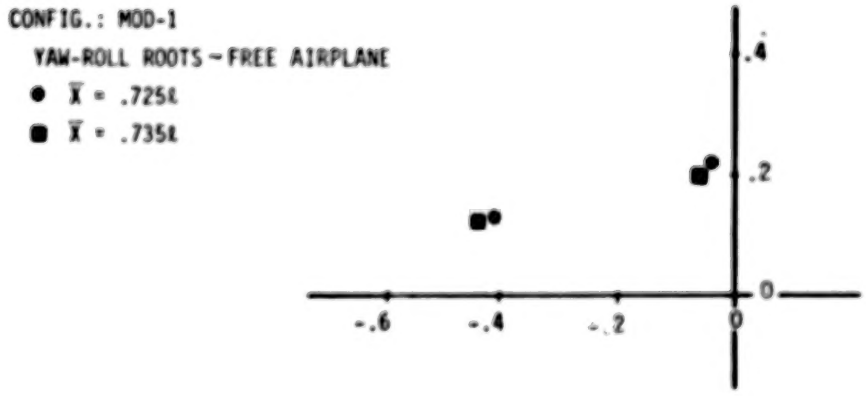

Figure 17 Yaw - Roll - Free Airplane M = 0.3

Table 3 Selected A/P Gains (Subsonic)

	K_e C1-MAE	K_q -GKFGAQ	K_I GKIGBZ	K_a C1-MAA	K_{Pa} -C3-MCDA	K_{yr} -C3-MCDR	K_r C1-MAR
					$K_{rr} = 1$		
NASA Baseline (Canard Retracted)	.7	3	.6	1.4	1	2	24
Canard $\bar{X}$ = .69	.5	3	.4	1.4	1	2	24
	.6	3	.6				
Canard $\bar{X}$ = .71	.5	3	.3	2	1	2	16
	.6	4	.6				
Mod 1 $\bar{X}$ = .723	.45	4	.6	2.4	.6	2	24
				1	1	8	6
Mod 1 $\bar{X}$ = .735	.45	.4	.6	2.4	.6	2	24

▷ Names used in Block Disgram of Appendix

▷ Names used in EASY Program

Transonic and Supersonic. The forms of the Space Shuttle autopilots for these two flight regimes were used as given in item 29 of table 2. Only one configuration, Mod 1 with the C.G. at 73.5 percent was analysed at these two flight conditions. The autopilot gains given in item 29 would not fly this configuration. Enough root locus analysis was done to select gains that produced stable responses that were reasonably close to fitting the Shuttle requirements envelopes. The transient responses are discussed in the section "Simulation and Results".

Hypersonic.-The principal problem at hypersonic speeds was pitch trim, as discussed previously in the section "Aerodynamics and Performance". The autopilot design was taken from item 30 of table 2. In order to match the shuttle responses in yaw and roll, the reaction control thrust was scaled up to produce the same angular acceleration on the CCV designs as on the shuttle. The relationship is:

$$T_{ccv} = \frac{(I/\ell)_{ccv}}{(I/\ell)_{shuttle}} \quad T_{shuttle}$$

Where I is the appropriate moment of inertia, ℓ is the lever arm and T the thrust. Flight control block diagrams used for the simulations are given in appendix B.

In the pitch axis, both the shuttle and the CCV configurations examined were near neutral stability at the trim angle of attack. As a result, the shuttle autopilot gains produced acceptable responses in the pitch axis also. However, the CCV requires substantial down elevon to trim which left insufficient control for maneuver. Early hypersonic simulation showed instabilities which were caused by the elevon hitting the stops. When the maximum down elevon was increased to 30 degrees, the problem was solved.

Simulation and Results.-In this section the transient response simulations are shown along with the resulting control deflections, rates and power requirements.

Comparison of Subsonic Transient Response for Various Vehicles.-Normal acceleration and roll responses are shown for various vehicles at a subsonic flight condition and a range of c.g. locations in figure 18.

The similarity of the responses shows that within the range of parameters of this study, the response can be made essentially independent of the free airframe stability.

The development of the autopilot gains used for these vehicles indicates that adequate gain margins can be maintained for vehicles of the type studied over the range of c.g.'s investigated.

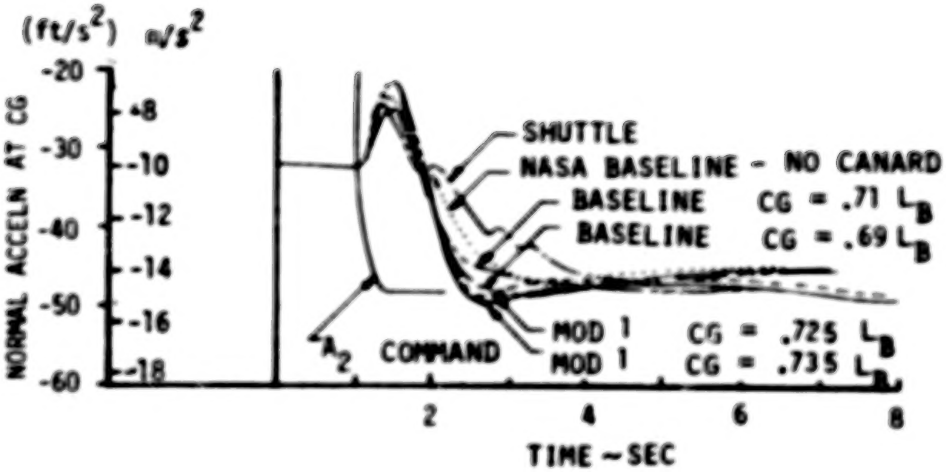

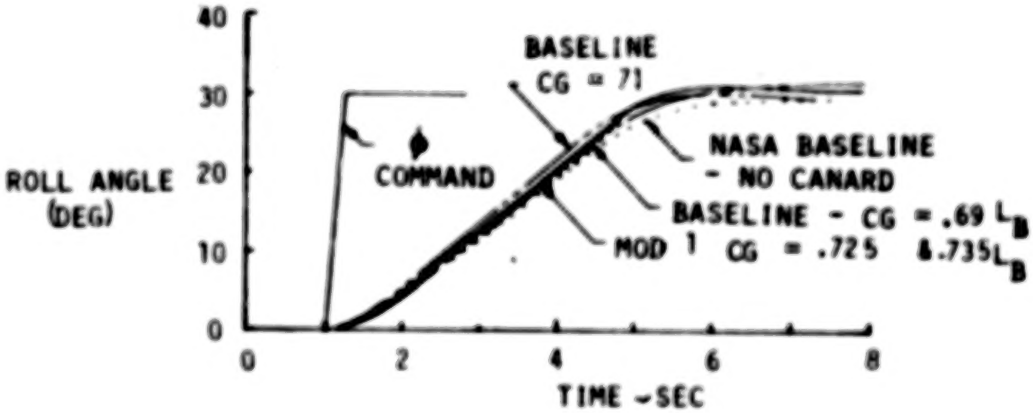

● TRIMMED FOR EQUILIBRIUM GLIDE.

INITIAL m = 0.3, $\alpha = 7^0 - 12^0$

Figure 18 Comparison of Subsonic Transient Responses for Various Vehicles

Comparison of Hypersonic Transient Responses for Various Vehicles.-Angle of attack and roll responses are shown for various vehicles at a hypersonic flight condition and a range of c.g. locations in figure 19 .

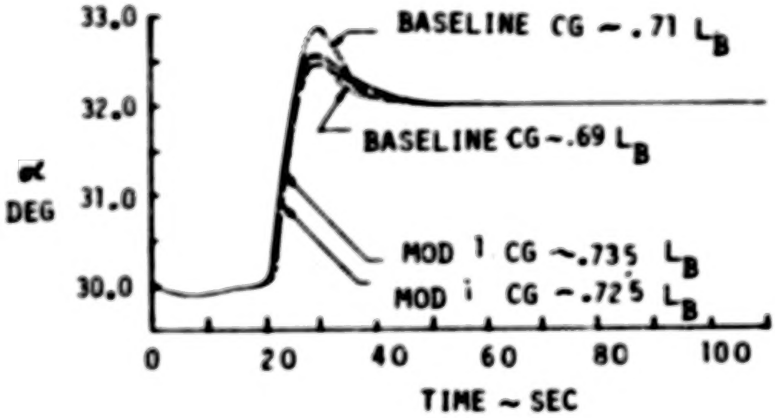

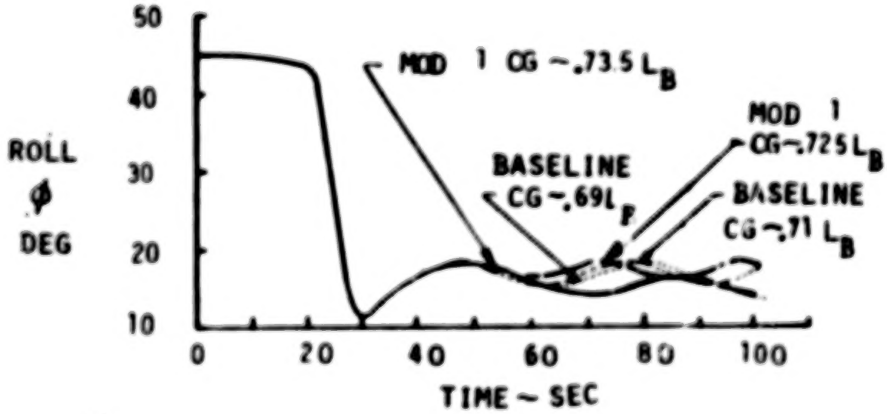

INITIAL M = 20, $\alpha = 30^0$

Figure 19 Comparison of Hypersonic Transient Response for Various Vehicles

These responses were obtained by using the shuttle autopilot configuration and gains. The reaction control thrust was scaled up from the shuttle by the ratio of the moments of inertia. The similarity of the responses exists because in this flight regime, thruster and inertia characteristics are more significant than the differences in aerodynamics between the configurations.

Pitch Response at Design Points.-CCV Mod-1 (c.g. 0.735 L_B).-The responses of the CCV Mod-1, to pitch axis commands are shown in figure 20 at each of the four design points. Shuttle response requirement envelopes are shown for comparison. Considering that the CCV moment of inertia is eight times that of the shuttle, and the CCV is over three times as unstable, the responses compare quite well with the shuttle requirements.

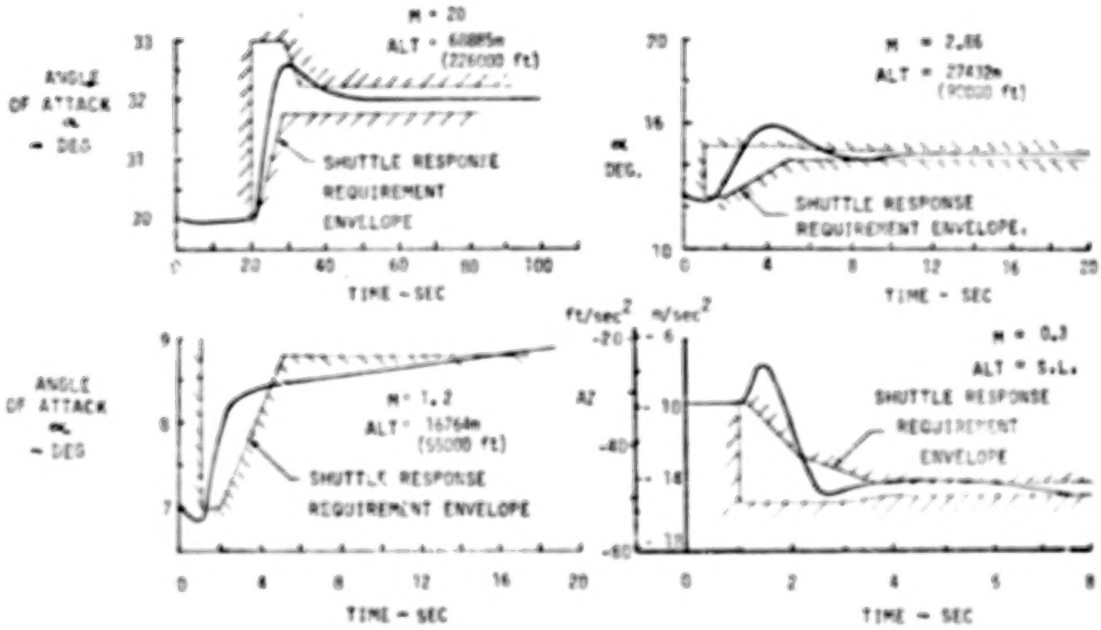

Initial Conditions Trimmed

Figure 20 Pitch Response at Design Points Mod 1 (c.g. = .735 L_B)

Roll Response at Design Points CCV Mod-1 (c.g. = 0.735 L_B) - The responses of the CCV Mod-1, to roll commands are shown at each of the four design points in figure 21 . Shuttle response requirement envelopes are shown for comparison. The CCV moment of inertia in roll is over sixteen times that of the shuttle. The responses obtained compare reasonably well with the shuttle requirements, showing that adequately fast and well damped dynamic responses can be maintained at all flight conditions.

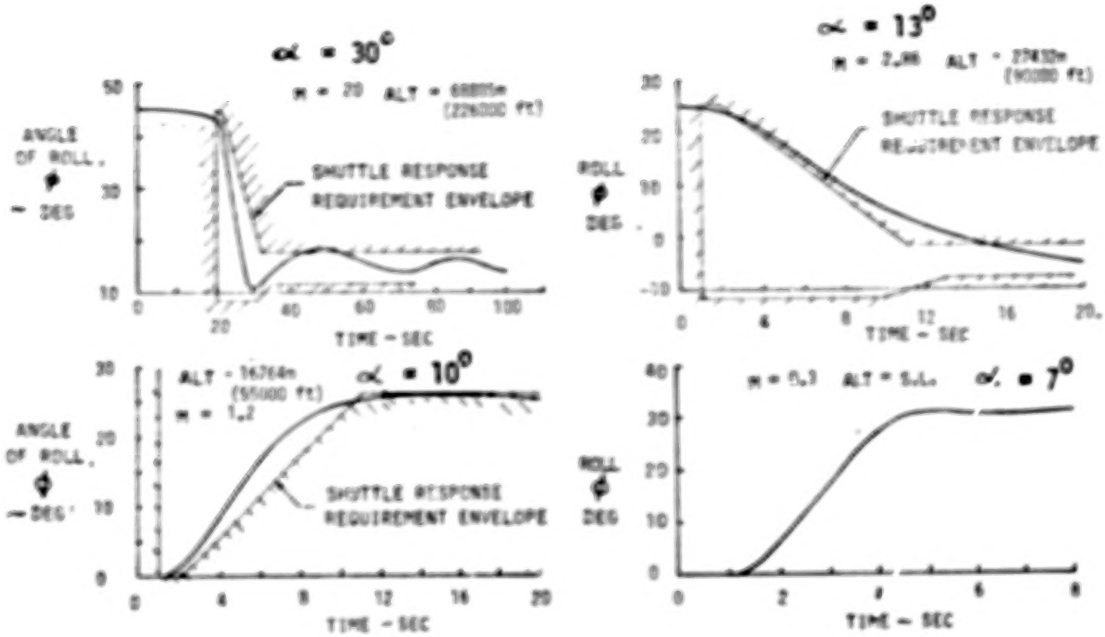

Mod 1 (c.g. = .735 L_B)

Figure 21 Roll Response at Design Points

Transient Response Comparisons, Shuttle and CCV Mod-1 - Direct comparisons of CCV Mod-1 (c.g. = 0.735 L_B) and Shuttle (c.g. = 0.675 L_B) responses are shown in figure 22 for subsonic and hypersonic flight conditions. For the subsonic case, a 0.5g pitch-up command and a 30 degrees roll command are applied simultaneously at t = 1 sec. The CCV response is somewhat faster in pitch and essentially the same in roll as the shuttle. In hypersonic case the command is a 60 degrees roll reversal. The responses are shown to be essentially the same for the two vehicles.

Transient Response Mod-1 (c.g. = 0.735 L_B) Subsonic.-A time history of responses to simultaneous 0.5g pitch up and 30 degree roll commands is shown for a subsonic flight condition in figure 23 All the variables are seen to be well-behaved. Angle of attack increases after the initial transient because the vehicle is slowing down markedly and the control system is calling for a constant normal acceleration. A command of this size would not be held for so long a time under real conditions.

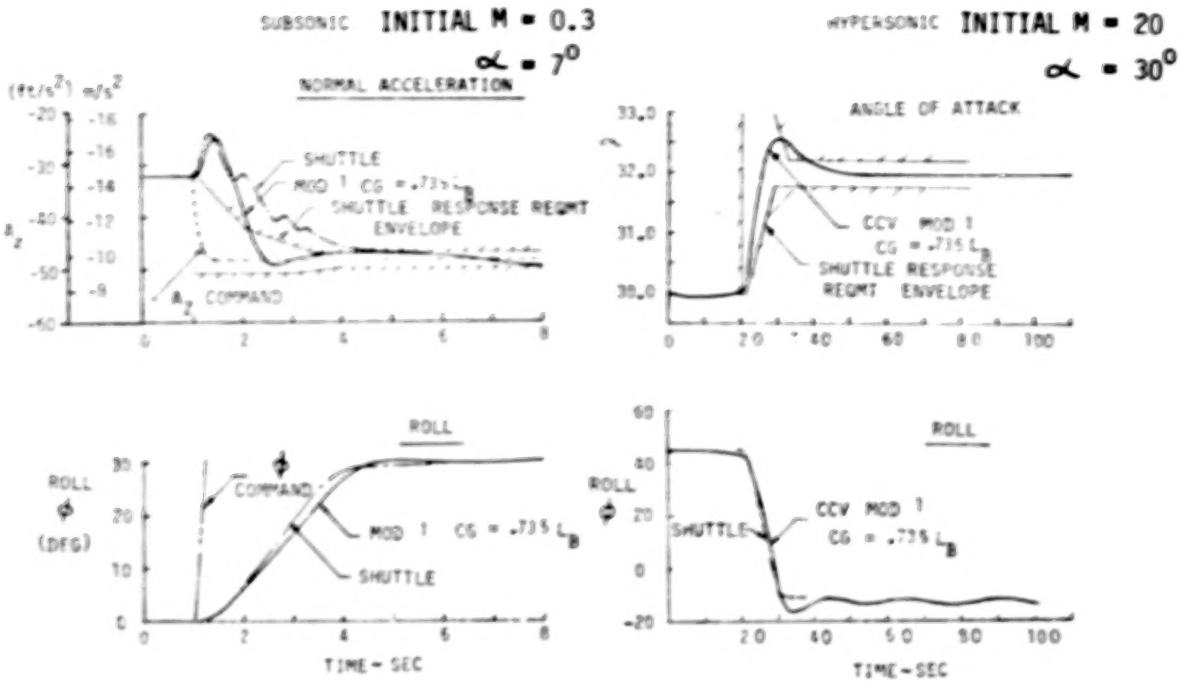

Shuttle and CCV Mod 1 (c.g. = 735 L_B)

Figure 22 Transient Response Comparisons

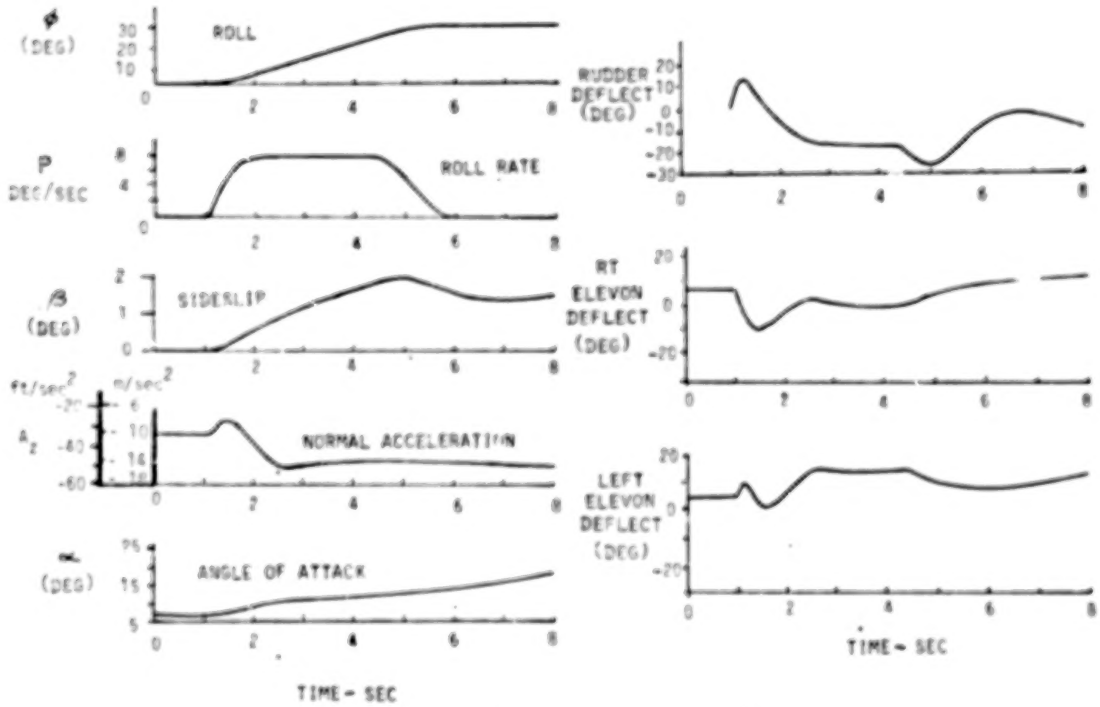

INITIAL M = 0.3 α = 7°

Figure 23 Transient Responses - Mod 1 (C.G. = .735 L_B) Subsonic

Transient Response Mod 1 (c.g. = 0.735 L_B) Hypersonic.-A time history of the responses to separate, two degree angle of attack and 30 degree roll, commands at a hypersonic flight condition is shown in figure 24 . The variables are seen to be well-behaved. The positive elevon deflection is seen to be a result of trim requirements rather than the maneuver. The largest elevon excursion from trim is about eight degrees for the combined pitch and roll maneuver.

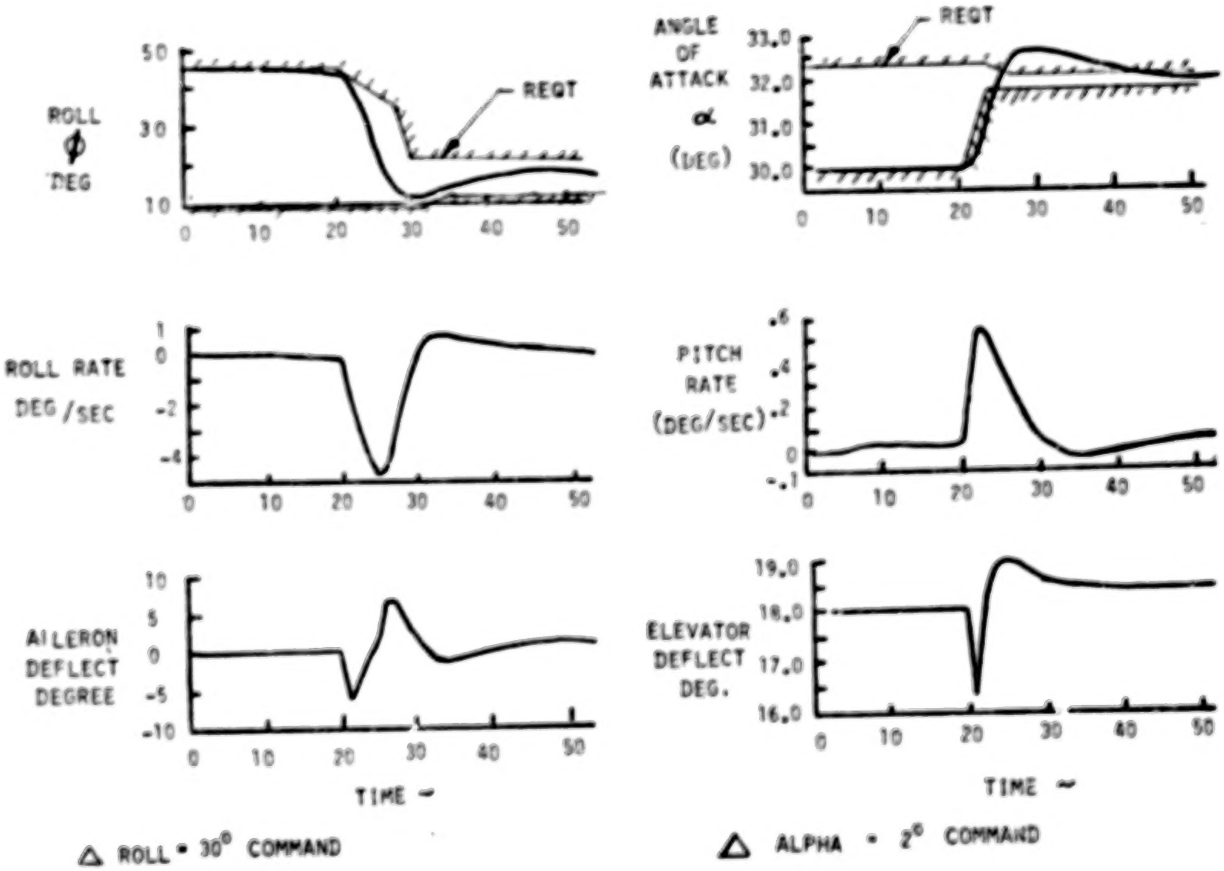

INITIAL M = 20 α = 30°

Figure 24 Transient Responses Mod 1 (C.G. = .735 L_B) - Hypersonic

Configuration Design

A number of design arrangement considerations are involved in the configuration development within the outline dimensions and lines provided by NASA LARC. Some of the more significant ones are discussed as well as the factors involved in the particular arrangement selection. These primary arrangement considerations include main engine arrangement and location, propellant tankage and feed lines, payload bay, landing gear and the crew cab. In addition, two configuration trade studies are presented. These are the LOX tank forward vs. aft trade study and the body cross section trade study.

Baseline, Modification 1, Conventional Main Engine Arrangements and Locations.-The Baseline, Conventional and Modification 1 (Mod 1) main engine arrangements and locations are the same. Six main engines are utilized; three are fixed 40:1 expansion ratio engines and three are two position nozzle engines, 50:1 expansion ratio in the first position and 150:1 expansion ratios in the second position. These engines are extrapolations of the current SSME LOX-Hydrogen engine and are projected to use 27579 K Pa (4000 psi) combustion chamber pressures. Two sources are utilized for the physical characteristics including weight of these engines. These sources are reference (2) and (3). These engines have a mass flow of approximately 900 kg/sec (1985 lb/sec.) requiring .457 m (18 in.) dia. feed lines for both LOX and hydrogen. This in turn establishes a minimum distance of 2.03 m (80 inches) between tank ends and the engine attach faces for bends, turning vanes, and flex sections. The power head diameter is 2.89 m (114 inches), and the nozzle maximum diameters are 2.34 m (92 inches) and 4.39 m (173 inches) for the fixed and two-position nozzles respectively. Small thrust variation of 10% did not change these requirements. Gimbal angle capability of $\pm 10^{0}$ in both axes is provided. Specific performance requirements may alter this requirement.

The nozzle thrust plane location is established by the necessity to protect the nozzles during entry with the body flap when the vehicle is at an angle of attack of 40^{0}. During entry, the engines are parked tilted up to their maximum limit. The engine arrangement is configured to provide the

necessary C.G. tracking capability during ascent. The baseline most aft ascent C.G. is assumed to be approximately 80% body length, or on the order of 6% to 10% further aft than the entry C.G.

Baseline, Modification I and Conventional (LOX Tank Aft) Propellant Tanks and Plumbing.-The propellant tanks and their provisions dominate the configuration of this class of vehicles. In that their surface and configuration are the most significant factors on vehicle weight, it is mandatory that this be multifunction to the maximum extent possible to achieve the mass fractions necessary for single stage vehicles. This results in the vehicle configuration being shaped by the tanks and the necessary fairings and attachments for the other subsystems.

The thrust structure incorporates composites in a waffle grid arrangement to which the vertical fin, the aft wing carry through structure, the main engines and the LOX tank attach. The aft hemispherical end of the tank is integrated into the forward face of the thrust structure. The forward hemispherical end of the LOX tank, the aft hemispherical end of the hydrogen tank and the intertank structure are an integrated structure providing multifunction support for the tanks, payload bay, and landing gear. The hydrogen tank external surface is shaped to provide the vehicle external lines with indentations for the nose gear well, crew cab, and payload bay.

The main hydrogen tank manifold is a jacketed 1.14 m (45 in.) diameter line which goes through the LOX tank on the centerline to a sprinkler head located within the thrust structure. From this sprinkler head, .457 m (18 in.) diameter lines go to each engine. The .457 m (18 in.) diameter LOX lines project straight aft from the LOX tank to the individual engines. This provides the simplest and most straight forward plumbing system. Not shown are the fill and vent plumbing systems which would be arranged to fill and vent the tanks when the vehicle is in the erected position.

Baseline and Modification I and Conventional (LOX Tank Aft) Payload Bay.-The 4.57 m (15 ft.) diameter by 18.29 m (60 ft.) long payload bay which is identical to the shuttle, is located approximately as it is on the shuttle i.e.,

one third of its length aft of the estimated C.G. It is half submerged in the hydrogen and LOX tanks. This provides good access to the bay while permitting full door opening without complex hinges or attachments.

Baseline, Modification I and Conventional Crew Cab.-The crew cab is located immediately forward of the payload bay. This provides the capability for payload bay access if required. Vertical height above the body upper surface is defined by approach attitude, approximately 12°, for forward vision, and entry hypersonic angle of attack, 15° to 30°, for shielding from heating. The required volume, approximately 33 m^3 (1130 $ft.^3$), has a length of 5.59m (220 ins.) by 5.08m (200 in.) wide by 2.29m (90 ins.) high. The crew cab envelope and outline requirements were established during the reference (1) studies.

Baseline, Modification I and Conventional Landing Gear.-The landing gear locations are positioned by three constraints. The first is that good practice positions the landing gear so that at rest the nose gear carries between 5% and 10% of the weight of the vehicle. The second constraint is that at the maximum landing angle of attack, approximately 16° at touchdown, tail scrape will not occur. The last provides that a 0.5g turn will not overturn the vehicle or overload the outboard wheels and tires. This results in a wheelbase of 34.92m (1375 inches) and a track of 19.10m (752 inches), with strut lengths of 3.05m (120 inches) for the nose gear and 15.08m (200 inches) for the main gear for the baseline vehicle.

Configuration Trade Studies.-Two trade studies were developed in sufficient depth to justify separate discussion. The summary results of these studies will be shown below.

LOX Tank Location.-The LOX tank and the LOX represent two of the larger mass elements of the configuration. In an effort to move the C.G. forward, particularly for the entry configuration, a configuration with the LOX tank forward, hydrogen aft, was developed in sufficient depth to permit assessment of this change on the vehicle. Figure 4 illustrates this arrangement.

Several factors were identified:

(a) The entry C.G. did move forward approximately 2.4% body length. However, the launch C.G. moved forward approximately 37%. Thus, the biggest impact would be on ascent with an excessively stable vehicle.

(b) The vehicle dry weight increased a little over 9% with much of this increase aft of the C.G. This weight was associated with the increase in the hydrogen tank weights necessary to support the LOX mass.

Figure 25 illustrates the basic tank unit weights with LOX forward and figure 26 illustrates the basic tank unit weights with LOX aft. A comparison of figures 25 and 26 reveals that not only does the placement of the LOX tank aft rather than forward of the LH tank save weight in the LH tank, but it

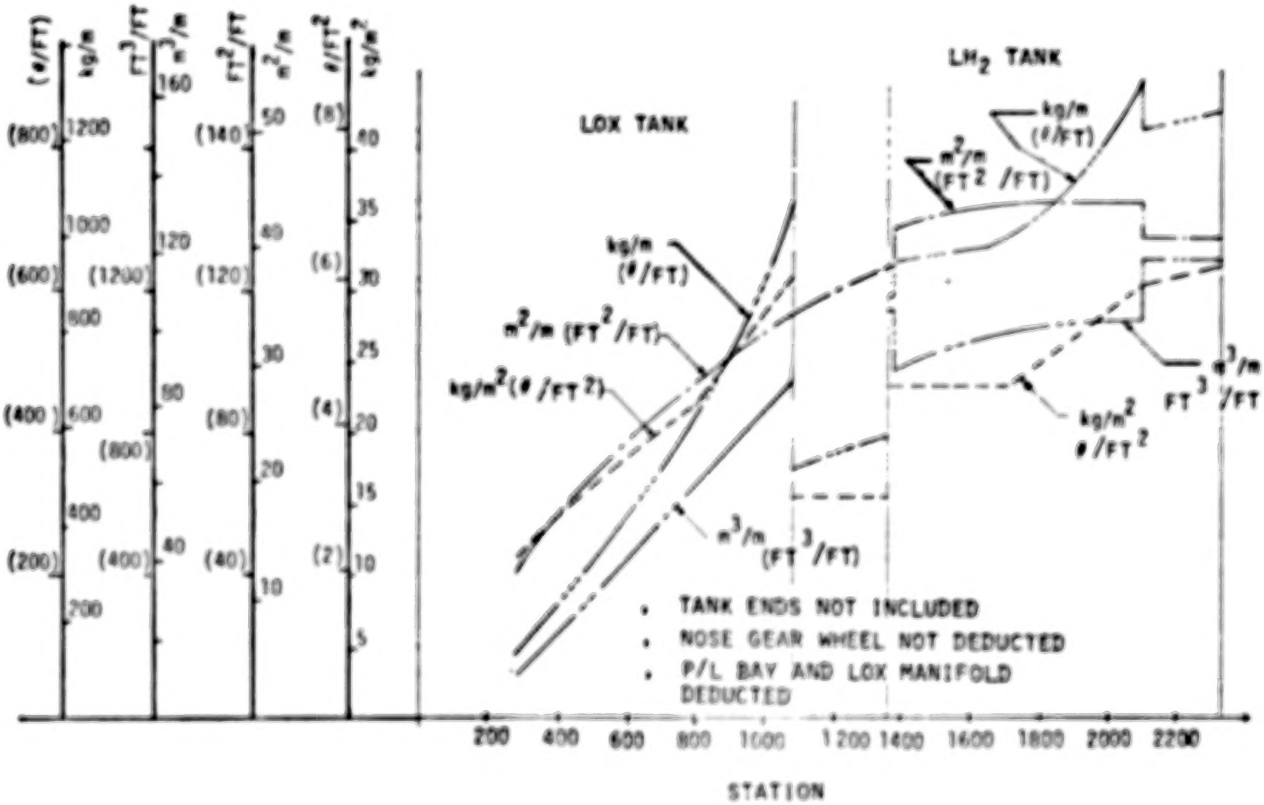

Figure 25 Conventional Tankage - LO_2 Forward

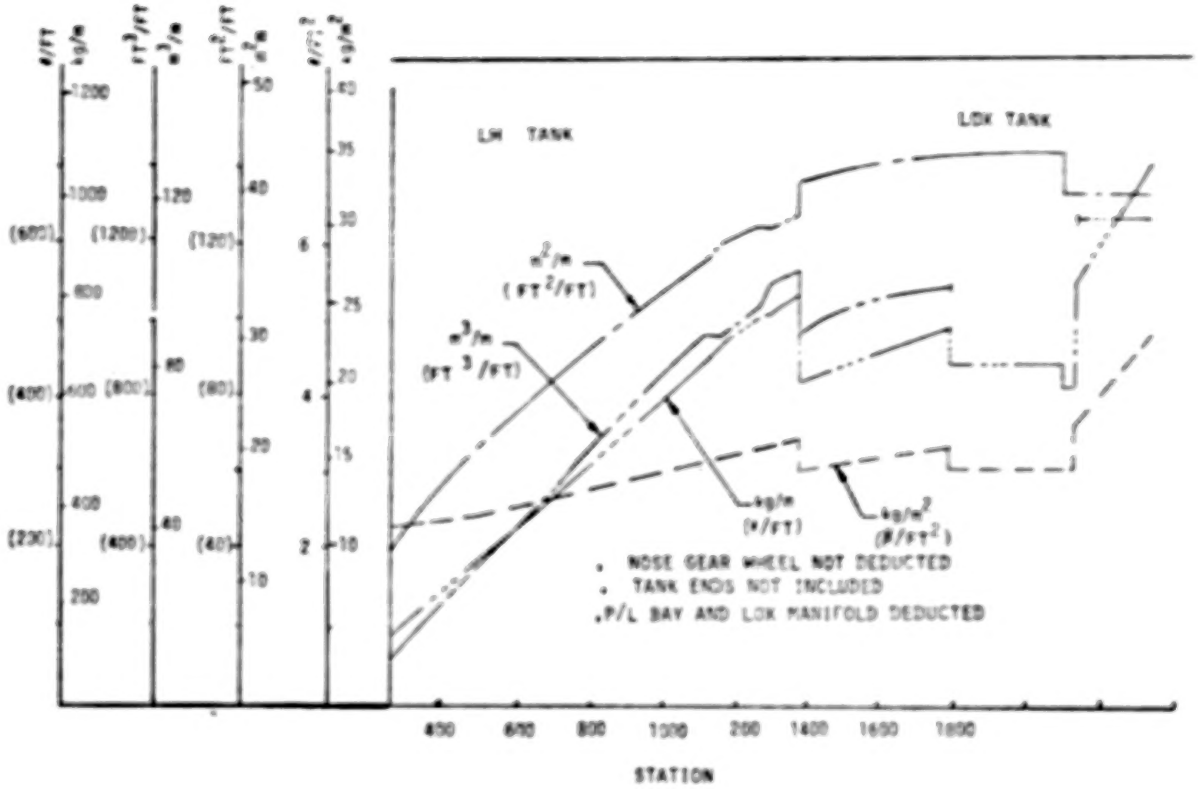

Figure 26 Conventional Tankage - LO_2 Aft

also provides a lighter LOX tank because of greater efficiency in both weight per unit area, but also in weight per volume. The aft located LOX tank has the same volume as the forward located LOX tank in a shorter length and, therefore, is subjected to a proportionately lower tank head pressures. The effect of head pressures on LOX tank weight is shown in figure 27 . Table 4 is a comparison of the mass properties of the two configurations. The increase in the LOX tank forward propulsion and hydraulic systems is due to the increased line length from the inter-tank area to the thrust structure.

Body Cross-Section Shape.-The drawings of the body lines provided by NASA LARC showed a flat sided body as shown on figure 28 . The cylindrical sided section appeared to be more efficient because the flat sides cause bending stresses to be imposed on the common membrane stresses. The analysis was conducted for the LOX tank. As can be seen for equivalent cross section area (volume), the flat sided section is approximately 49% heavier at the lower pressure and 33% heavier at the higher pressure.

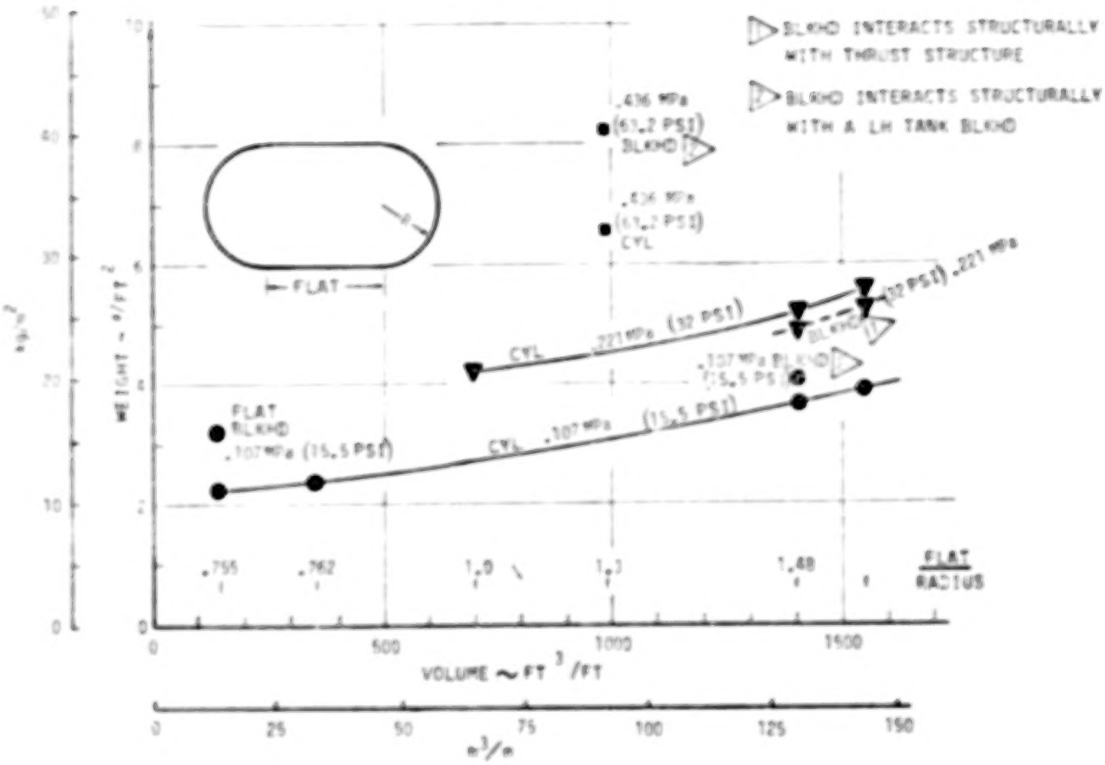

Figure 27 LO_2 Tank Unit Weights

Figure 28 shows the unit weights as a function of perimeter location and tabulates the results. Figure 27 shows the averaged unit weights as a function of internal tank press for the two configurations. In addition, the averaged unit weights for the bulkheads or tank ends are shown. These results indicate the weight efficiency of the cylindrical sided tanks over flat sided tanks. Figure 29 reflects these data for the cylindrical sided LOX tank design. This curve shows that weight increases slower than volume on a constant pressure curve. It also shows effect of pressure variation on weight. This data can be used to show that volumes being equal a short and large cross sectional area tank would be more weight efficient than a long and small cross sectional area tank when sized for typical boost pressure conditions.

Table 4 Mass Properties - Conventional - LO_2 Aft and LO_2 FWD -69% C.G.

CONVENTIONAL	LOX AFT			LOX FWD		
	WT - kg	STA		WT - kg	STA	
WING	17588	2255.9				
TAIL	1847	2664.6				
BODY	70681	1884.8		83765	1770.6	
INDUCED ENV. PROT.	13623	1845.8				
LANDING DOCKING & REC.	4994	1632		4994	1632	
PROPULSION	38540	2463.8		38711	2491.2	
PRIME POWER	464	1955				
ELECTRICAL	1391	1955				
HYDRAULIC	2556	2286		3418	1984	
CONTROL SURFACES	714	2547.3				
AVIONICS	1306	1220				
ENVIRONMENTAL CONTROL	1657	1220				
PERSONNEL PROVISIONS	361	1220				
GROWTH	12752			14102		
DRY WT.	168478	2064	78.5%	183945	1995.6	75.9%
PERSONNEL	263	1220		263	1220	
CARGO	23321	1745		7854	1745	
ACPS	46	1206.6		46	1206.6	
RESIDUALS	12595	2098.9		12595	1243.5	
LANDING WT.	204705	2028.5	77.1%	204705	1938.5	73.7%
ACPS PROPELLANT	3082	1206.6		3082	1206.6	
ENTRY WT.	207787	2016.3	76.70%	207787	1927.7	73.3%
RESERVE FLUIDS	12643	2386.8		12643	2072.5	
INFLIGHT LOSSES	305	1955		305	1220	
ASCENT PROPELLANT	1412221	2094.9		1412221	980.6	
GLOW	1632956	2081.1		1632956	1109.6	

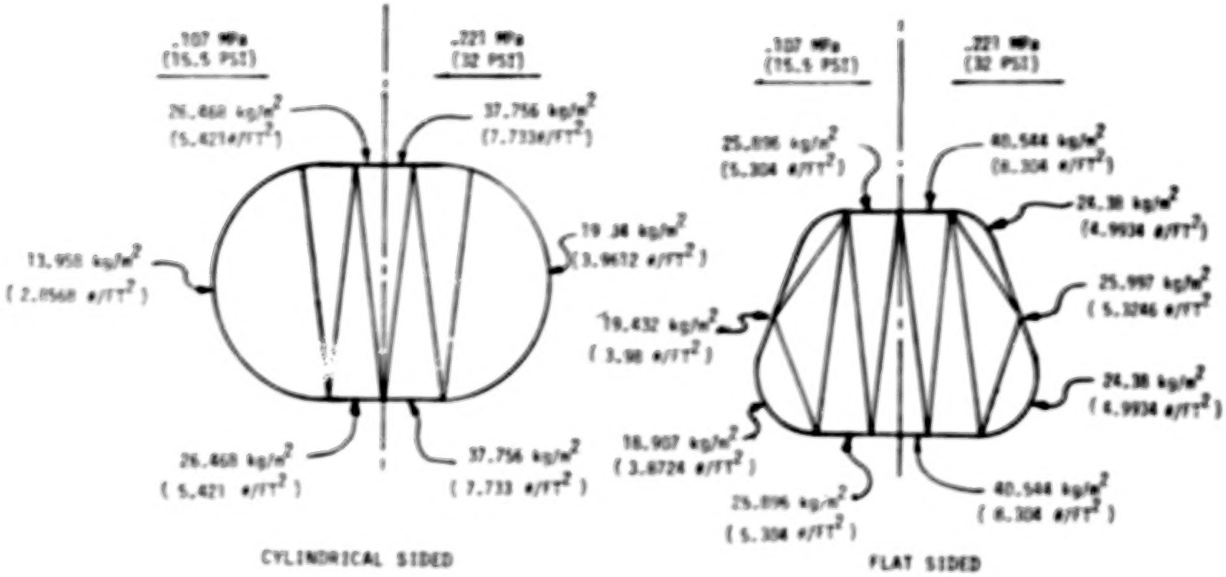

VOL 143.9 m^3/m (1549 FT^3/FT)	AVERAGE FACTOR kg/m^2 (lb/FT^2)				WEIGHT kg/m (lb/FT)			
	.107 MPa (15.5 PSI)		.221 MPa (32 PSI)		.107 MPa (15.5 PSI)		.221 MPa 32 PSI	
CYLINDRICAL	18.7	(3.8408)	26.4	(5.4083)	728	(489.2)	1155.4	(776.4)
FLAT SIDE	21.69	(4.4424)	30.67	(6.283)	1083.7	(728.2)	1532.7	(1029.9)

Figure 28 Cylindrical - Flat Sided Body Section

Subsystems Design

The various subsystems were assessed for impact of CCV design and where the impacts were minimal, the designs and results of reference (1) were utilized without significant revision. For example, the crew cab volume, accommodations, environmental control provisions, and weights are influenced primarily by crew size and mission duration and relatively unaffected by vehicle configuration. Other systems such as landing gear, electrical, and environmental control vary as a function of the landing weight of the vehicle with minimal design change involved. This will be true provided the entry trajectory and landing parameters remain closely similar. Those systems most affected by the design such as structures, secondary power, hydraulics, and propulsion were reviewed in more depth.

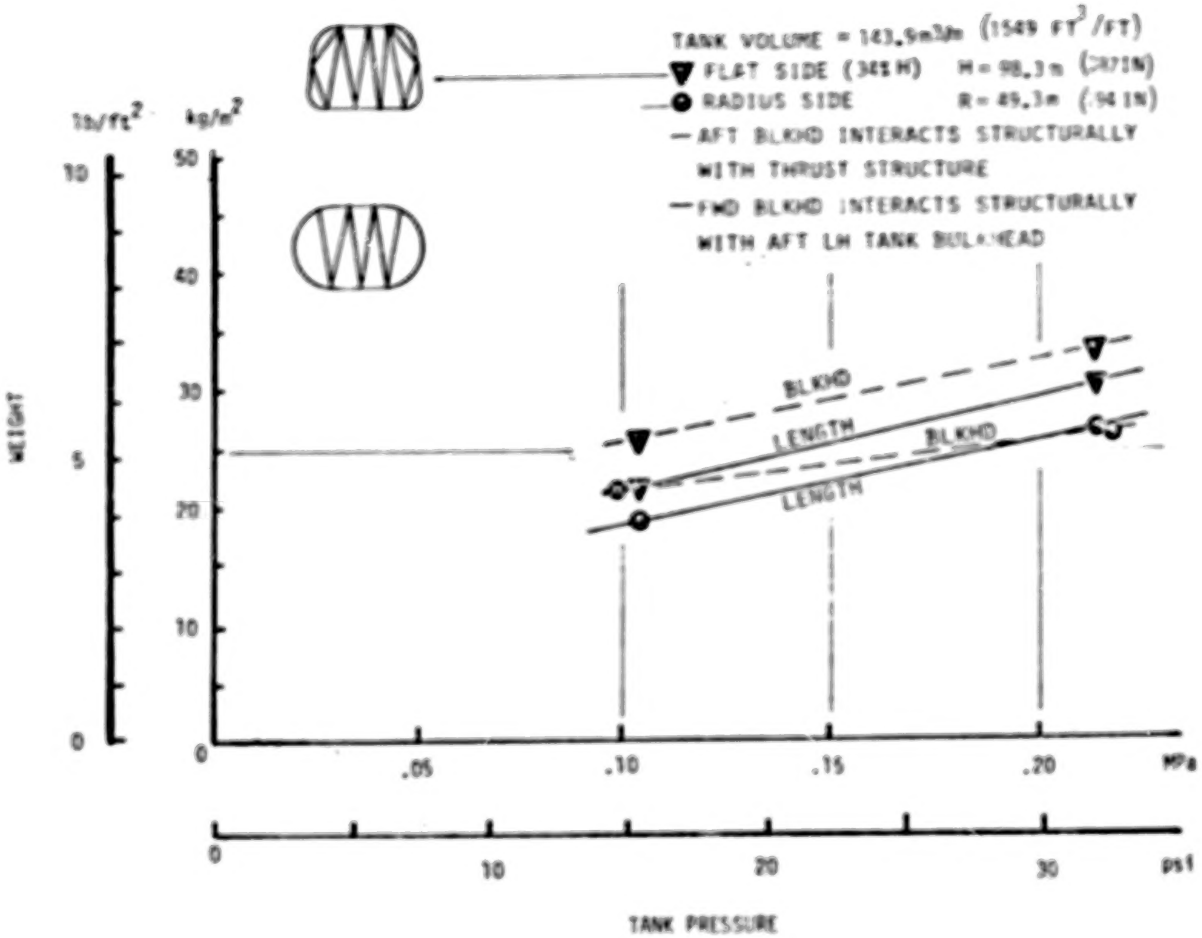

Figure 29 LO_2 Tank Unit Weights

Operating Environment.-The environment which most significantly impacts the subsystems is that associated with entry and landing. While certain ascent factors do impact the design, these are relatively constant for a given class and size of vehicles, i.e., the thrust vector control requirements do significantly impact the secondary power and hydraulic systems but are essentially constant and with a fixed ratio relative to lift off thrust.

The entry trajectory and landing parameters were supplied by NASA LARC and are shown on figure 30 . Time is shown from entry initiation and in that significant control or heating occurs subsequent to 300 seconds, the plot is shown from 300 seconds to touchdown. Utilizing the trajectory data of

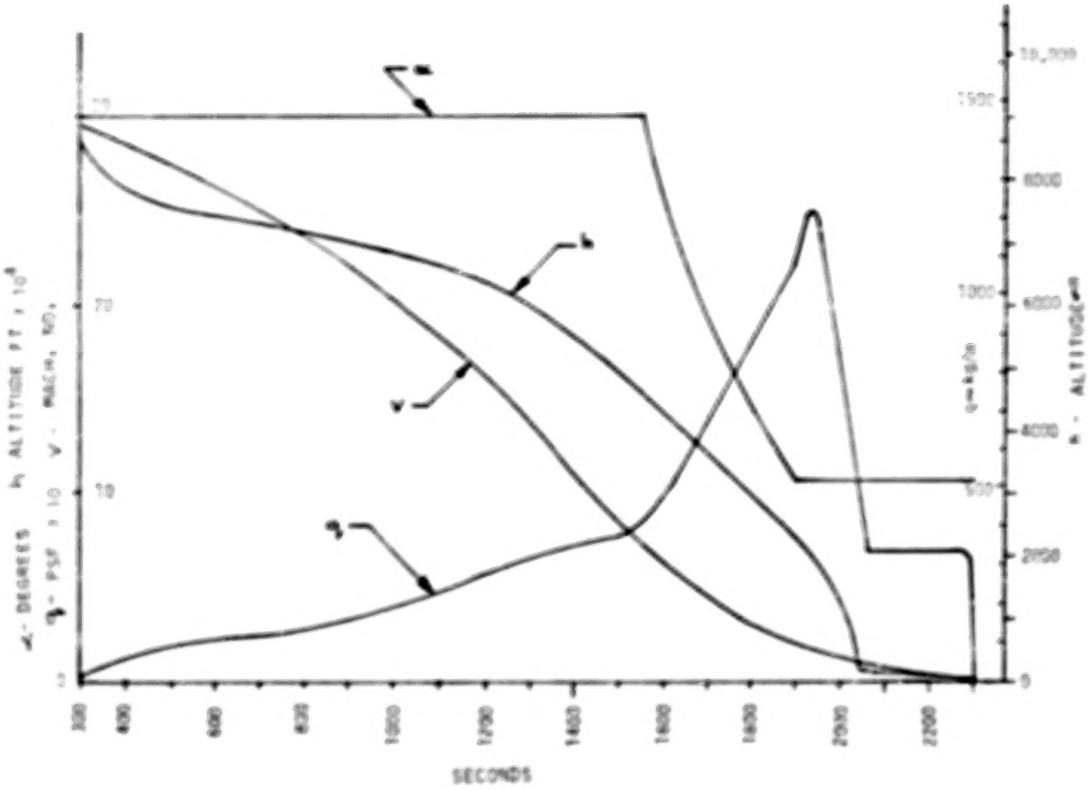

Figure 30 Entry Trajectory

figure 30 and the initial vehicle outline supplied by NASA LARC, entry heating was computed to establish peak temperatures as well as equilibrium isotherms. These were computed on the trapezoidal cross-section. These data are shown on figures 31 and 32 . For the circular cross-section, an adjustment was made to the TPS weights based on reference (1). Reentry heating distributions for the two cross-sections are similar, as is shown in figure 33 . Consequently, the impact on the TPS is minor. These data formed the basis for the selection of the specific thermal protection system configuration.

Structures Design.-The structures design is based on previous Space Transportation design studies. Much of this effort was reported in reference (1). The design criteria developed and utilized in these studies is shown on table 5 . The basic materials selections for the critical elements are also shown on table 5 . Aluminum brazed titanium honeycomb (H/C) is used

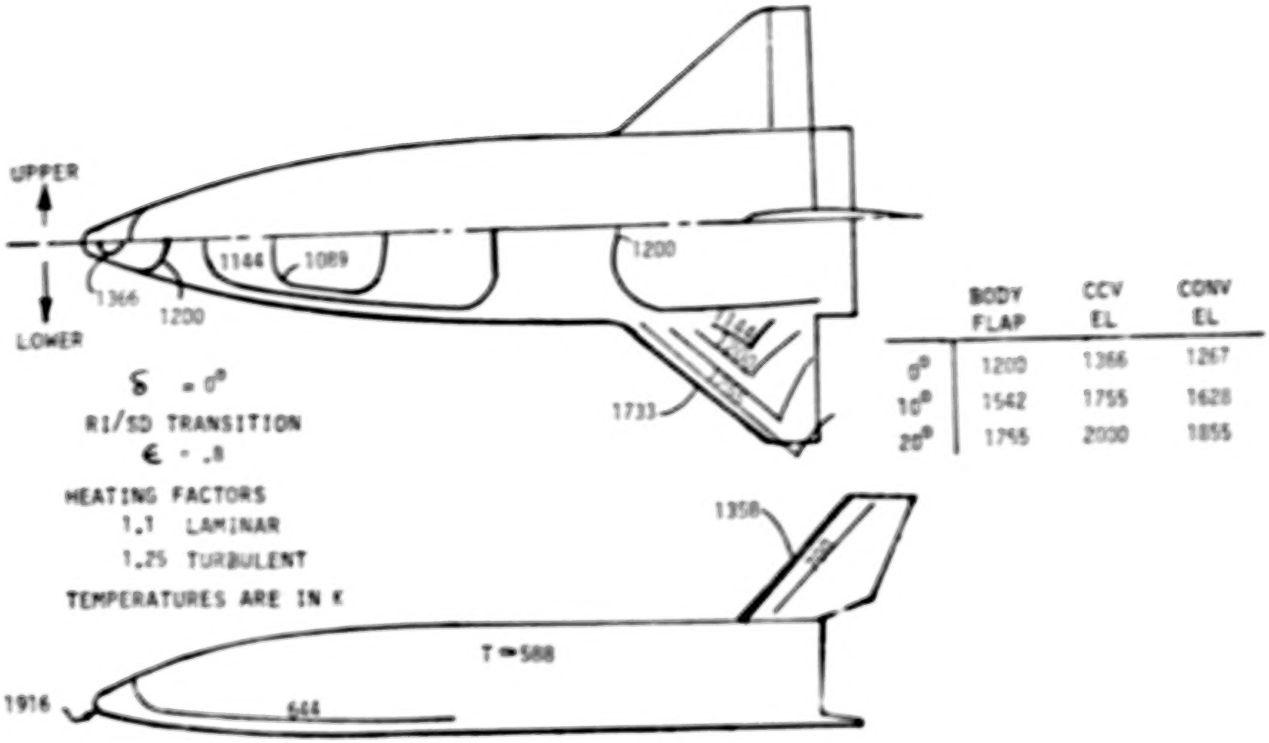

	BODY FLAP	CCV EL	CONV EL
0°	1200	1366	1267
10°	1542	1755	1628
20°	1755	2000	1855

Figure 31 Reentry Equilibrium Temperatures

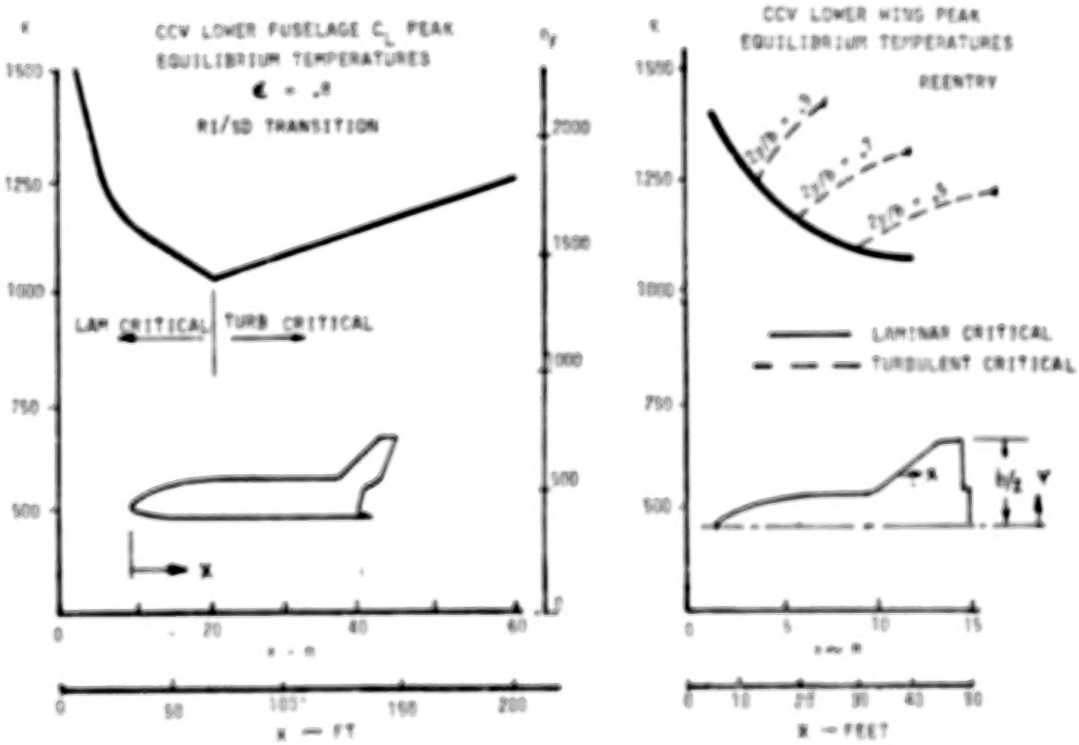

Figure 32 Reentry Equilibrium Temperatures

Table 5 Design Criteria

- 0.4G LIMIT LATERAL LOAD FACTOR
- F.S. = 1.5 LATERAL LOAD/LATERAL LOAD + PRESSURE
- F.S. = 2.0 PRESSURE ONLY SHEAR/BENDING ANALYSES
- F.S. = 1.0 PRESSURE ONLY LIMIT MEMBRANE PRESSURE STRESS ANALYSES
  FRAME 0.8 EFFECTIVE WITH SKINS TO A MAX. OF 22% OF MEMBRANE LOAD.
- 1.15 JOINT WEIGHT FACTOR INCLUDED
- SHEAR WEB t X 1.5 COVERS WEB + STIFFENER WEIGHT
- MIN. SKIN GAGE TANK WALLS AND SHEAR WEBS (0.015 INCHES) 0.381 mm
  MIN. FRAME CHORD AREA (0.20 SQ. IN.) 129 mm^2
- SURFACE STRUCTURE - ALUMINUM BRAZED TITANIUM HONEYCOMB SANDWICH
- FRAMES - 6AL-4V-T_1
- STRUTS - BORON/ALUMINUM L/ρ = 120 MAX AND D/t = 120 MAX.

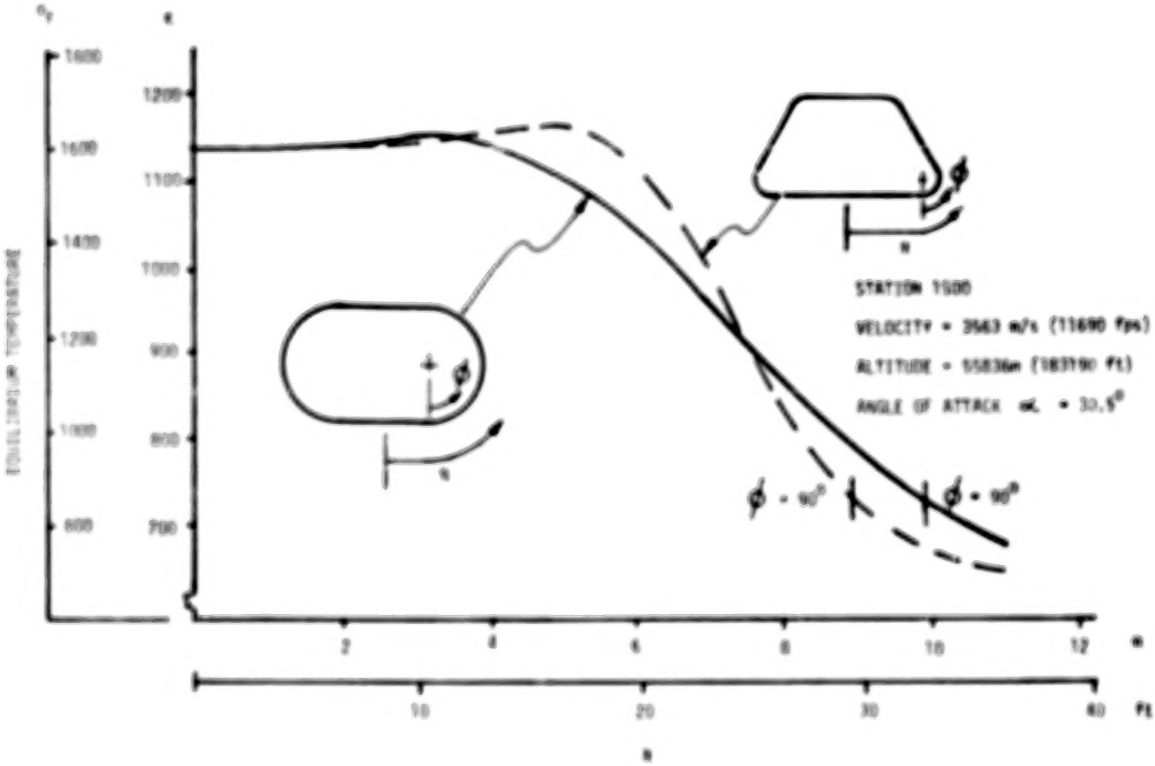

Figure 33 Comparison of Cross Section Temperature Distribution

as the structural skin. It was assumed that maximum outer H/C skin temperature during entry does not exceed 672°K (750°F), by selection of the proper thermal protection system (TPS). Outer frame and spar flanges are integral with the inner H/C skin. Flat surfaced body sections are braced with boron/aluminum struts attached to the inner Titanium frame flanges. Frames and spares are set at a 1.02m (40 inch) spacing. Table 6 shows the loads and analysis techniques, criteria, and governing conditions used in designing, sizing, and weighing the various elements of the LOX tank and is typical of the body sizing and weighing. The critical conditions in most instances are associated with the internal pressure in the tanks. This pressure is developed as a result of firtst, propellant vapor pressure, and second, static head pressure developed as a result of accelerations. Figure 34 shows these pressures in an aft located LOX tank at various stations along the tank length as a function of time from lift-off. The maximum total pressure occurs at the aft bulkhead at 130 seconds.

Table 6 LO_2 Tank Loads and Analyses

STRUCTURAL COMPONENTS	LOCATION	CRITICAL LOAD CONDITIONS-LIMIT LOAD -.0103 MPa (-1.5 PSI) TANK PRESSURE (32 PSI USED IN EXAMPLE ANALYSIS) BENDING OR SHEAR	.221MPa MEMBRANE STRESS	.4G LATERAL LOAD	SIGNIFICANT FEATURES-METHODS OF ANALYSIS
FRAME STRUT TUBES	TOP TO BOT	•		•	L/ρ & D/t
CHORDS	FLATS-TOP & BOTTOM	•			$M=\frac{wl^2}{12}$, $M=\frac{wl^2}{24}$
CHORDS	SIDES			•	$A=\left(\frac{M}{DF}\right)$
WEB	FLATS-TOP & BOTTOM	•			$t=\frac{V}{DF}$
WEB	SIDES			•	$t=\frac{V}{DF}$
SKINS	FLATS-TOP & BOTTOM	•	•		$M=\frac{wl^2}{12}$, $\frac{wl^2}{24}$, $\frac{PRd}{\Sigma d+.5A_{FR}}$
SKINS	SIDES		•		$f_t=\frac{PRd}{\Sigma d+.5A_{FR}}$
CORE CORE	FLATS-TOP & BOTTOM SIDE (MIN. DENSITY)	•			$f_s=\frac{V}{D}$

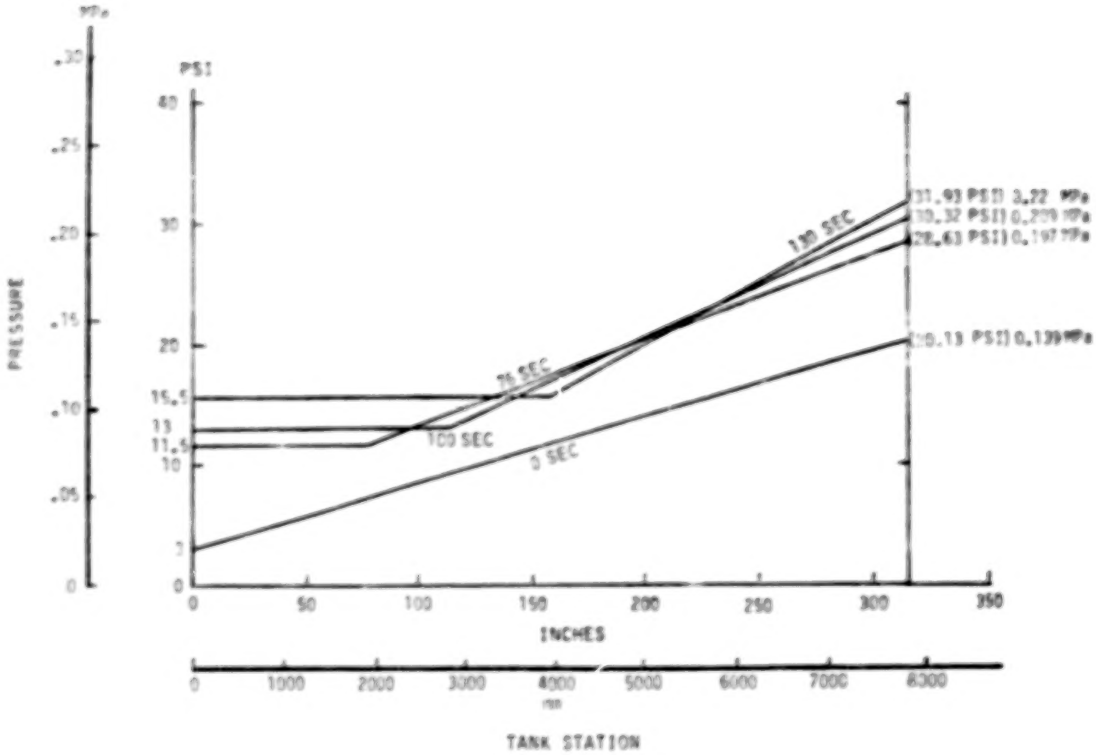

Figure 34 LO_2 Tank Pressure

Figure 29 reflects the averaged unit weights resulting from the sizing of forward and aft located LOX tanks. These unit weights are based on the configurations shown in figures 1 and 4 and are typical of the details shown on figure 5 . The unit weights and configuration data permit the generation of the plots shown on figure 35 and figures 25 and 26 , which define various tankage parameters for baseline, conventional LOX tank forward and conventional LOX tank aft, Respectively.

The thermal protection system (TPS) selected utilizes the data presented in reference (4) for performance and weights. This is reproduced on figure 36 for the 672^{0}K (750^{0}F) maximum back face temperature used with the aluminum brazed titanium H/C surfaces. Figure 37 plots the TPS unit weights for the tank/body external surface structure for the body system. Figure 38 shows the impact of deflection on peak surface temperature for the elevon and body flap and the corresponding weights associated with the necessary

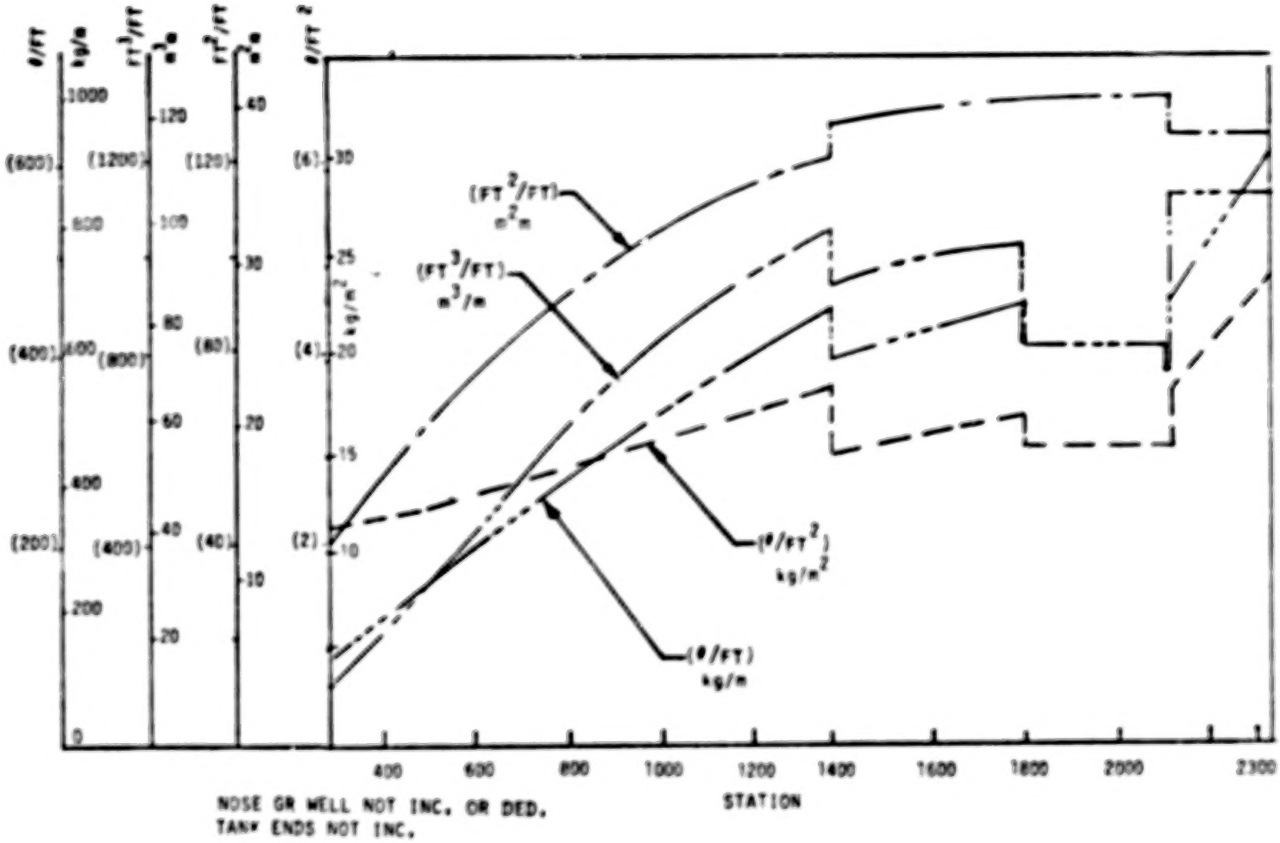

Figure 35 Baseline Tankage - LO_2 Aft

thermal protection and structural system. For example, a body flap deflection of 5^0 incurs a peak temperature of slightly more than 1366^0K (2000^0F). If this were the maximum deflection to be designed for, figure 36 indicates that TD-Ni-CR with Dynaflex[2] and Protecalor[3] insulation with a total thermal protection system weight of 11.23 kg/m^2 (2.3 lb/ft^2) would be adequate. To support this, a titanium in-structure of beams, ribs, and panels weighing approximately 12.69 kg/m^2 (2.6 lb/ft^2) of surface area or 25.39 kg/m^2 (5.2 lb/ft^2) of plan area would be required. This system then would weigh

[1] Registered trademark of Fansteel Corp.

[2] Registered trademark of Marmak Products Inc.

[3] Registered trademark of Protecalor Inc. (France)

36.62 kg/m^2 (7.5 lb/ft^2) of plan area. Significant features of this chart are first that for a given temperature limit (and unit weight) the body flap can be deflected twice as far as the elevon and secondly the conventional configuration elevon can be deflected 40% further than the Baseline elevon for identical constraints. The implication of this is that the high deflections required for trim should be accommodated first by the flap and only to minimum extent by the elevon.

The canard system installed on the baseline configuration is shown in figure 2 . The canard is a simple surface which is not movable once extended subsonically. These features minimize canard's weight and the body structural impacts.

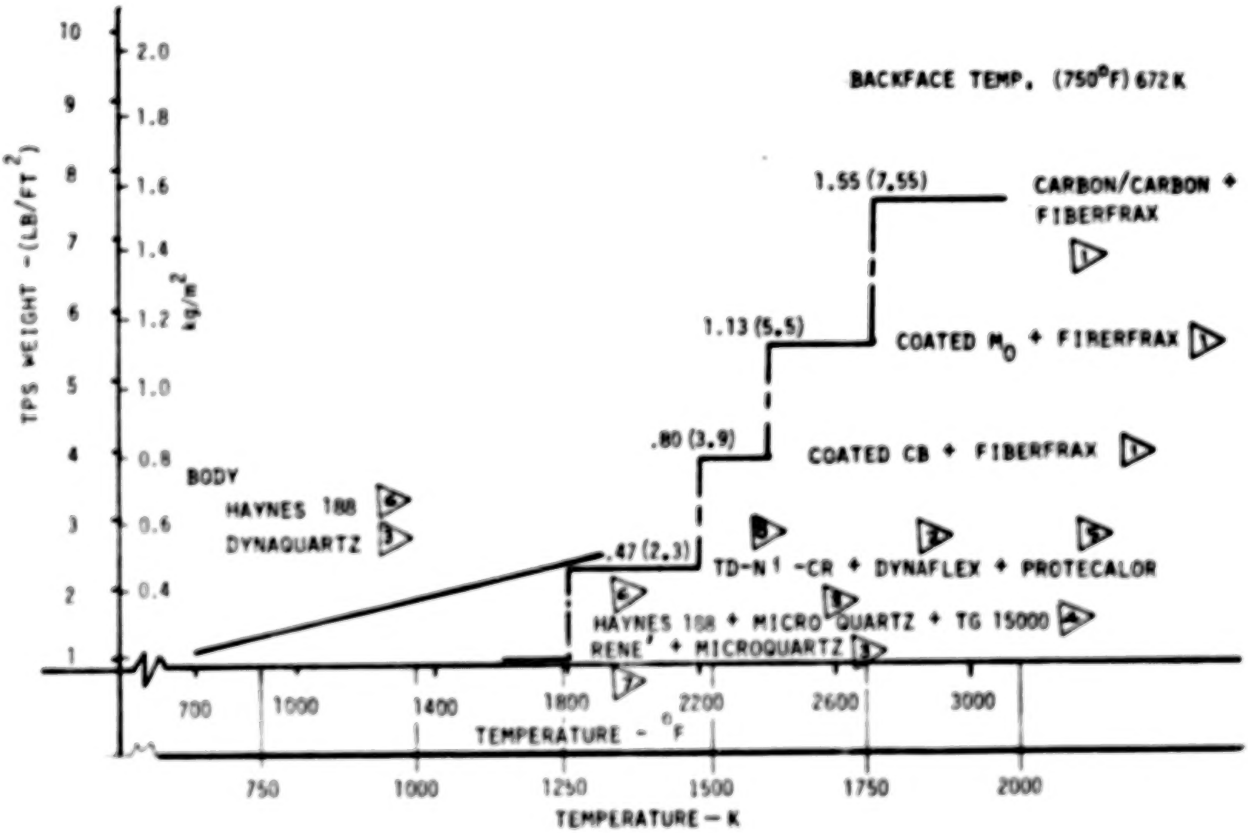

Figure 36 Thermal Protection System Weights

Registered trademark of the company mentioned

1. Carborundum Co.
2. Marmac Products Inc.
3. John Manville Fiberglass Inc.
4. Hitco
5. Protecalor (France)
6. Cabot Corp.
7. General Electric
8. Fansteel

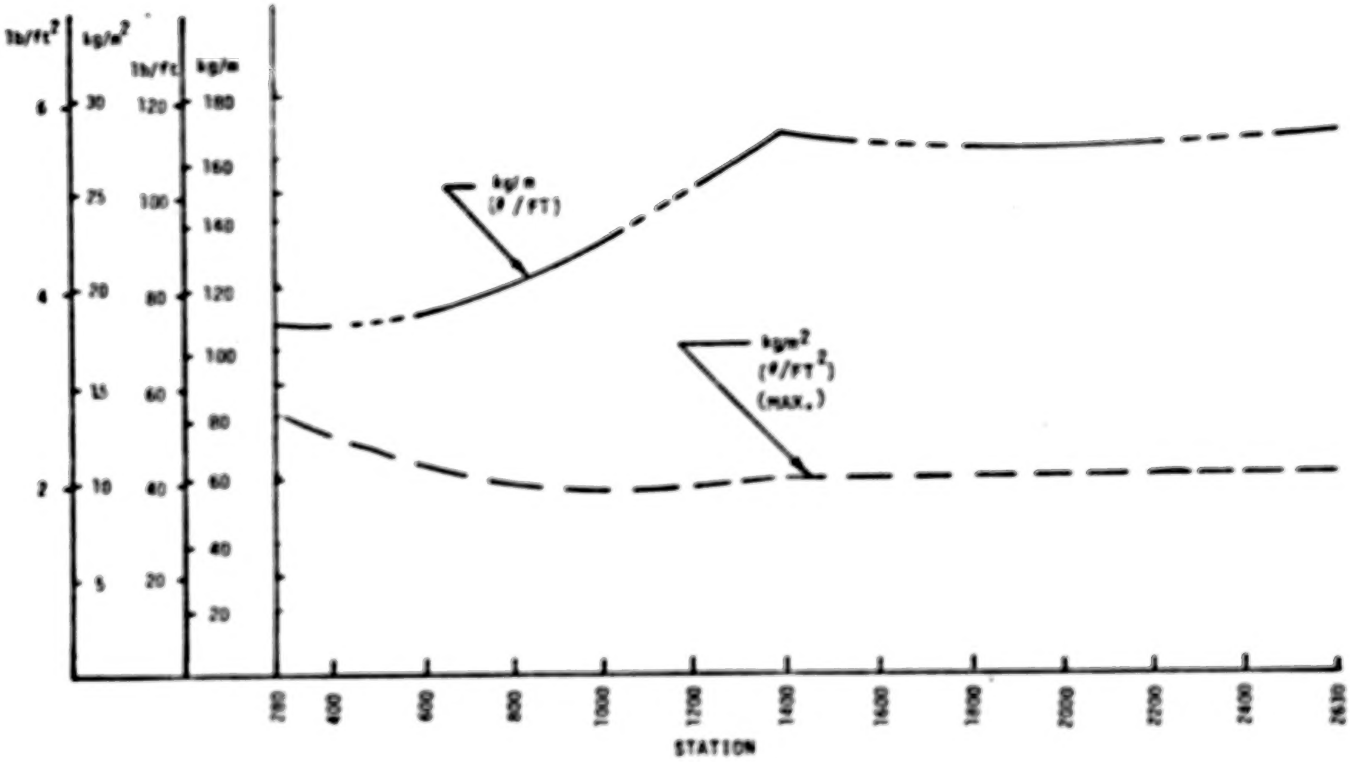

Figure 37 Conventional Body Thermal Protection System Weights

Secondary Power, Flight Control Actuation, Hydraulic and Reaction Control Systems.-The systems most impacted by CCV design are those effected by the flight path characteristics, stability and attitude control. As the C.G. progresses aft from extremely stable configurations, less power is required to perform a given manuever. At a point in this aft C.G. position, as the vehicle configuration becomes unstable, less fixed wing area is required; the control surfaces act to provide the required characteristics. The result is still lower weights for a specified payload. Further gains occur as the C.G. moves aft, however, the control systems are rapidly increasing in weight. The three configurations analyzed were all inherently aft. C.G., unstable vehicles. For this reason, all of the systems increased in size as the C.G. was moved aft.

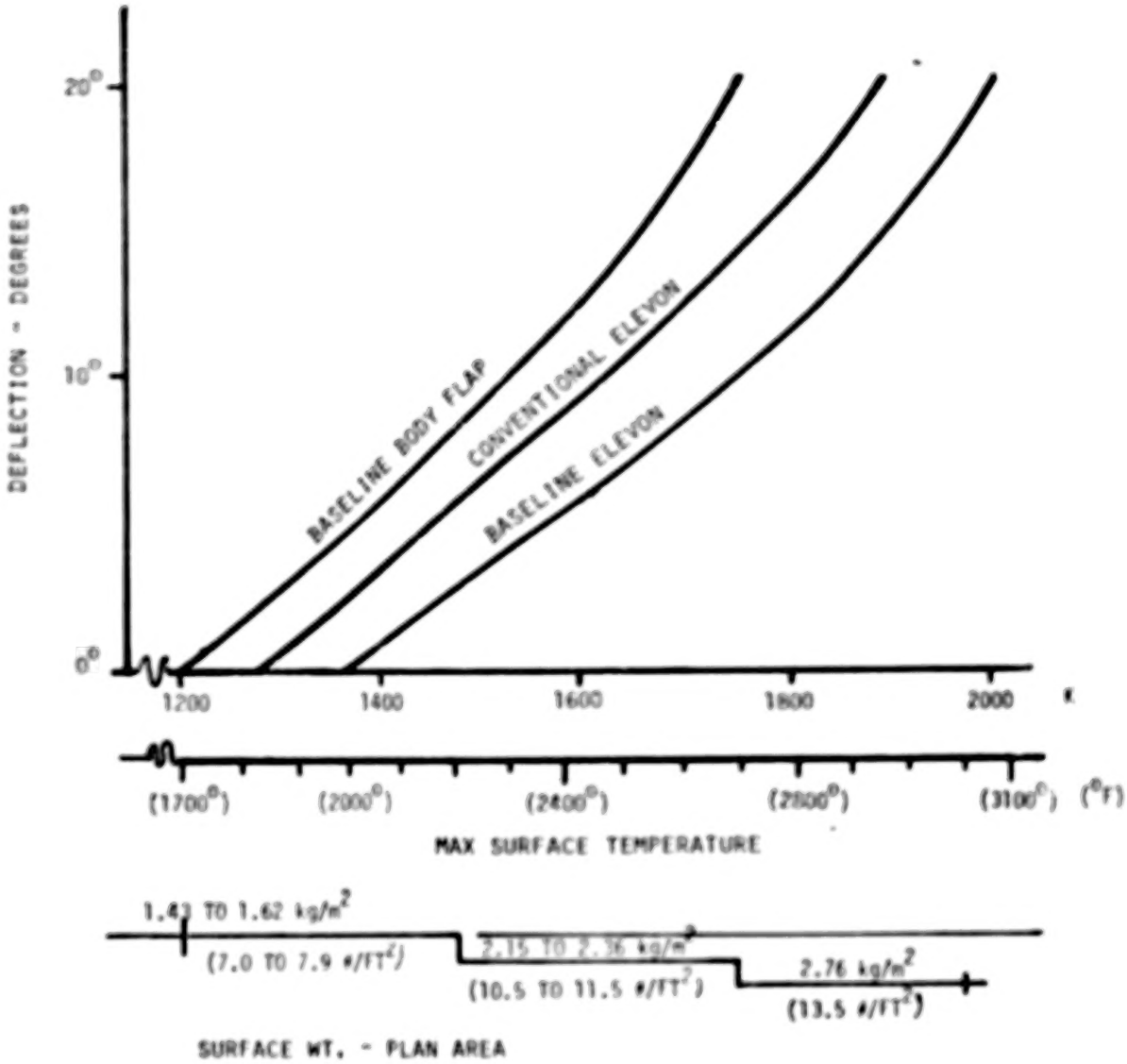

Figure 38 Elevon and Body Flap Surface Weights

Two primary inputs were utilized for system sizing. The first was the entry duty cycle developed for the Space Shuttle. The second was the data generated by the Flight Control computer runs which generated the surface deflections and hinge moments for specific manuevers for varying C.G. positions. Comparable data from Space Shuttle analyses permitted an estimate of power requirements relative to the shuttle.

Table 7 shows the shuttle duty cycle and a comparable duty cycle for the Baseline vehicle. Table 8 shows the significant characteristics for each of the surfaces.

The flight control system is configured as a computer controlled dual piston tandem actuator utilizing 34,473 K Pa (5000 psi) hydraulic systems. This is the hydraulic configuration previously developed under reference (1) studies. To provide the necessary redundancy, two elevons per side and two rudder panels are shown. The body flap which is a trim device is extrapolated from shuttle designs for power requirements and weight. Table 8 shows the actuation system weights for the various vehicle configurations studied.

Summarizing the entry duty cycle activity from table 7 permits the development of the horse power hours for the system as well as an assessment of the peak power and the point at which this occurs.

Table 7 Control System Entry Duty Cycle

SHUTTLE		BASELINE	
ELEVON			
1604 SECS	± 1°/SEC @ 1 HZ 25 % ON 75% OFF	1670 SECS	± 5° @ 1 HZ 25 % ON 75% OFF @ 20°/SEC
194 SECS.	± 1°/SEC @ .5 HZ CONTINUOUS	194 SECS	± 2.75° @ .5 HZ 5.5°/SEC
69 SECS	± 1.5°/SEC @ .5 HZ CONTINUOUS	69 SECS	± 4.13° @ .5 HZ 8.26°/SECS
4 SECS	± 7.5°/SEC @ .5 HZ CONTINUOUS	4 SEC	± 20° @ .5 HZ 40°/SEC
RUDDER			
200 SECS	± .75°/ SEC @ .5 HZ CONTINUOUS	200 SECS	± .75° @ .5 HZ 1.5°/SEC
194 SECS	± .5°/ SEC @ .5 HZ CONTINUOUS	194 SECS.	± 1.43° @ .5 HZ 2.86°/SEC
69 SECS	± 1.5°/SEC @ .5 HZ CONTINUOUS	69 SECS.	± 4.3° @ .5 HZ 8.6°/SEC
120 SECS	± 1.5°/SEC @ .5 HZ CONTINUOUS	120 SECS.	± 4.3° @ .5 HZ 8.6°/ SEC

Table 8 Surface Actuation System Weights and Power Requirements

	SURFACE	DEFLECT DEGREES	MAX. RATE DEG/SEC.	HINGE MOM SURF $\frac{ft}{ft^2}$	TOT SURF WTS - α_g	C.G. STA.	WT - α_g & C.G.	DUTY CYCLE PK KW	KW-HRS	% KW-HRS
.69 CONV	ELEVON	+ 30° -30°	80	3.05	325	2440	714	732	91.6	92.8
	RUDDER	+ 45°	60	1.50	160	2610	STA 2547.3			
	FLAP	+ 20° -15°	6	2.09	270	2600		39.6	3.1	
.725 CONV	ELEVON	"	"	4.23	651	"	867	1017	71.7	172.8
	RUDDER			1.50	160		STA 2531.2			
	FLAP			2.09	270			39.6	3.1	
.69 NO CANARD	ELEVON	"	"	2.87	307	"	690	679	47.8	85.2
	RUDDER			1.50	160		STA 2557			
	FLAP			2.09	270			39.6	3.1	
.69 BASE	ELEVON	"	"	2.87	307	"	690	679	47.8	85.2
	RUDDER			1.50	160		STA 2557			
	FLAP			2.09	270			39.6	3.1	
.71 BASE	ELEVON	"	"	3.23	345	"	823	777	54.7	93.7
	RUDDER			2.24	289		STA 2559			
	FLAP			2.09	270			57.0	4.7	
.725 MOD	ELEVON	"	"	5.56	597	"	1332	1336	94.2	133.1
	RUDDER			2.24	289		STA 2584.9			
	FLAP			4.70	470			57.0	4.6	
.735 MOD	ELEVON	"	"	5.97	636	"	1814	1434	101.0	147.3
	RUDDER			2.89	347		STA 2549			
	FLAP			4.70	470			74.72	5.99	

NOTE: REDUNDANCY FACTOR OF 1.73 INCLUDED
TVC KW-HRS ADDED

The secondary power generation and distribution systems are configured using the hydrazine APU of the shuttle as a basis for extrapolation to the required power levels for power generation and previous studies of reference (1) for the 34,473 K Pa (5000 psi) distribution system. The basic specific weights utilized for these elements as well as the resulting weight are shown on table 9 . The line lengths shown are for the Baseline LOX aft configuration. Thrust vector control requirements are included, but as noted, these requirements vary from a high of 40% of the total for the more stable configurations down to 27% of the total horsepower hours for the larger systems.

Table 9 Secondary Power System Weights

TVC POWER RATIOED TO SHUTTLE

BASELINE	237 KW	34.3 KW - HRS
CONVENTIONAL	263 KW	38.0 KW - HRS

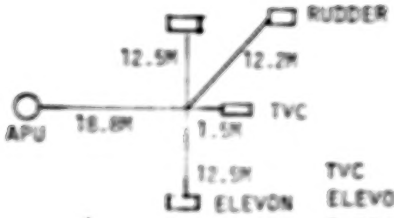

	Σ M
TVC	20.3
ELEVON	63.0
RUDDER	31.0

	PK KW (DTYCYC) / KW-HRS	HYD SYS RES FL 1.4 $K_{\#}$ / K_W	APU PUMP ALT .46 $K_{\#}$ / K_W	APU FUEL TANK 1.22 $K_{\#}$ / KW-HRS	APU FUEL FUEL 3.3 $K_{\#}$ / KW-HR	HYDLINES .06 $K_{\#}$ / KW-M	Σ SYSTEM	Σ SYSTEM + ACTRS
.69 CONV.	771 / 92.8	1078	351	112.8	305	1477	3325	4039
.725 CONV.	1055.9 / 112.8	1477	482	137	370	2015	4481	5322
.69 NO CANARD	717.4 / 85.2	1005	327	103	280	1374	3400	4091
.69 BASE	717.4 / 85.2	1004	327	103	280	1374	3400	4091
.71 BASE	834.4 / 93.7	1167	380	114	308	1594	3564	4387
.725 MOD 1	1394.7 / 1331.1	1951	636	162	437	2651	5837	7169
.735 MOD 1	1508.6 / 141.3	2110	688	172	464	2866	6301	7754
C.G. STA		2240	1955	1955	1955	2320		

Mass Properties Analysis

A detail build-up of the mass properties of each of the configurations studied was developed. The basis for establishing subsystem weights is shown in table 10 . The detailed analysis of the significant elements has been described. The factors shown are those developed through the studies of reference (1). The propulsion formula is the formula developed through reference (2) studies modified by the weight reduction developments of reference (3).

Table 10 Mass Property Table

WEIGHT ASSESSMENT	
WING	DETAIL BUILD UP OF WEIGHTS
TAIL	
BODY	
INDUCED ENVIRONMENTAL PROT	
PRIME POWER	
HYDRAULIC	
CONTROL SURFACES	
LANDING DOCKING AND RECOVERY	.0244 X LANDING WEIGHT
ELECTRICAL	.0068 X LANDING WEIGHT
ENVIRONMENTAL CONTROL	.0061 X LANDING WEIGHT
PROPULSION	FORMULA WITH 6.4% REDUCTION
AVIONICS	SAME AS VTO STUDIES
PERSONNEL PROVISIONS	
PERSONNEL	
ACPS	.015 X ACPS PROPELLANT

Where specific factors have previously been developed as in the case of propellants and weight margins, these have been repeated on table 11 for reference. The subsystems factor of 4% has been accepted due to the high percentage of components which are either off-the-shelf or which require minimum development. Table 12 is the chart of the mass properties of the Baseline vehicle as developed for two assumed C.G. locations, 69% and 71% body length. Shown in the table are calculated C.G. locations.

Table 13 is the chart of the mass properties for the Modification 1 vehicle. The conventional vehicle is shown on table 14 with table 4 reflecting the variations associated with LOX tank location. The LOX tank trade

Table 11 Mass Property Analysis

WEIGHT FACTORS

- ASCENT PROPELLANT
  - FLIGHT PERFORMANCE RESERVES - .85% ΔV AT BO. = 75.65 m/S (248.2 FPS)
  - RESIDUALS

    GASES LO_2 = 1.698 x VOL. m^3 = kg (.106 x VOL. FT^3 = LB)

    LH_2 = .224 x VOL. m^3 = kg (.014 x VOL. FT^3 = LB)

    TRAPPED PROPELLANT .000321 x THRUST = kg (.00315 x THRUST = LB)

    PROPELLANT UTILIZATION ERROR .068% x ASCENT PROPELLANT

    TRAPPED PROPELLANT IN ENGINES .000086 x THRUST = kg (.00084 x THRUST = LB)
  - OMS PROPELLANT 198.12 MPS ΔV AT 4642.5 ISP (650 FPS Δ V AT 473.4 ISP)
  - RCS PROPELLANT

    30.48m (100 FPS) ON ORBIT + 12.19m (40 FPS) RE-ENTRY + 6.09m (20 FPS) RESERVES AND RESIDUALS.

    SPLIT EQUALLY FWD AND AFT FWD I_{SP} N_2O_4 - MMH = 2843.9 SECS. (290 SECS.)

    AFT I_{SP} LO_2 - LH_2 = 3922.6 SECS. (400 SECS.)
  - MARGINS STRUCTURES 10% SUBSYSTEMS 4%

was analyzed at an assumed C.G. of 69% body length. For consistency, the body length for all configurations was 66.8 m (2630 in.). This dimension is measured from the body lines vanishing point at the nose to the hinge line of the body flap on the Baseline vehicle.

Figure 39 summarizes the impact of the analyses shown on tables 12, 13, and 14 and 4 on payload in the payload bay as a function of vehicle entry C.G. location. Figure 39 adjusts the vehicle payload and C.G. to account for the vehicle entry C.G. being different in the final calculations than the originally assumed C.G. First the weight of the control systems affected by C.G. location is plotted as a function of vehicle entry C.G. The control systems elements which are significantly impacted by C.G. location and which are included in the buildup of weights are the surface actuators, hydraulic system including lines, valves, filters, reservoirs, fluid, and pumps, the APU, and the APU fuel and tankage. Then the value shown as "cargo" in the Mass Properties Table is distributed first as the delta to the system for the specific C.G. location and secondly, the residual is apportioned as required to achieve the desired C.G. between ballast

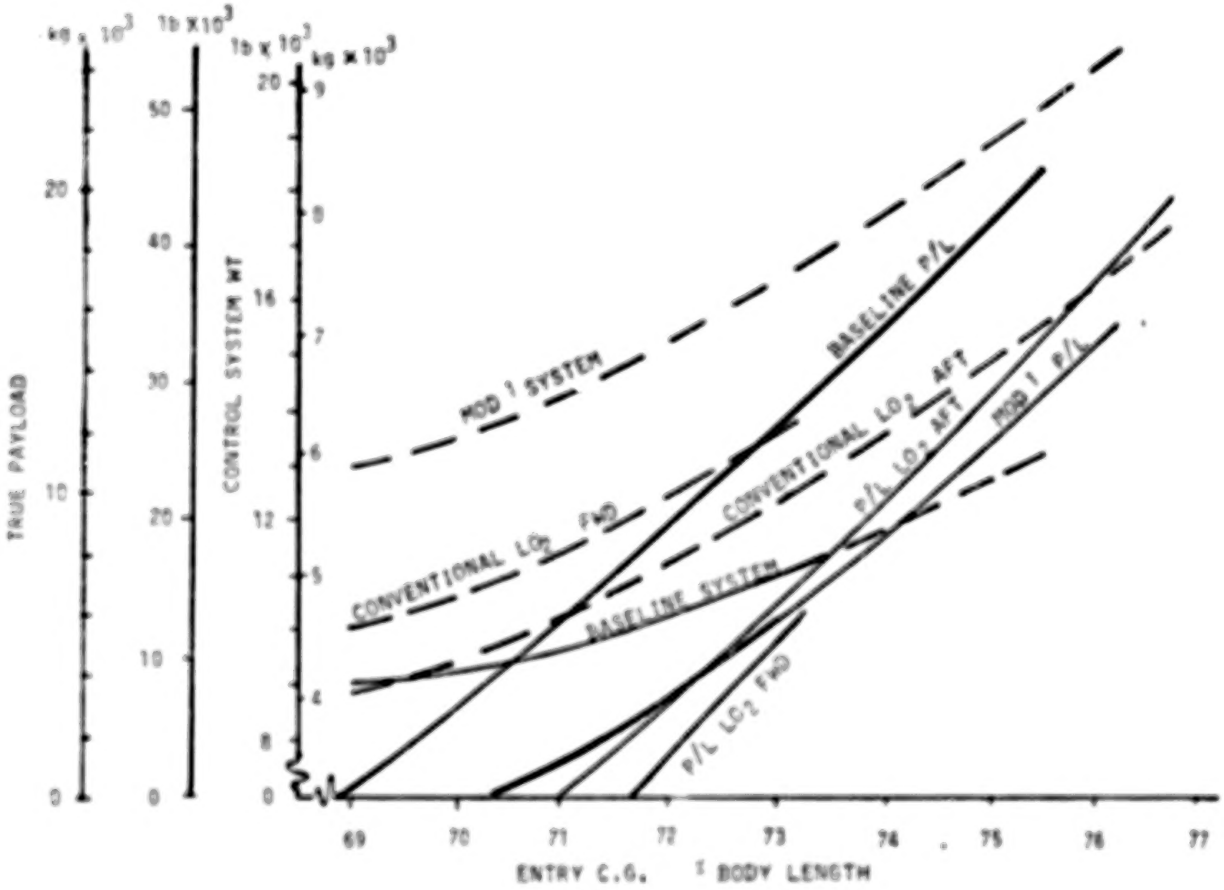

Figure 39 Payload vs C.G.

Table 12. Mass Properties - Baseline - 69% and 71% C.G.

Baseline with Canard	69%			71%		
	WT kg	STA		WT kg	STA	
WING	1100.4	2274.2		11004	2274.2	
TAIL	1847	2664.6		1847	2664.6	
BODY	66359	1807.5		66359	1807.5	
INDUCED ENV. PROT.	13120	1877.1		13120	1877.1	
LANDING DOCKING & REC.	4521	2000		4521	2000	
PROPULSION	34683	2464.6		34683	2464.6	
PRIME POWER	431	1955		494	1955	
ELECTRICAL	1260	1745		1260	1745	
HYDRAULIC	2377	2286.2		2762	2286.2	
CONTROL SURFACES	690	2551		823	2559	
AVIONICS	1306	1220		1306	1220	
ENVIRONMENTAL CONTROL	1500	1220		1500	1220	
PERSONNEL PROVISIONS	361	1220		361	1220	
GROWTH	11389			11413		
DRY WT.	150855	2030.3	77.2%	151458	2031.5	77.2%
PERSONNEL	263	1220				
CARGO	22910	1745		22279	1745	
ACPS	41	1206.6				
RESIDUALS	11388	2049.7				
LANDING WT.	185458	1994.9	75.8%	185430	1996.8	75.9%
ACPS PROPELLANT	2744	1206.4				
ENTRY WT.	188202	1983.4	75.4%	188174	1985.3	75.5%
RESERVE FLUIDS	11434	2386.8				
INFLIGHT LOSSES	279	1955		308	1955	
ASCENT PROPELLANT	1269439	2094.9				
GLOW	1469357	2082.9	79.2%			

Table 13 Mass Properties - Modification 1 - 72.5% and 73.5% C.G.

BASELINE WITH MOD I	72.5%			73.5%		
	WT - kg	STA		WT - kg	STA	
WING	11372	2286.3		11372	2286.3	
TAIL	1847	2664.6		1847	2664.6	
BODY	66753	1813.1		66753	1813.1	
INDUCED ENV. PROT	13747	1914.8		13747	1914.8	
LANDING, DOCKING & REC.	45.4	2000		4512	2000	
PROPULSION	34684	2464.6		34684	2464.6	
PRIME POWER	798	1955		860	1955	
ELECTRICAL	1258	1745		1258	1745	
HYDRAULIC	4602	2286		4977	2286	
CONTROL SURFACES	1332	2544.9		1454	2549	
AVIONICS	1306	1220		1306	1220	
ENVIRONMENTAL CONTROL	1498	1220		1498	1220	
PERSONNEL PROVISIONS	362	1220		362	1220	
GROWTH	11657			11679		
DRY WT.	155730	2042.8	77.2%	156310	2043.9	77.7%
PERSONNEL	263	1220				
CARGO	17877	1745		17272	1745	
ACPS	41	1206.6				
RESIDUALS	11388	2049.7				
LANDING WT.	185301	2013.1	76.5%	185275	2015	76.6%
ACPS PROPELLANT	2744	1206.6				
ENTRY WT.	18804	2001.3	76.1%	188018	2003.2	76.2%
RESERVE FLUIDS	11434	2386.8				
INFLIGHT LOSSES	437	1955		464	1955	
ASCENT PROPELLANT	1269439	2094.9				
GLOW	1469357	2084.4	79.3%			

Table 14 Mass Properties - Conventional - 69% and 72.5% C.G.

CONVENTIONAL LOX AFT	69%			72.5%		
	WT - kg	STA		WT - kg	STA	
WING	17588	2255.9		17588	2255.9	
TAIL	1847	2664.6		1847	2664.6	
BODY	70681	1884.8		70681	1884.8	
INDUCED ENV. PROT.	13623	1845.8		13623	1845.8	
LANDING DOCKING & REC.	4994	1632		4994	1632	
PROPULSION	38540	2463.8		38540	2463.8	
PRIME POWER	464	1955		619	1955	
ELECTRICAL	1391	1955		1391	1955	
HYDRAULIC	2556	2286.2		3492	2286.2	
CONTROL SURFACES	714	2547.3		841	2531.2	
AVIONICS	1306	1220		1306	1220	
ENVIRONMENTAL CONTROL	1657	1220		1657	1220	
PERSONNEL PROVISIONS	361	1220		361	1220	
GROWTH	12752			12801		
DRY WT.	168478	2064	78.5	169745	2065.5	
PERSONNEL	263	1220		263	1220	
CARGO	23321	1745		21965	1745	
ACPS	46	1206.6		46	1206.6	
RESIDUALS	12595	2098.9		12595	2098.9	
LANDING WT.	204705	2028.5	77.1%	204613	2031.9	77.3%
ACPS PROPELLANT	3082	1206.6		3082	1206.6	
ENTRY WT.	207787	2016.3	76.7%	207696	2019.6	76.8%
RESERVE FLUIDS	12643	2386.8		12643	2386.8	
INFLIGHT LOSSES	305	1955		396	1955	
ASCENT PROPELLANT	1412221	2094.9		1412221	2094.9	
GLOW	1632956	2087.1	79.4%	1632956	2087.6	

assumed to be at station 270 and payload at station 1745. The payload is then plotted versus C.G. position for each of the configurations. As can be seen for the conventional LOX forward vehicle charted in table 4 , the subsystem elements were generated for an assumed C.G. location of 69%; however, the actual C.G. of 73.7% was so far aft that when the entire value of cargo was distributed as above, the most forward C.G. with no payload was 71.7%. The maximum payload occurred at 73.3%. With a C.G. aft of this, the cargo value is reduced by the increase in control subsystems weight further reducing payload. The Modification 1 configuration which was configured for a more aft C.G. appears to offer lower payloads than the Baseline at a given C.G. This is influenced by the constraint that vehicles other than the conventional vehicle have identical Gross Lift-Off Weights. This limits the available mass fraction for subsystems and payload. The necessity for several iterative cycles of design is required to establish the optimum configuration.

Figure 39 is not presented to solve the total payload, c.g. control surface weight/area and vehicle configuration equation. For example trim angle and elevon temperatures have to be considered as limits to the aft movement of the C.G. to increase payload. Approximate elevon temperatures are included on the payload curves. For example on the Baseline vehicle at an entry C.G. of 69.3%, the elevon temperature will attain 1755°K (2700°F) and at a C.G. of 72% will reach 1978°K (3100°F). At constant elevon temperatures, the percentage of difference between Baseline and Modification 1 payloads is much less than at constant C.G. A much greater payload improvement at constant elevon temperature is noted with 1.633 X 10^{6} kg (3.6 million pound) GLOW on the Conventional vehicle over the 1.469 X 10^{6} kg (3.24 million pounds) GLOW of the Baseline and Modification 1 vehicles. Further discussion of payload and vehicle C.G. is presented in the following Section.

CCV/Conventional Vehicle Performance Summary

Summary comparisons are made in figure 40 of the various CCV and conventional vehicle designs in terms of landing speed, hypersonic trim and temperatures and payload as affected by C.G. location. For an assumed TPS temperature limit of 1755°K (2700 degree F) with down elevons, estimated payload for the conventional design (with increased GLOW) is higher than the baseline CCV. However, when the GLOW for the conventional vehicle is

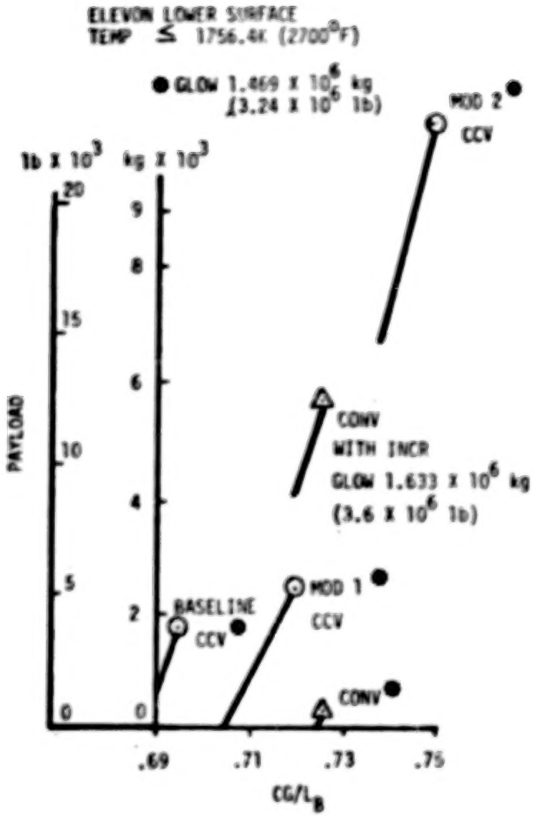

PAYLOAD

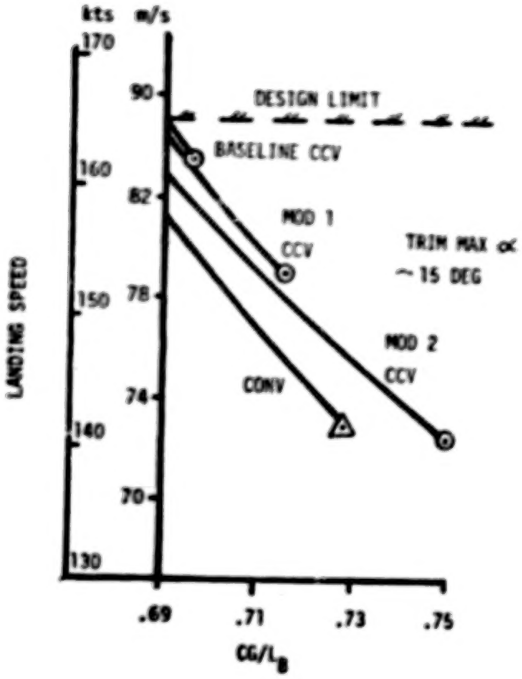

LANDING SPEED

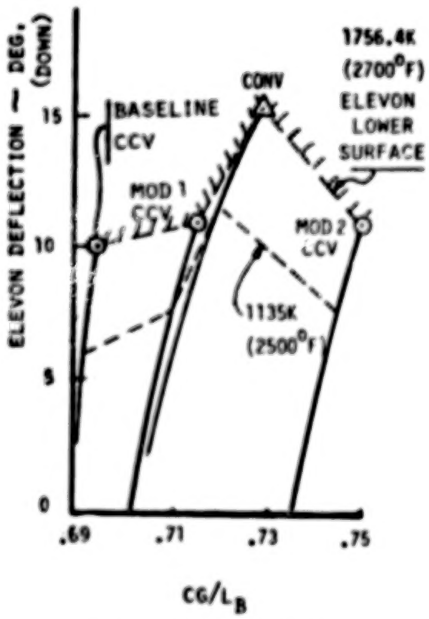

HYPERSONIC TRIM/TEMP.

Figure 40 Performance Summary

reduced from 1.633 (3.60) to 1.469 X 10^6 kg (3.24 million lb) (the value for CCV designs) with reestimated performance, using mass fraction and propellant ratios, the CCV designs show a gain in payload. Payload gains up to 2.267 X 10^3 kg (5000 lb) for Mod 1 over the conventional vehicle (at same GLOW) are indicated. Further, payload gains can be realized by aerodynamic configuration changes. By incrasing body nose camber (to a straight flat bottom) and wing incidence to 5 degrees, the permissible C.G. for trim moves aft from 0.71 L_B to 0.75 L_B which, in turn, reduces ballast weight penalities. This configuration is designated as Mod 2 on the charts, and it is estimated that the payload gains increase to about 9.071 X 10^3 kg (20,000 lb). Since no flight control transient responses at C.G.'s as far as 0.75 L_B were analyzed, some caution must be expressed on the validity of these large payload gains. This suggests a point of departure for follow-on studies.

ADVANCED TECHNOLOGY FOR CCV DESIGNS

The criteria used in this study for evaluating technology advancement is improvements in payload or dry weight reduction (costs were not considered). Candidates for improvement are categorized in the following technical areas: performance, flight control, structural/subsystems, propulsion, and aerodynamic configuration.

CCV Vehicle Performance

Candidates for improving flight control efficiently, such as sensors, gyros and avionics have impacts on system reliability and cost, but little effect on weight reduction. Use of optimal control methods and piloted simulators appear to have some potential for improving CCV designs. However, payload gains should only be in the order of a few thousand pounds.

Recent SSTO results have identified structural and subsystems as candidates for significant technology advancement, examples are; composite materials, hydraulics, integrated power control and actuator packages. CCV designs focus more emphasis on hydraulic and actuator subsystems as candidates for weight reductions. Potential weight reductions are from 2.265 X 10^3 to4.531 X 10^3 kg. Propulsion systems that affect aft C.G. location are

of most interest to CCV design. Dual fuel propulsion systems may offer a favorable control over aft C.G. locations. Preliminary estimates indicate potential saving in the 4.5×10^3 to 9.071×10^3 kg range. The major candidate for weight reduction is the design of the aerodynamic configuration which impacts hypersonic trim, aft C.G., and aero heating and potential payload gains up to 9.071×10^3 kg are possible. From this overview presented in figure 41 the assessment examines, in more detail, flight control, structures, subsystems, and propulsion advanced technology in the following sections.

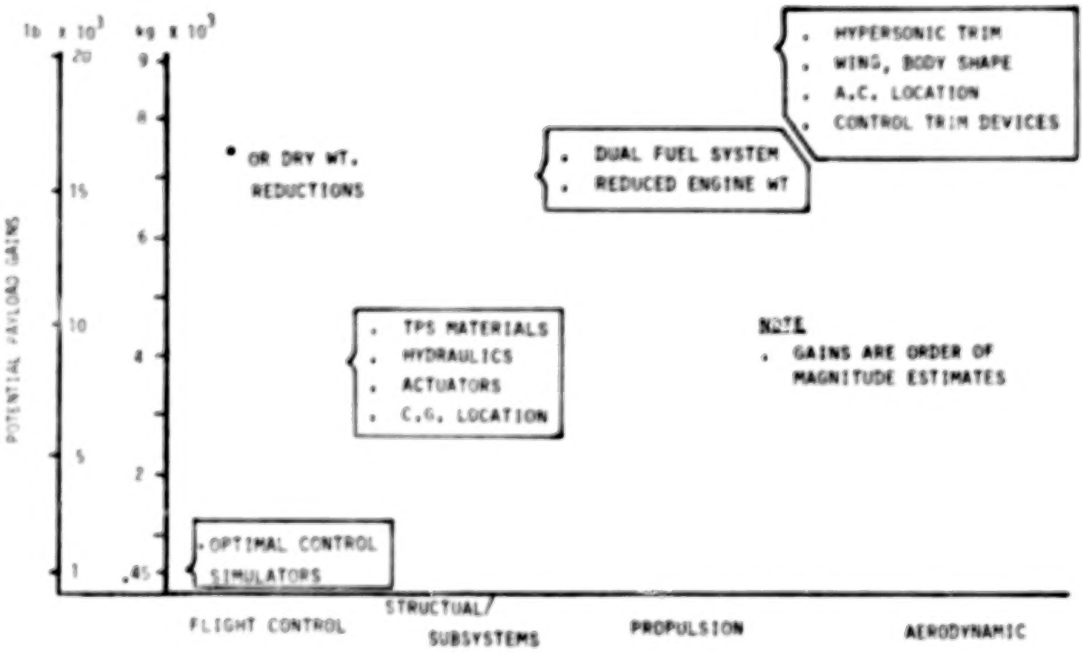

Figure 41 Advanced Technology for CCV Designs

CCV Design Process

As a result of this study, a CCV design process for large re-entry vehicles (SSTO type) has been formulated for application to follow-on CCV studies. The elements of this design process are presented in the following discussion.

The first cut at the configuration should design for re-entry trim using near zero elevon deflection. Body-wing camber, body flap and C.G. location are the variables available. Subsonic trim, also at $\delta_e \approx 0^o$ accomplished by canard incidence and body flap angle.

A gust/turbulence environment must be established as a function of flight condition (V, h) as well as a set of maneuver response envelopes. At each flight condition two flight controllers should be designed, one for gusts and one for maneuvers. A digital autopilot could reconfigurate itself for each of these tasks by examining the change in commands.

The control surface (elevon) size is varied and the resulting maximum surface deflection, rate, hinge moment and power requirements are noted. There will be a minimum surface size that can handle the disturbance and maneuver requirements. This may or may not be the lowest weight configuration depending on the actuation requirements that result. However, the minimum weight system can be inferred from the above studies.

Flight conditions for which the vertical fin becomes effective, directional stability and rudder power reduce the requirement for elevon size to accomplish roll maneuvers, so these should be varied also to find the minimum system weight. However, the fin and rudder size will probably be determined by the cross wind landing requirements. Here again there is a trade between fin and rudder size.

One configuration variable that can be varied within limits with almost no weight penalty is dihedral angle. This should be optimized by the control dynamicist to reduce the control surface size and actuation requirements.

Use of an optimal control design technique is recommended because it reduces the variation in the control surface and actuation requirements of the several configuration variations that could result from different degrees of tailoring of the autopilot to each individual configuration.

Structures/Subsystem

There are a number of technology developments which will enhance CCV design. Many of these are under development for other programs and should be available as off-the-shelf technology for the time frame considered. Significant items are listed below:

Structures.-There are a number of developments which are applicable to CCV design in that better mass fractions will result from the incorporation of the technology projected. Many of these have been incorporated in the configurations shown for this study. Some of the significant items are listed below:

- Insulation - Dynaquartz/Microquartz - Improved insulation characteristics with lower density. These developments are being pursued with immediate application to the Shuttle.
- High Strength/High Temperature Composite Structures - These developments are being developed through a number of approaches with immediate application to supersonic aircraft as well as the Shuttle. This also offers a potential application for lighter landing gears and brakes.
- Brazed Titanium and Rene'Honeycomb Structures.-This development has application to all space transport vehicles including shuttle but has had limited support at present.
- Radiative Thermal Protection Systems - As shown by reference (1) developments in this area are proceeding even if not at a highly funded pace.

Propulsion and Secondary Power.-The principal area for development is the extension of the SSME capability. Whereas a new engine development program may not be realistic, logical extensions of the SSME may be acceptable. For this study, the engines projected are approximately twice the thrust rating of the SSME and are projected to use 27579 K Pa (4000 psi) chamber pressure. At this time, there are no plans for such an engine development.

A Reaction Control System using liquid oxygen and hydrogen has had periodic development effort and does show significant improvements in I_{SP}. A similar situation exists for a liquid oxygen and hydrogen APU. Neither of these developments are being pursued at present and no obvious impetus is projected.

Fuel cell development has been focused to a specific application in the main. New technology developments have been limited for this reason. As new approaches to solutions for the energy shortage are explored, this power generation source may receive additional interest.

Hydraulics.-The most significant development in this area is the evolution of a 34474 K Pa (5000 psi) or higher pressure system. This development is the cumulative development of a wide range of necessary elements encompassing pumps, actuators, valves, seals, fittings and fluids. Developments are under way sponsored by industry and government.

Electrical/Electronic.-A wide number of developments proceeding to provide lower weight, higher reliability, lower cost elements for computers, solid state relays, sensing and data transmission, power generation, transmission, and conversion, etc. These developments receive impetus from a wide range of sources assuring the probability of success for these programs.

Environmental Control Systems, Crew Accommodations, Display, Communications, etc.-As in the above case these areas have a very wide application and for this reason technology improvements providing lower weights, cost and volumes with higher reliability are predictable.

CONCLUSIONS

A fundamental goal of this study was to determine the applicability of the control configured design approach to earth orbital transportations systems. The baseline system chosen for study analysis was a reusable vertical take-off/horizontal landing single-stage-to-orbit vehicle having mission requirements similar to the Space Shuttle orbiter.

The applicability and benefits were identified by technical analyses of aerodynamic, flight control and subsystem design characteristics. Evaluations were made in terms of time responses to step disturbances, static margins and trim control, and subsystem actuator and fluid control power. Figures of merit were assessed on vehicle dry weight and payload injected to low earth orbit. Specific study conclusions are as follows:

- Unstable static margins for CCV designs can be controllable and have acceptable flying qualities by employing state-of-the-art automatic flight control techniques.
- Major design parameters for CCV designs are the hypersonic trim/aft C.G./lower control surface heating interfaces.
- Critical task for CCV designs is the development of aerodynamic body/wing hypersonic configurations.
- Optimized CCV designs can be controllable and provide substantial payload gains over conventional non-CCV design vehicles.

RECOMMENDATIONS

Overall recommendation is to proceed with follow-on studies of CCV designs for Advanced Orbital Transportation Systems. Recommended study tasks should include:

- Application of Advanced Flight Control Techniques
  - Optimal Control of Unstable Aft C.G. CCV Designs
- Improve Current Subsystems
  - Advanced Hydraulics
  - Actuator Weight Reductions
- Initiate Optimized Aerodynamic Configurations for CCV designs
  - Body/Wing Shaping for Hypersonic Trim
  - Body Nose Camber and Wing Incidence
  - A.C. and C.G. Interface
  - Static/Active Auxiliary Control Devices

REFERENCES

(1) Technology requirements for Advanced Earth Orbital Transportation Systems Contracts NAS 1-13944 and NAS 1-13944 (Mod 1)

(2) Lusher, W. P. and Hellish, J. A., "Advanced High Pressure Engine Study for Mixed-Mode Vehicle Applications, NASA CR-135141, 1977"

(3) SSME Extended Capabilities Study by Rocketdyne, Contract No. NAS 8-32340

(4) AIAA Conference Paper, March 24/25, 1977 Structures and Composites, Vol. A; Bohon, H. L., Shideler, J. L., and Rummler, D. R.; "Radiative Metallic Thermal Protection Systems - A Status Report".

(5) Application of the "EASY" Dynamic Analysis program to aircraft modeling. BCS Document No. 40120; J. D. Burroughs and A. W. Warren; November 15, 1976.

APPENDIX A - AERODYNAMIC CHARACTERISTICS

Many of the aerodynamic coefficients were obtained from wind tunnel tests of the Baseline CCV Configuration (unpublished NASA/Langley data). For those not available, estimates were made using scaled Shuttle Orbiter values or DATCOM methods. Estimated values are shown in the following tables.

	MACH NUMBER			
Rotary Derivatives (Per Rad.)	Subsonic	Transonic	Supersonic	Hypersonic
C_{Mq}	(0.3)	(1.2)	(2.86)	(20)
	-2.00	-2.00	-2.00	-2.0
C_{np}	0.13	0.15	0.10	-.02
C_{nr}	-0.30	-0.60	-0.60	-0.30
C_{lp}	-0.30	-0.28	-0.22	-0.30
C_{lr}	0.15	0.16	0.07	0.05
$C_{Y\delta R}$	.0032	.0030	.0010	0.0
$C_{Y\delta A}$	-.0030	-.0010	.0000	0.0
$C_{n\delta R}$	-.0006	-.0010	-.0005	0.0
$C_{n\delta A}$	.0010	.0000	.0000	.0005
$C_{\ell\delta R}$	.0008	.0006	.0003	.0001
$C_{\ell\delta A}$	.0030	.0020	.0005	.0015
Hinge Moment (Per DEG)				
$C_{h_{\delta e}}$	-.0068	-.0170	-.0100	-.0150
$Ch_{\alpha e}$	-.0076	-.0100	-.0060	-.0150
$C_{h\delta R}$	-.0100	-.0170	-.0100	0.0
$C_{h\beta}$	.0050	.0180	.0190	0.0
$C_{\ldots BF}$		-.03500	-.1800	-.0600

Configuration: Baseline CCV

(for Mod-I Relative to Baseline Configuration)

(per Deg)	MACH NUMBER Subsonic (0.3)	Transonic (1.2)	Supersonic (2.86)	Hypersonic (20)
ΔC_{n_β}	-.0002			Same as Baseline
ΔC_{ℓ_β}	.0001			"
ΔC_{Y_β}	.0005			"
ΔC_{L_α}	.0005	.0010	.0031	Obtain from Hypersonic Aero Program
ΔC_{m_α}	-.0010	-.0015	-.0020	"
$\Delta C_{m_{\delta e}}$	-.0020	-.0010	-.0005	"
$C_{Y_{\delta R}}$	←	(0.942 $C_{Y_{\delta R}}$ Baseline)	→	Same as Baseline
$C_{n_{\delta R}}$	←	(0.942 $C_{n_{\delta R}}$ Baseline)	→	"
$C_{\ell_{\delta R}}$	←	(0.942 $C_{\ell_{\delta R}}$ Baseline	→	"
$C_{Y_{\delta A}}$	←	$C_{Y_{\delta A}}$ Baseline	→	"
$C_{n_{\delta A}}$	←	$C_{n_{\delta A}}$ Baseline	→	"
$C_{\ell_{\delta A}}$	←	$C_{\ell_{\delta A}}$ Baseline	→	"

$S_{REF_{MOD-1}} = 59.1\ m^2\ (6365\ Ft^2)$ $\bar{C} = 18.48m\ (60.62\ Ft.)$

For MOD-I configuration with increased size of body flap and elevons adjust aero characteristics by area ratios for forces and tail volume coefficient ratios for moments, i.e.

For body flap increase

Tail volume coefficient,

$$\bar{V} = \frac{\ell S_{BF}}{\bar{c} S_{REF}}$$

where, ℓ = moment arm C.G. to body flap A.C.

$\bar{c}$ = MAC Ref. Wing

S_{REF} = Ref. Wing Area

S_{BF} = Body Flap Area

B.F. Chord Mod-I = B.F. Chord Baseline + 1.52m (5 ft)

thus,

$$\frac{\bar{V}\ \text{Mod-I}}{\bar{V}\ \text{Baseline}} = \frac{.124}{.0918} = 1.27$$

$$\Delta C_{m_{BF}})_{MOD-1} = 1.27 \times \Delta C_{m_{BF}}\ \text{Baseline}$$

For elevon increase:

Elevon Chord MOD-I = Elevon Chord Baseline + 0.91m (3 ft.)

thus,

$$\frac{\bar{V}\ \text{MOD-I}}{\bar{V}\ \text{Baseline}} = 1.26$$ (using Elevon characteristics in place of body flap)

$$\Delta Cm_{ELEVON\ MOD-1} = 1.26 \times \Delta Cm_{ELEVON}\ \text{Baseline}$$

The following table summarizes all the changes in Aero characteristics that were used in obtaining MOD-I from baseline Aero coefficients

CONTENTS

	Page	
SUMMARY	1	1/A7
INTRODUCTION	2	1/A8
SYMBOLS	4	1/A10
VEHICLE DESCRIPTION	6	1/A12
Baseline	7	1/A13
Mod 1	7	1/A13
Conventional	7	1/A13
FLIGHT DYNAMIC SIMULATION DESCRIPTION	13	1/B10
STUDY APPROACH	15	1/B12
RESULTS AND DISCUSSION (Tasks I, II, III)	17	1/B14
Literature Survey (Task I)	17	1/B14
Aerodynamics and Performance	24	1/C7
Flight Control	29	1/C12
Configuration Design	47	1/E3
Subsystem Design	54	1/E10
Mass Properties Analysis	67	1/F9
CCV/Conventional Vehicle Performance Summary	74	1/G2
ADVANCED TECHNOLOGY FOR CCV DESIGNS (Task IV)	76	1/G4
CCV Vehicle Performance	76	1/G4
CCV Design Process	78	1/G6
Structures/Subsystem	79	1/G7
CONCLUSIONS	81	1/G9
RECOMMENDATIONS	82	1/G10
REFERENCES	83	1/G11
APPENDICES	84	1/G12

APPENDIX B FLIGHT CONTROL SIMULATION BLOCK DIAGRAMS

Analysis Tool Selection

The EASY program was selected because it provides a uniquely applicable set of capabilities. The model is set up by "wiring together" system components, which include a six degree of freedom module and various transfer functions and non-linear components from which autopilot compensations and actuators can be readily constructed. The autopilots selected for use at subsonic speeds are diagrammed in figure 42.

In figure 43 the block labeled D6 simulates the basic six degree of freedom equations. Block AV, which receives the outputs of D6, produces variables required for aircraft simulation such as α, β, total velocity, dynamic pressure, etc. This block in turn feeds LO and LD which are the longitudinal and lateral-directional aero equations respectively. Thus the entire basic airframe simulation is contained in figure 43

The pitch autopilot for subsonic speeds is shown in figure 44 block GBZ sums the normal acceleration command and the feedback (FZ2LO) and applies the integral + proportional transfer function. GAQ sums the acceleration error with the pitch rate feedback times its gain and also supplies the pitch loop gain control. Note that the block MAA drives XP, not GAQ. An improved arrangement will make this evident. XP transforms pitch, yaw and roll autopilot channel outputs into right and left elevon and rudder commands. These then drive the control surface actuators, each represented by the three blocks MCA, SAA, GDA. These three blocks form a first order lag with independently settable limits on rate and position, such that the rate is forced to zero when the output position is limited.

The roll and yaw autopilots for subsonic speeds are in figure 45 GAP sums roll command and the sensed roll angle. The body axis roll and yaw rates times their respective gains are summed with the roll error in MCDA. The roll channel gain and output are in MAA in the preceeding figure. The yaw channel can be driven by roll command through a washout filter in LE

actually this was not used. Yaw rate and side-slip feedback signals are summed in MCDR and the yaw channel gain is contained in MAR. The rudder servo consists of MCA1, SAA1, GDA1 and is not well drawn. The feedback closing the loop for the first order lag can be seen going to the left from GDA1 to MCA1.

The program has the capability of determining trim conditions for any selected flight condition, linearizing the problem about the trim condition, and performing all the usual linear analyses such as root locus and frequency response. The same program will also run a complete six degree of freedom, non-linear simulation. This is particularly attractive in that the aero data have only to be entered into one program.

The aero data can be entered as stability derivatives (which may be functions of several variables) or as coefficients, just as they are recorded in the wind tunnel or any combination.

For performing the analyses, individual states can be easily frozen to simplify the problem. For example, the lateral-directional states and forward velocity can be frozen to reduce the problem to the pitch axis short period. Examples of root locus, gain selection and control coupling are presented in figures 46 and 47.

The simulation at hypersonic speeds is block diagrammed in figure 48 At supersonic ($M < 3$) speeds the yaw jets are turned off. Presented in figures 49 to 53 are more detailed block diagrams of the simulation which were obtained from NASA item 30 of table 2 based upon the Space Shuttle orbiter flight control system.

PITCH AUTOPILOT

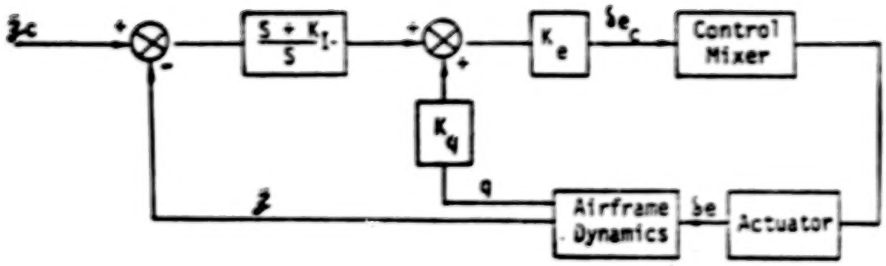

YAW - ROLL AUTOPILOT

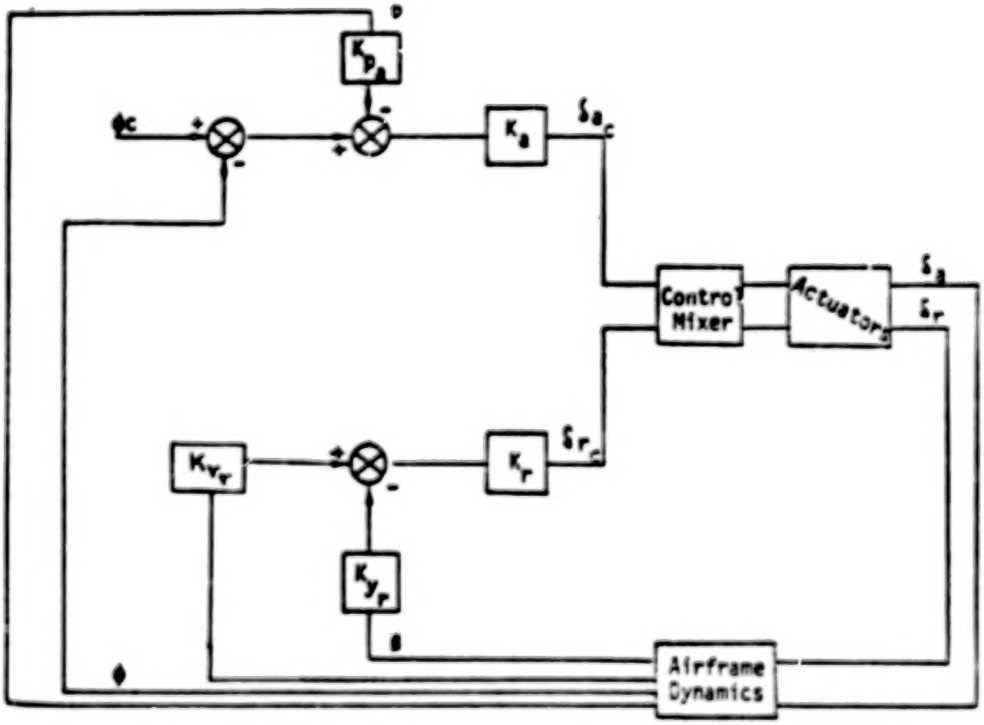

Figure 42 Subsonic Autopilot

Microfilmed From
Best Available Copy

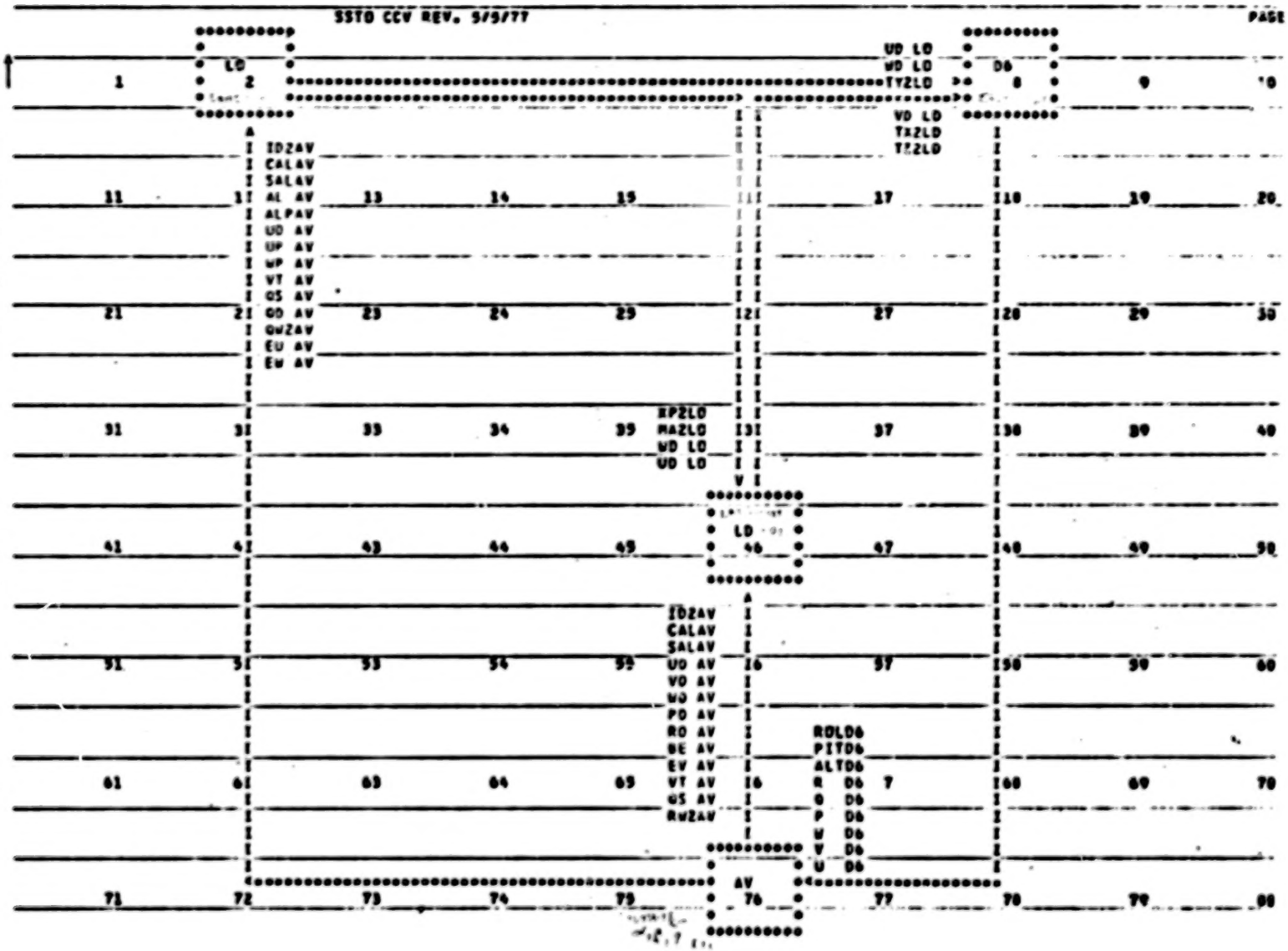

Figure 43 Airframe Dynamics

Microfilmed From
Best Available Copy

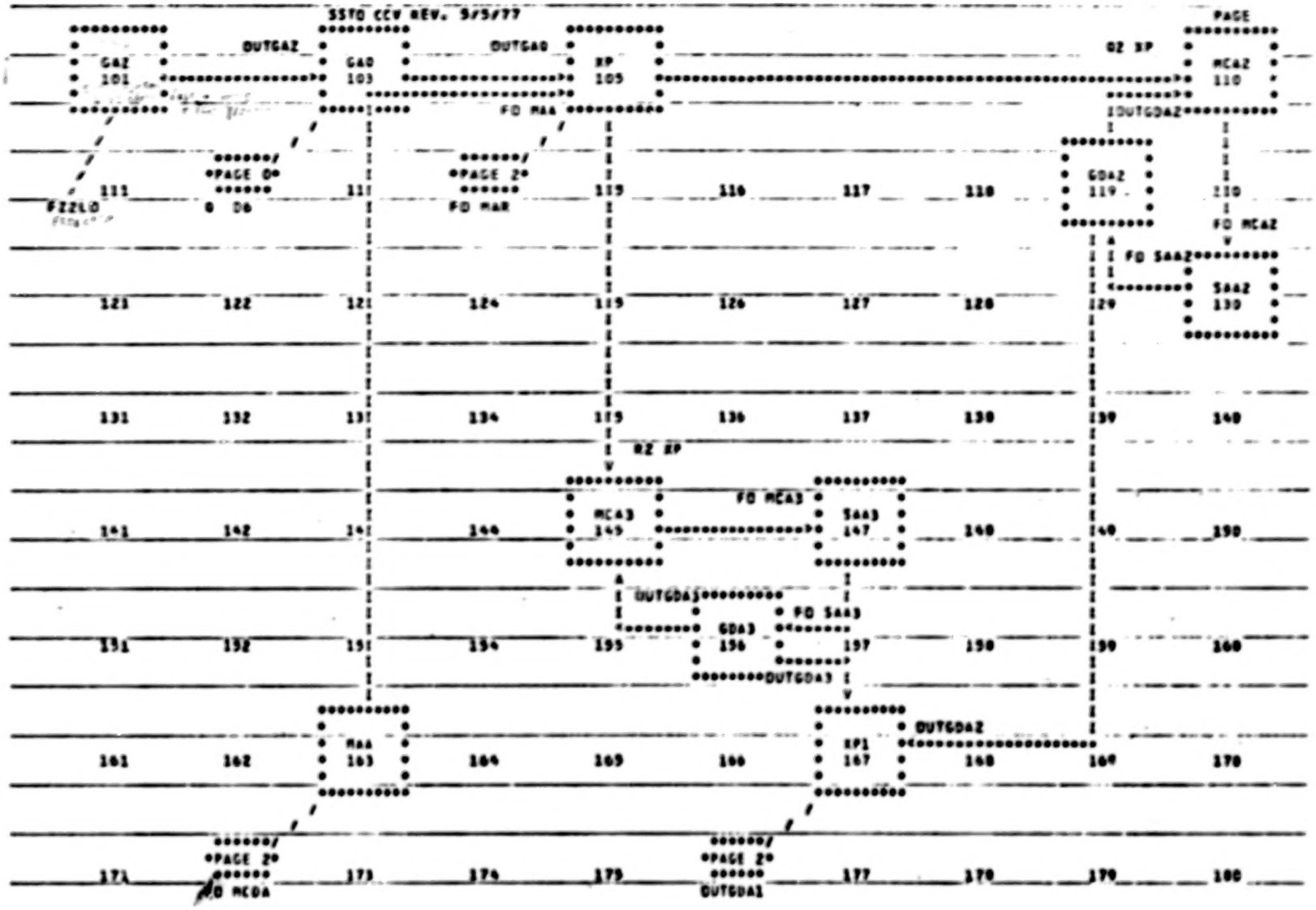

Figure 44 Pitch Autopilot

Microfilmed From
Best Available Copy

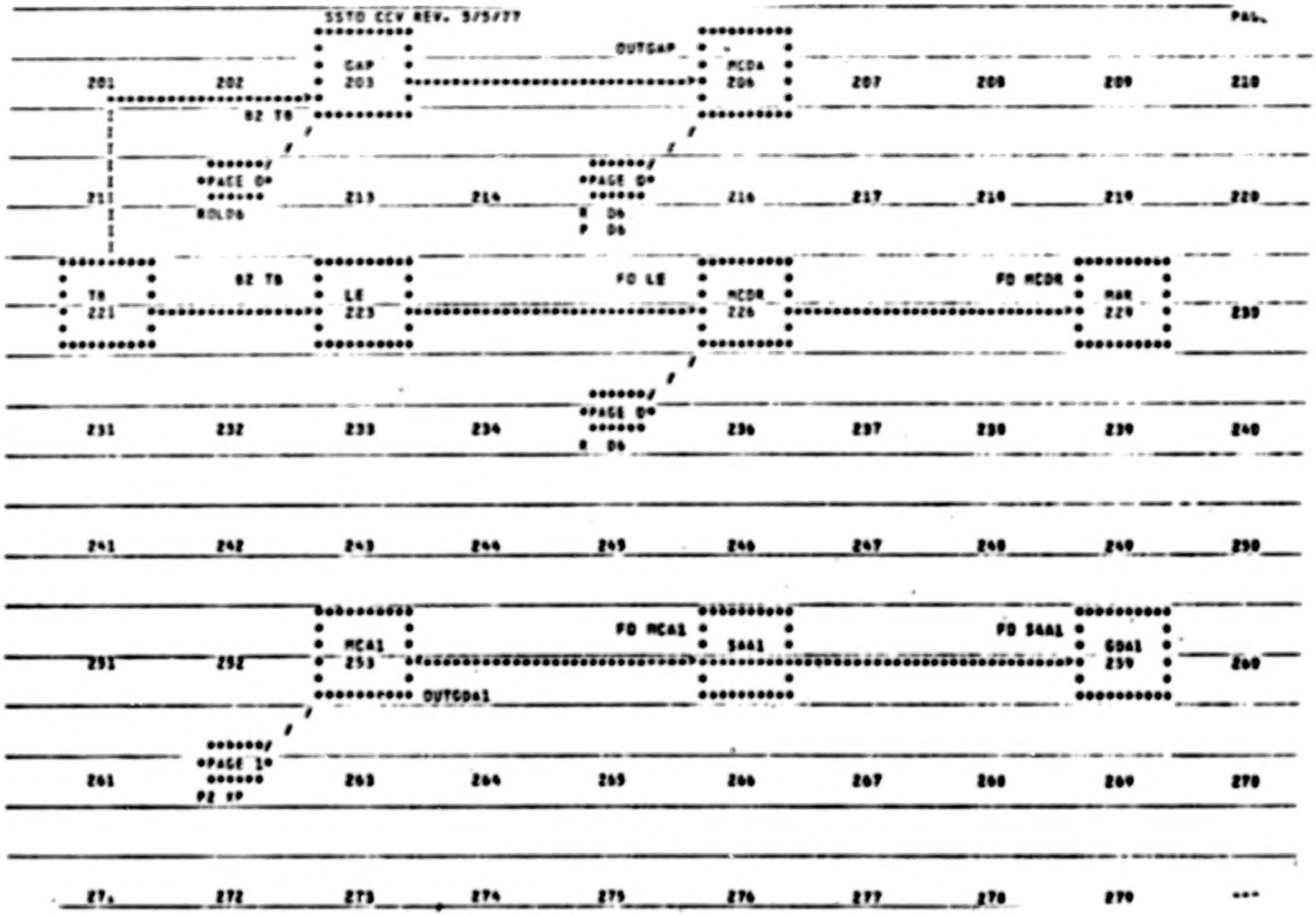

Figure 45 Yaw-Roll Autopilot

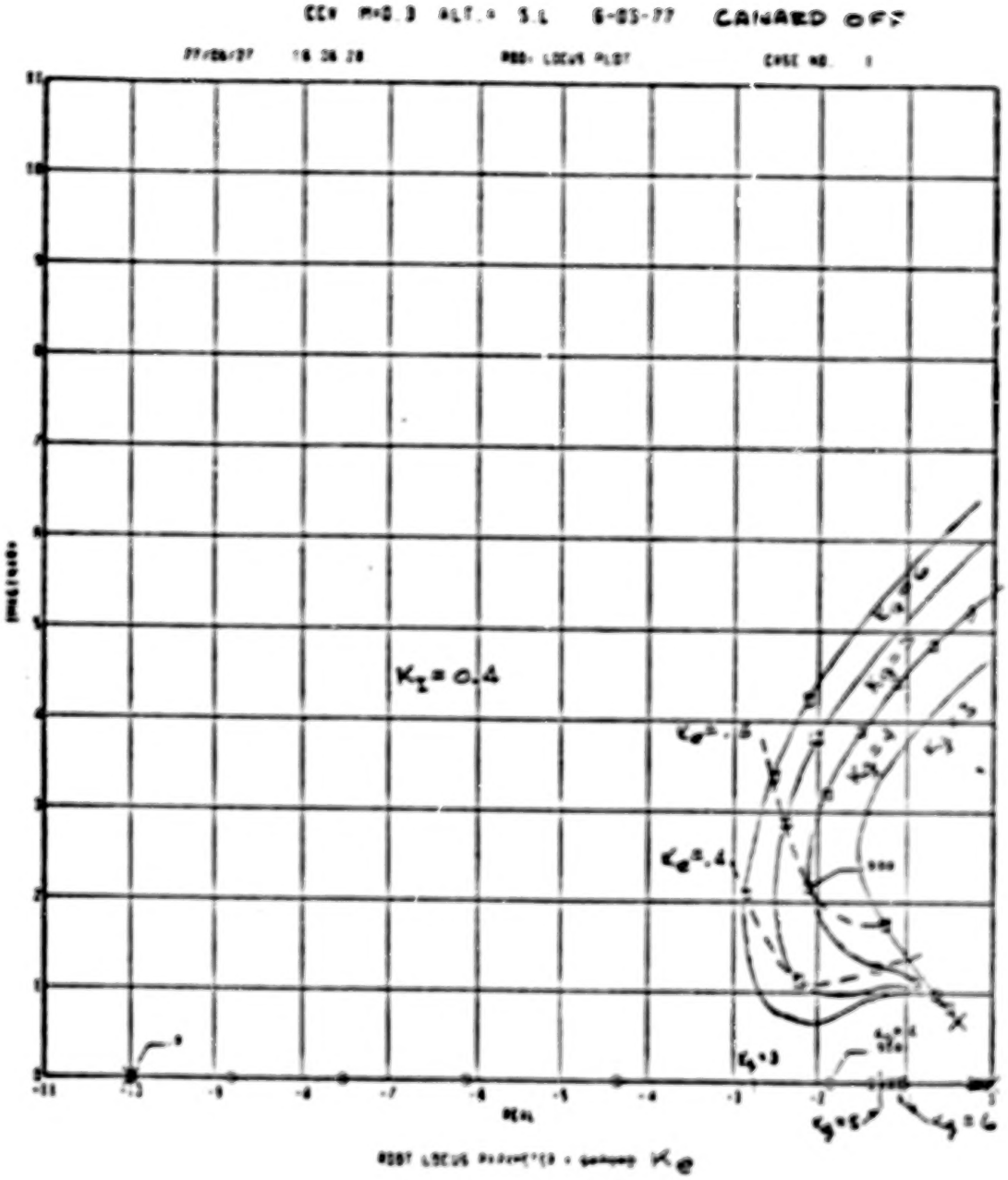

Figure 46 Pitch Axis Root Locus

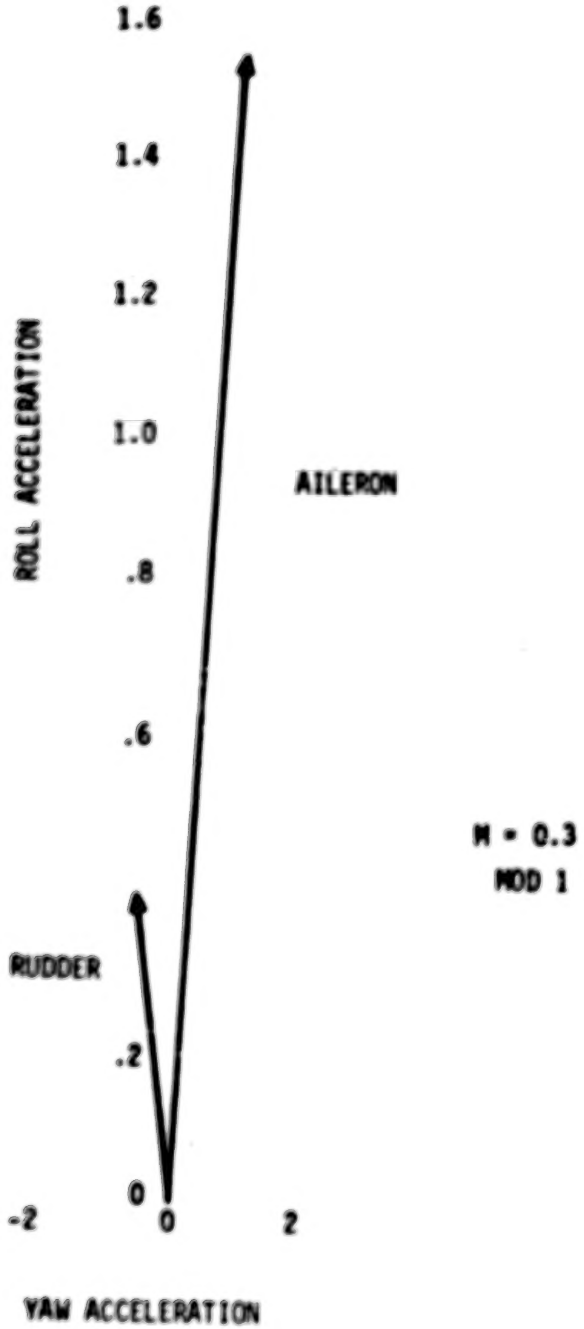

Figure 47 Control Coupling

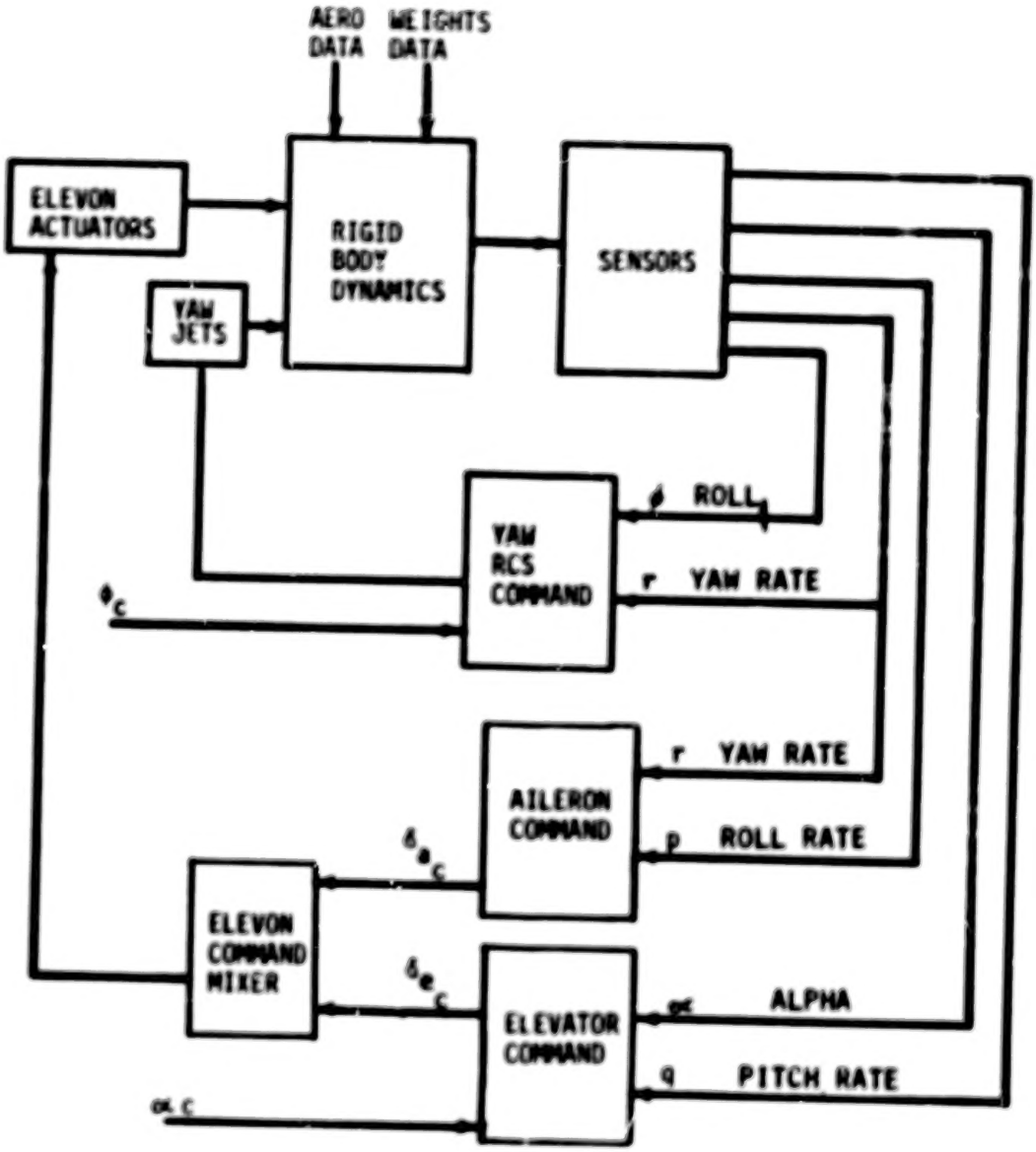

Figure 48 Hypersonic Simulation Configuration

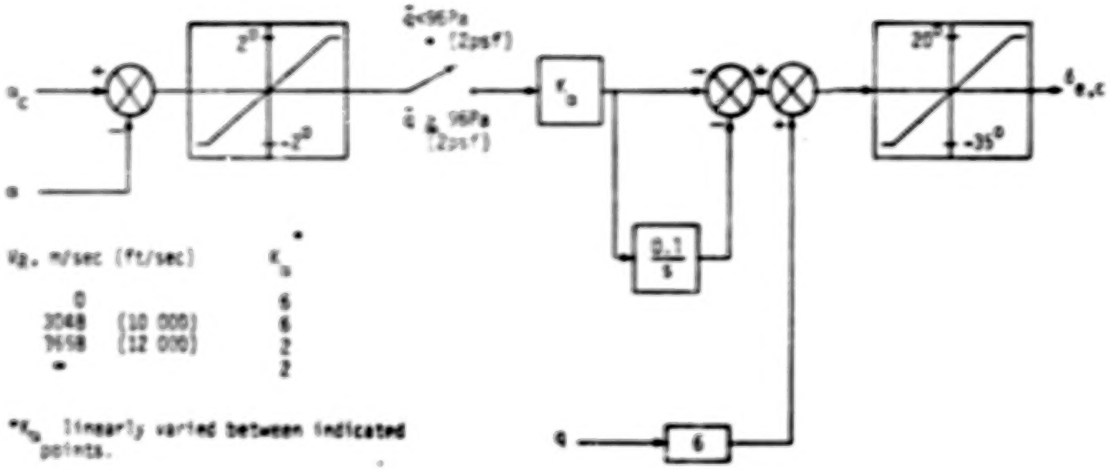

Figure 49 Elevator Command Block Diagram

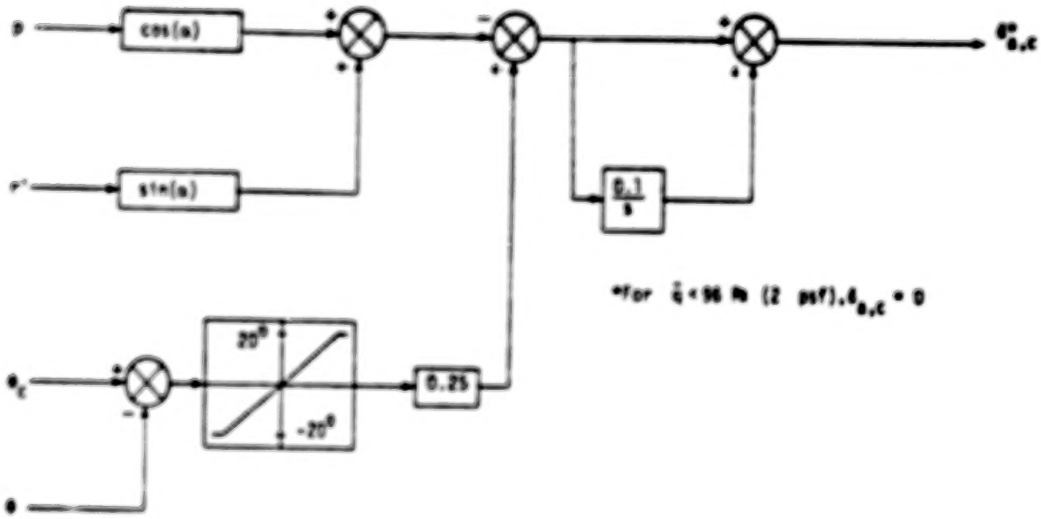

(a) $\phi \leq 18^0$ and $M \leq 5$.

Figure 50 Aileron Command Block Diagram

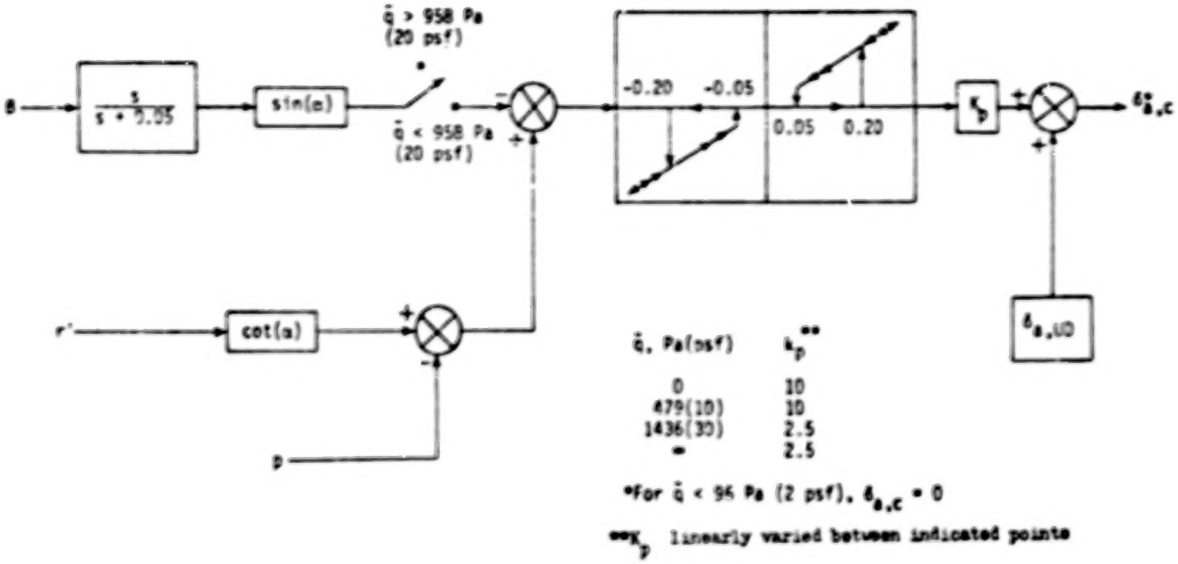

(b) $\alpha > 18^{\circ}$ or $M > 5$.

Figure 50 Concluded.

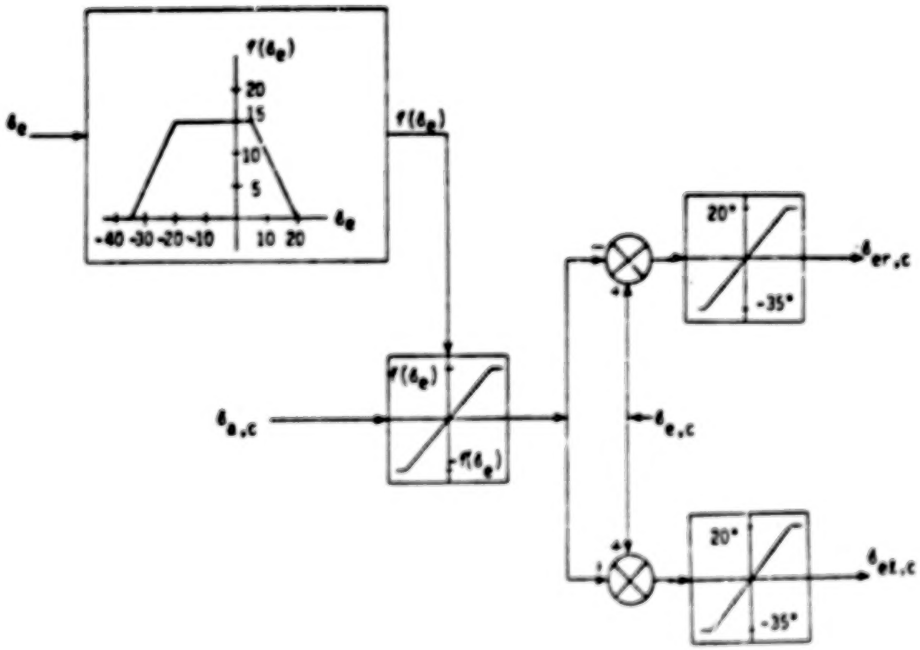

Figure 51 Right and Left Elevon Panel Commands

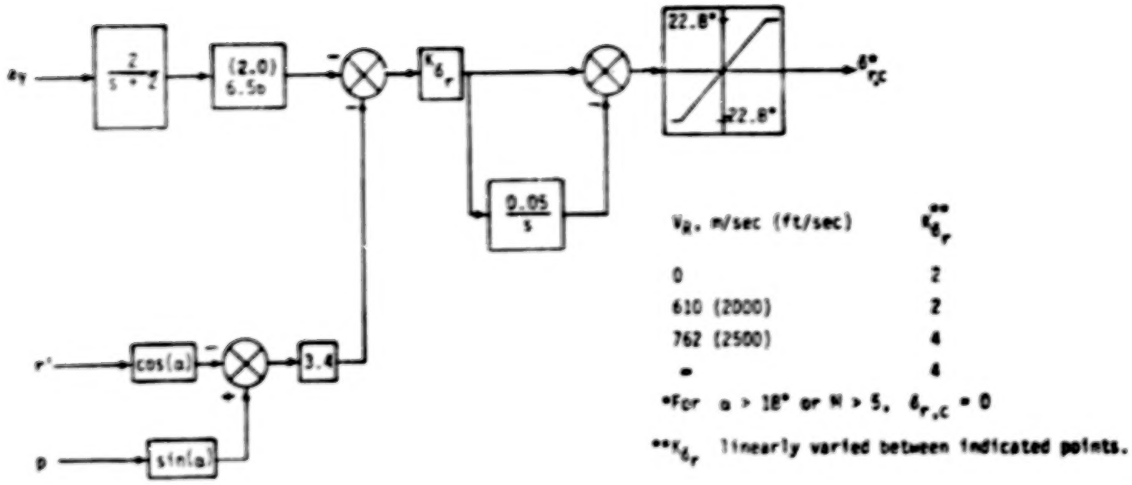

Figure 52 Rudder Command Block Diagram. Numbers in parentheses are in U.S. Customary Units.

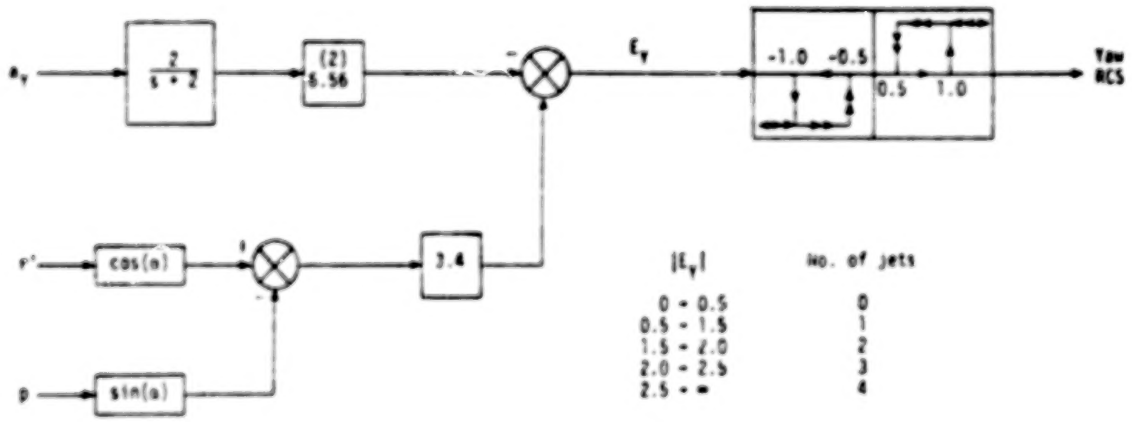

(a) α ≤ 18° and M ≤ 5.

Figure 53 Yaw RCS Error-Signal Block Diagram

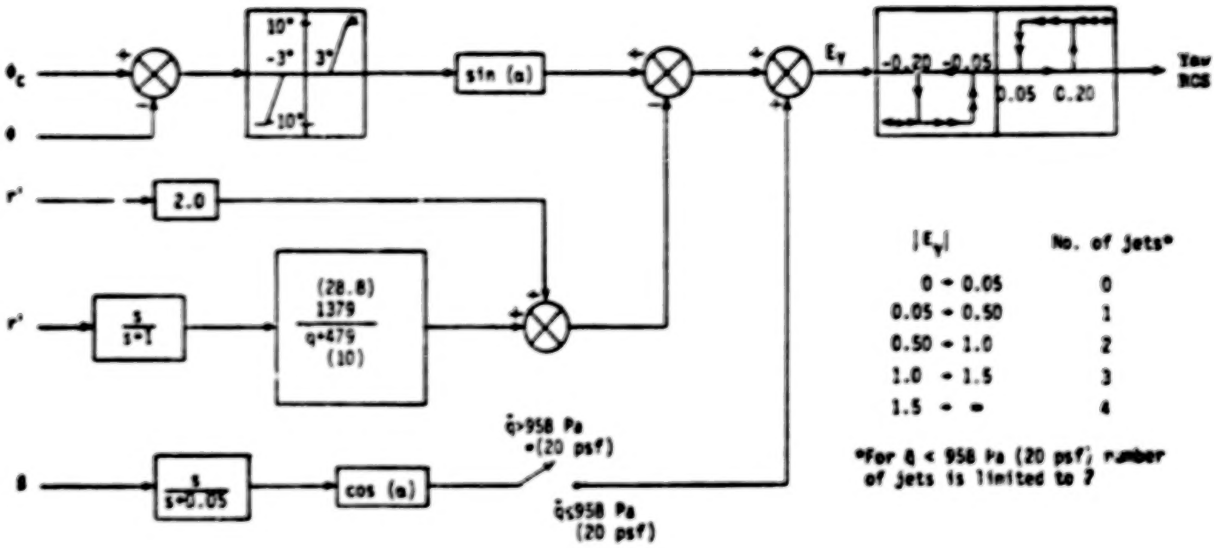

(b) $\alpha > 18^{\circ}$ or $M > 5$.

Figure 53 Concluded.

1. Report No.	2. Government Accession No.	3. Recipient's Catalog No.
NASA CR-2723		

4. Title and Subtitle	5. Report Date
Applicability of the Control Configured Design Approach to Advanced Earth Orbital Transportation Systems	August 1978
	6. Performing Organization Code
7. Author(s)	8. Performing Organization Report No.
Andrew K. Hepler, Howard Zeck, William H. Walker, Daniel E. Shafer	
9. Performing Organization Name and Address	10. Work Unit No.
Boeing Aerospace Company Kent, Washington 98031	
	11. Contract or Grant No.
	NAS1-14833
	13. Type of Report and Period Covered
12. Sponsoring Agency Name and Address	Contractor Report, Final
National Aeronautics and Space Administration Washington, D. C. 20546	14. Sponsoring Agency Code

15. Supplementary Notes

Langley Technical Monitor: Delma C. Freeman, Jr.
Final Report

16. Abstract

The present study addresses the Applicability of the Control Configured Design Approach (CCV) to Advanced Earth Orbital Transportation systems. The baseline system chosen to investigate is a fully Reusable Vertical Take-Off/Horizontal Landing Single-Stage-to-Orbit vehicle and had mission requirements similar to the Space Shuttle orbiter. Technical analyses were made to determine aerodynamic, flight control and subsystem design characterisitcs. Figures of merit were assessed on vehicle dry weight and orbital payload.

The study results indicated that the major parameters for CCV designs are hypersonic trim, aft C.G., and control surface heating. The study demonstrated that optimized CCV designs can be controllable and provide substantial payload gains over conventional non-CCV design VTO vehicles.

17. Key Words (Suggested by Author(s))	18. Distribution Statement
Control Configured Vehicles (CCV) Advanced Space Transportation Systems Single Stage to Orbit (VTO)	Unclassified - Unlimited Subject Category 08

19. Security Classif. (of this report)	20. Security Classif. (of this page)	21. No. of Pages	22. Price*
Unclassified	Unclassified	103	$6.50

*For sale by the National Technical Information Service, Springfield, Virginia 22161

NASA-Langley, 1978

90

50

END

DEC 11 1978